Illuminating the Effects of the US-China Tariff War on China's Economy[*]

Davin Chor
Dartmouth and NBER

Bingjing Li
HKU

December 2022

Abstract

How much has the US-China tariff war impacted economic outcomes in China? We address this question using high-frequency night lights data, together with measures of the trade exposure of fine grid locations constructed from Chinese firms' geo-coordinates. Exploiting within-grid variation over time and controlling extensively for grid-specific contemporaneous trends, we find that each 1 percentage point increase in exposure to the US tariffs was associated with a 0.59% reduction in night-time luminosity. Combining these with structural elasticities that relate night lights to economic outcomes, we find that this negative impact was highly skewed across locations: While grids with negligible direct exposure to the US tariffs accounted for up to 70% of China's population, we infer that the 2.5% of the population in grids with the largest US tariff shocks saw a 2.52% (1.62%) decrease in income per capita (manufacturing employment) relative to unaffected grids. By contrast, we do not find significant effects from China's retaliatory tariffs, and offer suggestive evidence of several channels through which Chinese firms might have mitigated the impact of tariffs on imported inputs. We obtain similar findings from a parallel analysis conducted at the prefecture level, indicating that these grid-level impacts had discernible negative aggregate consequences.

Keywords: US-China tariff war; Night lights.

JEL codes: E01, F10, F13, F14, F16

1 Introduction

Starting in early 2018, the US and China engaged in a series of high-profile tariff actions that escalated over the next two years. This steadily unwound the progress on trade liberalization and economic cooperation achieved since the mid-1990s between the two countries. At the height of this "tariff war" in September 2019, US tariffs on China had surged by 20.7 percentage points on average; these increases covered 93.0% of all Harmonized System (HS) 6-digit products, affecting 14.2% of the value of China's total exports (or 74.7% of China's exports to the US) in 2017. In response, China enacted retaliatory tariffs on goods from the US averaging 16.6 percentage points; these affected 84.3% of HS 6-digit products, that accounted for 5.6% of the value of China's total imports (or 66.0% of imports from the US) in 2017.[1]

This paper studies the impact of the US-China tariffs on China's economy. Did higher US tariffs exert downward pressure on economic activity within China, and if so, by how much? Likewise, did China's retaliatory tariffs affect domestic economic activity, by limiting access to inputs from the US? There have to date been relatively few studies assessing this impact on China, due in no small part to reporting lags and limited access to Chinese data especially at the sub-national level. To the best of our knowledge, firm-level customs data for the tariff war period (2018 and after) are not publicly available yet to researchers, possibly due to the sensitive nature of the information, nor do the Chinese authorities have a consistent practice of releasing statistics on production and employment at the local level for detailed industries.[2] There is moreover no prevailing consensus on how severely the tariff war affected the Chinese economy, given that China was already experiencing a slowdown prior to the trade disputes which could reflect other macroeconomic shocks with a timing coincident with the tariffs.[3] A key aim of this paper is therefore to identify and quantify the effects of the US-China tariffs on income and employment growth across locations in China.

To overcome data constraints, we use satellite readings on night-time luminosity. Total visible light emitted from Earth's surface at night has become a commonly-used proxy for local economic performance, given the strong correlation it exhibits with conventional measures such as real GDP per capita. In addition to its higher frequency, the night lights data have several

---

[1]Average tariff rates reported here are simple averages across all HS 6-digit codes. The imports by China from the US amounted to 154.4 billion USD in 2017. China's retaliatory tariffs in Lists 1-3 targeted imports of 110 billion USD, which is around 72% of the value of imports from the US. We found a lower coverage ratio of 66.0% for two reasons. First, in Jan 2019, there was a large wave of exemption on auto parts. Second, although the List 4 targeted 75 billion USD imports from the US, most targeted products overlap with those in List 1-3. That is, China only added an additional 10 percent tariff to the existing retaliatory tariffs.

[2]While a number of provincial statistical agencies periodically report industry-level output and employment, this is for relatively aggregate two-digit industries.

[3]It has been hypothesized that, besides weak external demand, China's economic slowdown since 2015 has been partly driven by structural problems including the debt-ridden financial system, weakening property markets, and the diminishing return from investment in infrastructure (*New York Times*, 17 Oct 2019).

advantages. First, it has a high spatial resolution; our analysis will be based on readings from nearly one hundred thousand 11-km-by-11-km grid cells across mainland China. Second, the data is less subject to manipulation and censoring compared to official statistics, a relevant concern in the context of China (Nakamura et al., 2016; Chen et al., 2019).

Figure 1 provides an illustration of the detailed variation in the night lights data, which can help in uncovering possible slowdowns in economic activity induced by the tariff hikes. The area shown is Suzhou, a prefecture-level city in the coastal province of Jiangsu. In it, we have outlined two regions – the New & Hi-tech Zone (Huqiu District) in red, and the Suzhou Industrial Park in green – which both have a high concentration of manufacturing firms; for example, the two largest categories of exports by value in the Industrial Park were electronics products and machinery, equipment, and components.[4] Night lights dimmed between Q1/2018 to Q1/2019 across the city, but there was substantial within-city variation. The year-on-year change in mean log night lights was -0.105, -0.085, and -0.067 for the New & Hi-tech Zone, the Industrial Park, and the rest of Suzhou respectively. The larger decline in night lights in industrial districts with a high export exposure hints at a link from the tariffs to an adverse impact on local economic activity. If US tariffs shrank export orders for Chinese firms, the resulting contraction in production and in their labor demand would in principle reduce lights emitted from factory night-time operations and from the worker dormitories often situated adjacent to these factories.

To establish the causal nature of this link, we adopt a Bartik (or shift-share) design. We construct a measure of exposure to the US tariffs for each micro-geographic location within China that is based on the initial product composition of its exports. Intuitively, grids that specialized in selling products to the US that were subsequently hit by tariffs were more directly exposed to the resulting decline in export demand. At the same time, China's retaliatory tariffs could have disrupted production for firms that source inputs from the US. To explore this, we construct a second Bartik measure of input tariff shocks that combines the initial composition of a location's intermediate and capital goods imports with product-level retaliatory tariffs. As described, this empirical strategy requires information on the structure of trade flows at the detailed grid level. We assemble this using web-mapping services (Google Maps and Amap) to geo-locate firms in the 2016 China customs dataset; we moreover use the Bartik variables constructed from geo-coordinates from one mapping service to instrument for the corresponding variables built from the second, to address possible coefficient attenuation due to measurement error in any individual source.

We perform our main analysis on a grid-level panel dataset constructed at the quarterly

---

[4]Based on Annual Industrial Park Statistics in 2017, the Industrial Park exported 16.97 billion dollars in electronic products and 13.94 billion dollars in machinery, equipment and components, which accounted for 40.7% and 33.4% respectively of its total exports; around half of this value was exported to the US.

Figure 1: Motivating Evidence: Night Lights Intensity in Suzhou in Q1/2018 and Q1/2019
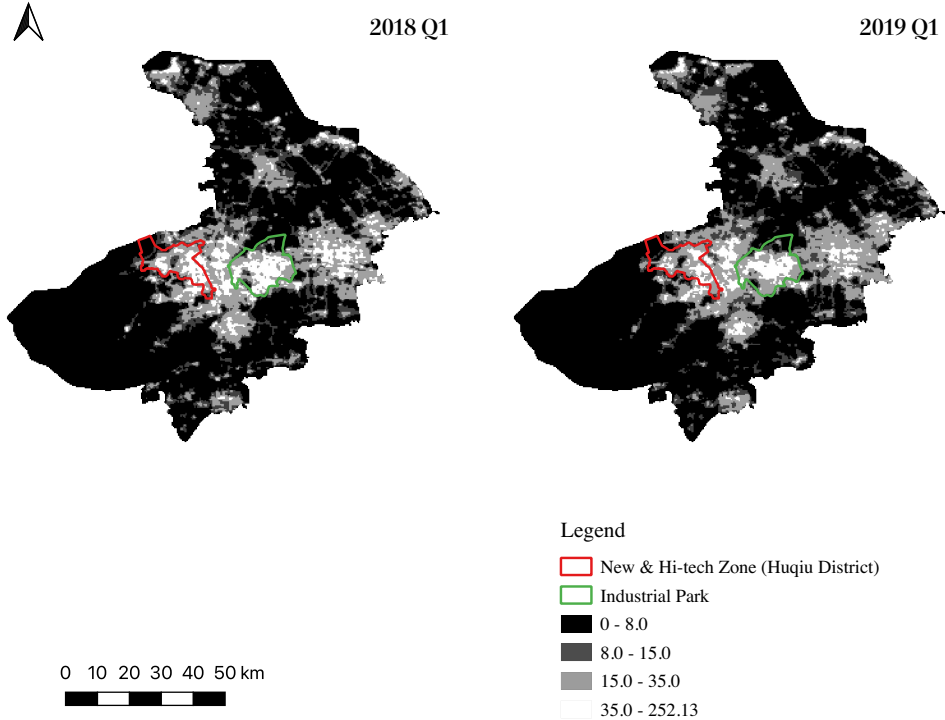
Notes: From the VIIRS-DNB.

frequency. Specifically, we examine the impact of the tariff shocks that unfolded over the period Q1/2018-Q3/2019 on the year-on-year growth in night lights intensity over Q2/2018-Q4/2019. We find that each one percentage point increase in exposure to the US tariffs lowered night lights intensity by 0.59 log points, this being a point estimate on the conservative end of the range of magnitudes across different specifications. By contrast, we do not find statistically significant effects for the retaliatory tariffs on inputs, and explore several potential explanations. In particular, we document a striking increase in the share of Chinese imports conducted under the processing trade regime, suggesting that this was a key channel through which Chinese producers sidestepped (at least partially) the additional burden from the retaliatory tariffs.

We further provide a discussion of the orthogonality conditions required for our Bartik strategy to be valid (c.f., Goldsmith-Pinkham et al., 2020; Borusyak et al., 2022); in this empirical setting, we view the case for causal identification as stemming from the plausible exogeneity of the initial product-level trade shares for the granular grid cells. Related to this, we perform extensive checks to show that the results are not confounded by pre-trends, including trends associated with other initial grid characteristics that could be correlated with trade shares. Our results are likewise unaffected when we control explicitly for contemporaneous policy shocks, including changes in China's MFN tariff rates and exchange rate movements. We also perform a Monte Carlo exercise to allay concerns related to possible over-rejection in

statistical inference with the use of Bartik measures (Adão et al., 2019).

How do these effects on night lights translate to economic outcomes such as income? To address this, we follow the statistical framework of Henderson et al. (2012) to estimate an inverse elasticity of night lights with respect to GDP per capita. We propose a novel approach for recovering this elasticity parameter, that leverages on the time series dimension of the night lights and income data available at the more aggregate prefecture level. This enables us to infer the change in GDP per capita that matches the change in night-time luminosity induced by the tariff shocks; we also use the same methodology to compute implied effects on manufacturing employment.

A key message that emerges is that the exposure to and hence the impact of the US tariffs was very skewed across locations. Grids that saw zero direct export exposure to the US tariffs accounted for more than half (close to 70%) of China's population. At the other end of the spectrum, the cumulative US tariff shock over Q4/2017-Q42019 at the 97.5th population-weighted percentile bin was 9.1 percentage points; for this tail 2.5% population bin, we infer that GDP per capita was 2.52% lower and manufacturing employment was 1.62% lower relative to unaffected grids. These grids that experienced the largest US tariff shocks were located in close to two-thirds of China's prefectures and were thus spread across China. We moreover find that this impact was particularly concentrated in grids with a high commuting intensity, suggesting that the negative demand shock prompted a reallocation of labor in line with the spatial general framework of Monte et al. (2018). Due to the difference-in-difference nature of our regression models, our estimates should be interpreted as speaking to partial equilibrium effects which net out any overall impact the tariff war may have had that was common across all grid cells. In particular, even grids with no direct tariff exposure could have been impacted if there were spillovers through economic interactions with firms located in the rest of China. We nevertheless show that such general equilibrium effects – to the extent that these are captured by weighted-averages of nonlocal tariff shocks, as in the framework of Adão et al. (2020) – likely reinforced the negative direct impact of the tariffs. In this sense, we view our quantitative estimates as constituting lower bounds to the full adverse impact of the US tariffs on China's economy. Last but not least, we uncover similar results – both directionally and in the size of the estimated effects – in a parallel analysis conducted at the prefecture level. Although we lose some statistical precision here relative to the preceding analysis, these findings confirm that the grid-level impact of the US tariffs were meaningful and consequential when aggregated up to these key administrative units.

This paper contributes to a growing body of research into the effects of the US-China tariff war on economic activity (see Fajgelbaum and Khandelwal, 2021, for a recent survey). The bulk of the work to date has focused on the implications of the US tariff increases and China's retaliatory tariffs on a comprehensive set of outcomes in the US, including: pass-through to

domestic prices (Amiti et al., 2019; Fajgelbaum et al., 2020; Flaaen et al., 2020; Cavallo et al., 2021), consumption (Waugh, 2019), employment (Flaaen and Pierce, 2019; Benguria and Saffie, 2020; Goswami, 2020), investment (Amiti et al., 2020), supply chains (Handley et al., 2020), and political economy (Blanchard et al., 2019; Fetzer and Schwarz, 2021).

Less is known in contrast about how China's economy has weathered this trade tension, due to the limited availability of micro-level data. Several studies have thus turned to information for publicly-listed Chinese firms, to document patterns of abnormal stock returns around the tariff announcements (Huang et al., 2022), or to study the effects of trade policy uncertainty on firm investments and profits (Benguria et al., 2022). Jiao et al. (2022) use proprietary data from a single prefecture-level city, to investigate the adjustments of Chinese exporters' sales across different markets. In addition, several studies leverage China's monthly customs data at the product level to study non-tariff barriers during the trade war (Chen et al., 2022) and the impacts of China's retaliatory tariffs on its export performance (Jiang et al., 2022).[5] Instead of focusing on a particular subset of firms/locations or the variations at the product level, our paper exploits the satellite coverage to observe the impact on granular grid locations that span mainland China.

In parallel, other researchers have performed model-based assessments of the impact of the tariffs on China's economy (Ferraro and Leemput, 2019; Ju et al., 2020; Zhou, 2020), by building general equilibrium trade models that account for global value chain linkages in their structure (following for example, Caliendo and Parro, 2015). We also seek to assess the quantitative impacts of the tariff war on China's economy, but our approach exploits quasi-experimental variation in cross-location exposure to the tariff shocks to identify their differential impact on economic outcomes. This approach is similar in spirit to Cui and Li (2021), who find that the US tariffs curtailed new firm registrations in China, and to He et al. (2021), who find that the US tariffs resulted in fewer online job postings and lower wage offers.[6] While our immediate focus is on the tariffs' impact on economic outcomes, it bears noting that negative economic shocks have been shown to have repercussions too for social stability and local leaders' careers within China's political system (Campante et al., 2019).

Our paper is naturally related to the wider literature on the use of night lights in empirical research. It is now well established that night lights are strongly correlated with standard measures of economic activity at the national as well as sub-national levels, including: GDP (Chen and Nordhaus, 2011; Henderson et al., 2012; Hodler and Raschky, 2014; Storeygard, 2016), average income in both national accounts and household surveys (Pinkovskiy and Sala-

---

[5]Relatedly, Tian et al. (2022) employ the firm-level information from Chinese customs data to evaluate tariff pass-through and the implications of retaliatory tariffs via import-export linkages within firms.

[6]Interestingly, He et al. (2021) also find that China's retaliatory tariffs did not have a statistically significant influence on their labor market measures

i-Martin, 2016), geographic features (Henderson et al., 2017), population density (Bleakley and Lin, 2012), and various development indicators (Michalopoulos and Papaioannou, 2013). The regularity and reliability of the satellite data collection has enabled researchers to explore questions related to economic development in novel and convincing ways, in otherwise data-scarce environments (Donaldson and Storeygard, 2016). Newer vintages of satellites have further made it possible to monitor higher-frequency changes in night lights; recent applications include studies of the short-run responses to the 2015 trade disruption between India and Nepal (World Bank, 2017), and the 2016 Indian demonetization episode (Chodorow-Reich et al., 2019). As with these studies, our analysis adopts quarterly night lights data across fine sub-national geographic units, which allows us to examine the effects of the multiple rounds of US-China tariffs actions.

The paper is organized as follows. Section 2 describes the key data sources. Section 3 lays out the empirical strategy for identifying the effects of tariff shocks on measured night lights, and reports these findings. Section 4 translates these estimates into implied effects for GDP per capita and manufacturing employment. Section 5 concludes. The Appendix documents more details on the data, as well as additional empirical analysis.

2 Data

This section describes the main sources that we employ to compile the grid-level dataset of tariff shocks and night lights intensity, on which our empirical analysis is based.

2.1 Product-level Data on Tariffs

Our primary source of information on the US-China tariffs is Bown (2021), which identifies and dates tariff actions that came into force starting in January 2018. From this source, we obtain: (i) tariffs imposed by the US on imports from China, available at the Harmonized System (HS) 10-digit product level; and (ii) retaliatory tariffs imposed by China on US goods, available at the HS 8-digit level. The ebb and flow of these tariff actions is well-documented in prior studies (e.g., Bown and Kolb, 2021), with each round of increases by the Trump administration prompting China to respond in short order with retaliatory tariffs.

Our analysis includes the Section 201 tariffs on solar panels and washing machines (which came into effect in February 2018), the Section 232 tariffs on aluminum and steel products (March 2018), as well as the four rounds of Section 301 tariffs (July 2018 to September 2019). We focus on these tariff actions up until September 2019, prior to the Phase One Trade Agreement between the US and China, though we have also coded up the tariff changes to end-2020. We are careful to incorporate the information from Bown (2021) on tariff exemptions, that were

granted by either the US or Chinese authorities after each tariff round to particular products on a case-by-case basis; these exemptions are netted out from the tariffs.[7] When aggregating the data to either the monthly or quarterly level, we scale the tariffs by the number of days that they were in effect. As the China customs data that we will use are at the HS 6-digit level, we take a simple average over all associated 10-digit or 8-digit tariff changes (for the US and China tariffs respectively) to obtain tariff shock measures for HS6 codes. We complement the above with data from Most Favored Nation (MFN) tariff schedules from China's General Administration of Customs starting in 2017, to keep track of discretionary changes made to those tariffs by the Chinese authorities. By comparison, MFN tariffs for the US were stable during this period.

We have provided in the Introduction a sense of how far-reaching the tariff increases were. Appendix A contains a more detailed timeline and description of these changes, which are also illustrated in Figure A.1. The biggest ramp-up in both the US tariffs on China and in Chinese retaliatory tariffs occurred during September 2018, with the third round of Section 301 tariffs (see Tables A.1-A.2). Somewhat less well known is the fact that China also undertook cuts to its MFN tariffs – on product codes that accounted for more than a third of its total imports in 2017 – in part to mitigate the impact of the US tariffs (Table A.3); we will control for these in our empirical analysis.

We verify in Appendix C that the tariffs substantially affected trade flows at the product level. The lead-lag specifications there show that Chinese product-level exports to the US declined after US tariff increases, with statistically significant cumulative effects kicking in after two to three months (Figure C.1, Panel I.A); this corroborates Amiti et al. (2019) and Fajgelbaum et al. (2020) on the swift response of these trade flows to the tariffs. Interestingly, we do not find evidence that exports were diverted to other destinations, as China's exports to the rest of the world remained relatively stable (Panel I.B). We separately confirm that China's imports from the US fell sharply immediately following retaliatory tariff actions (Panel II.A).

2.2 Firm Geographic Coordinates and Grid-level Trade Flows

We require information on initial export and import activities at the grid level, in order to capture a location's exposure to the tariffs. For this, we draw on 2016 Chinese customs data, which covers the universe of China's exporters and importers. For each trading firm, the customs provides a breakdown of its trade flows by destination/origin countries for HS 6-digit products. However, the precise geo-location of firms is not directly available.[8] To pin down each firm's

---

[7]The tariff exemptions by the respective authorities affected a meaningful share by value of China's total exports and imports; please see A for details.

[8]The prefecture where each firm is located can be inferred from the customs authority's unique firm identifier, but this is too coarse for mapping to a grid cell.

geographic coordinates (i.e., longitude and latitude), we turn to web-based geo-location services. Using the Google Maps API, we search firm names to recover each firm's geo-coordinates. If this yields no result, we then search for the firm using its address and zipcode, conditional on that information being available in the customs dataset. (Firm addresses are missing for more than 57% of the firms.)

With the geo-information in hand, we then map firms to 0.1 arc-degree grid cells (approximately 11-km-by-11-km) to compute grid-level exports and imports in the baseline period (i.e., 2016, indexed by 0). In particular, the value of exports of product k to the US from grid i are given by: $X_{ik0}^{US} = \sum_{f \in i} X_{fk0}^{US}$, where the sum is taken over the exports of this product to the US by firms f located in the grid cell (X_{fk0}^{US}). Similarly, we define grid-level imports of product k from the US to be: $M_{ik0}^{US} = \sum_{f \in i} M_{fk0}^{US}$, where M_{fk0}^{US} is the corresponding imports by firm f located in grid i. Note that we exclude all trade flows by intermediary firms, as these transactions may not reflect actual production in a grid location.[9]

The geo-coordinates obtained from a single mapping service could be subject to some inaccuracy – for example, there could be different thresholds for accepting a search outcome that is a potential false positive – and this constitutes a source of measurement error in the inferred export and import structure at the grid level. To cope with this concern, we repeat the above procedure using the Amap API, to construct a second measure of grid-level trade exposure. Amap is a web-based mapping, navigation and location service, akin to Google Maps, that is maintained by the Alibaba Group. There are about 283,000 non-intermediary firms in the 2016 Chinese customs data. The Google Maps API recovered location information for 95.9% of these firms, while the corresponding share was 79.9% for Amap. Importantly, the two sets of geo-coordinates are highly correlated, with a small mean distance between Google Maps and Amap locations, as we report in detail in Appendix B. We employ alternative APIs not only to cross-validate the firm geo-data, but also to design an IV strategy that addresses the attenuation bias introduced by measurement error that is particular to each individual source.

2.3   Night Lights Intensity

Given the paucity of detailed statistics on Chinese economic activity at the sub-national level, we turn to a common proxy measure of local economic performance, namely data on human-generated night lights. The luminosity of night lights is known to be more intense in locations with concentrations of population or economic activity (Henderson et al., 2012). In the context of China, night lights emanating from industrial areas (such as that in Figure 1) in principle

---

[9]Intermediary firms are identified on the basis of their Chinese character firm names. Following Ahn et al. (2011), firms with names containing Chinese characters that are the English-equivalent of "importer", "exporter", and/or "trading" are excluded.

reflect the intensity of factory operations during night shifts, as well as occupancy in adjacent dormitories (where migrant workers employed in the factories are often housed).

We use the VIIRS-DNB dataset, which provides a monthly average of night lights intensity in 15 arc-second geographic grids commencing in April 2012.[10] These readings are filtered by the data provider to exclude observations impacted by lightning, lunar illumination, and cloud-cover. Two night lights series are available. The first excludes any data impacted by stray light during the summer months. The second adopts a stray-light correction procedure; this raises the coverage for Northern China during the summer time, but relies on the quality of the applied corrections.[11] We use the first series as our baseline measure, and the second for a robustness check. Compared to prior vintages of night lights data, the VIIRS-DNB has the key advantage that it is not top-coded.[12] The satellite overpass however occurs later at night (around 1:30am). Improvements in satellite technology notwithstanding, the accuracy of the readings can still be affected by local weather conditions, and so the night lights data on any given day should be viewed as a proxy for economic activity that is observed with noise.

We aggregate this data to 0.1 arc-degree grids. There are 97,313 grid cells of this size in mainland China, and these serve as the geographic units for the analysis in Section 3.[13] We will mostly work with night lights intensity at a quarterly frequency, by taking the simple average of the observations across available months. Appendix C provides a basic proof of concept that product-level tariffs affected economic activity as captured by this proxy. We illustrate there using a lead-lag specification that US tariffs levied at the product level were accompanied by a decline in the night lights intensity of grids that prior to the tariff war were engaged in exports of that product.[14]

---

[10]The night-time imaging capacity in the VIIRS-DNB is an advance over its predecessor – the Defense Meteorological Program Operational Line-Scan System (DMSP-OLS) – in radiometric accuracy, spatial resolution and geometric quality (Hu and Yao, 2022). (https://eogdata.mines.edu/products/vnl/#reference) Many existing studies use night-lights data from the DMSP-OLS (including papers cited in the literature review in Section 1), but this data series ceased after 2013.

[11]See Mills et al. (2013) for technical details.

[12]Figure 4 in the IMF working paper version of Hu and Yao (2022) shows that while the DMSP-OLS night lights intensity is increasing in country real GDP per capita, the slope of this relationship tapers off in the top range of the latter variable. In contrast, the relationship between the VIIRS-DNB night lights and real GDP per capita is distinctly linear. Relatedly, Bluhm and Krause (2022) show that top-coded night lights from DMSP-OLS understate the extent of economic activity in the biggest urban areas.

[13]We use the ArcGIS tool "Fishnet" to create a net of rectangular cells with width 0.1 arc-degree for mainland China, based on a map from the China Data Center at the University of Michigan.

[14]Related to this, Appendix C reports additional suggestive evidence to corroborate the negative economic impact of the US tariffs, using the available time series data from China's National Bureau of Statistics on year-on-year changes in industrial value added and in electricity generation.

3 Tariff Shocks and Night Lights: Grid-Level Analysis

In this section, we investigate the effects of the US-China tariff war on night lights as observed for the close to 100,000 grid cells in mainland China. We describe the empirical strategy and grid-level tariff shock measures in Section 3.1, before reporting the findings in Section 3.2.

3.1 Empirical Strategy

Our primary interest is in studying the economic impact on China of the following trade barriers: (i) the US tariffs imposed on goods from China; and (ii) the retaliatory tariffs imposed by China on goods from the US. We therefore relate grid-level changes in night lights intensity to local exposure to the tariff shocks via the following empirical model:

$$\Delta \ln(Light_{it}) = \pi_1 \Delta USTariff_{i,t-1} + \pi_2 \Delta CHNInputTariff_{i,t-1} + D_{pt} + D_i + W_{i0} \times D_t + u_{it}. \quad (1)$$

Here, $Light_{it}$ is the night-time luminosity of grid i during time t, and the Δ operator denotes the difference between the time t and $t-4$ values for a given variable. (We refer to the unit of time, e.g., Q2/2019, as the year-quarter.) The variable $\Delta USTariff_{i,t-1}$ captures exposure to US tariff shocks during time $t-1$ faced by Chinese exporters geo-located in grid i, while $\Delta CHNInputTariff_{i,t-1}$ measures the exposure of importers in that location to changes in the retaliatory tariffs levied against inputs sourced from the US; we focus on tariffs on inputs, since these would in principle have raised production costs for Chinese manufacturers (though we will also explore broader import tariff shocks in a later check). We lag the tariff shocks on the right-hand side by one period to accommodate a lagged response of local economic activity to the tariff increases.

The fixed effects structure in (1) comprises a full set of prefecture-by-year-quarter (D_{pt}) and grid dummies (D_i). The D_{pt}'s account in a flexible manner for unobserved shocks common to all grids within a prefecture p; in particular, these absorb the effects of policy moves or directives enacted at the prefecture level that could have affected local economic activity. The use of the D_i dummies further means that we are exploiting within-grid variation over time in night lights intensity. Note that with these fixed effects, the π_1 and π_2 coefficients are difference-in-difference estimates of the effects of exposure to the tariffs. We control in addition for a vector of initial grid-level characteristics interacted with year-quarter fixed effects, $W_{i0} \times D_t$; as we elaborate on shortly, this will help to bolster the causal interpretation of the tariff shock coefficients.

In our estimation, we regress stacked year-on-year changes in log night lights intensity over the period Q2/2018 to Q4/2019 on stacked year-on-year changes in grid-level tariffs over Q1/2018 to Q3/2019, which covers all the major tariff increases by the Trump administration

as well as China's responses. To guard against the influence of outliers, we winsorize the $\Delta \ln(Light_{it})$ observations that are above the 99th percentile or below the 1st percentile within each period t. Standard errors are clustered at the province level to account for serial correlation over time as well as spatial correlation across grids within a province. To generate population-relevant estimates, we weight the regression observations by grid population in 2015.[15]

We adopt a Bartik (or shift-share) construction for the key tariff shock explanatory variables. For the exposure of location i within China to the US tariffs, we compute:

$$\Delta USTariff_{it} = \sum_k \frac{X_{ik0}^{US}}{X_{i0}} \Delta USTariff_{kt}, \qquad (2)$$

where X_{ik0}^{US}/X_{i0} is the value of product-k exports from grid i to the US, expressed as a share of total grid-level exports, in 2016 prior to the tariff war. The variation in $\Delta USTariff_{it}$ stems from: (i) cross-grid differences in initial export product composition and in the importance of the US as a destination for those exports; and (ii) cross-product differences (at the HS 6-digit level) in the US tariff increases over time, $\Delta USTariff_{kt}$. A location is therefore exposed to a bigger decline in external demand if it specializes in exporting products to the US market that subsequently face larger US tariff hikes.

Analogously, our baseline measure of location i's exposure to the retaliatory tariffs is:

$$\Delta CHNInputTariff_{it} = \sum_{k \in \mathcal{K}} \frac{M_{ik0}^{US}}{M_{i\mathcal{K}0}} \Delta CHNTariff_{kt}, \qquad (3)$$

where $\mathcal{K}$ denotes the set of products k classified as inputs.[16] $M_{ik0}^{US}/M_{i\mathcal{K}0}$ is the base-year value of product-k imports from the US, expressed as a share of total grid-level imports of inputs. As constructed, $\Delta CHNInputTariff_{it}$ leverages: (i) cross-location differences in initial import composition and in the importance of the US as a source country for these inputs; and (ii) variation across products and over time in China's retaliatory tariffs, $\Delta CHNTariff_{kt}$.

Our baseline measures in (2) and (3) implicitly assume that only grids with firms exporting to or importing from the US are affected by the tariff shocks. This formulation is more aligned with our regression analysis that focuses on the short-run responses of local night lights growth to the tariff actions during the trade war. That said, we will later verify the robustness of our results under alternative constructions of tariff shocks using China's trade shares with all

---

[15]We impute a population of 1 for cells with a reported zero population, though our results are virtually unchanged even if we were to entirely drop these grids from the sample (see Table D.4 in the appendix). A description of data sources for all auxiliary variables, including grid-level population, is in Appendix B.

[16]More specifically, this is the set of HS 6-digit products classified as either an intermediate input or a capital good by the United Nations' Broad Economic Categories (BEC), Revision 5, coding system.

destination (or origin) countries as weights.[17]

Another view is that, regardless of export destinations or import origins, all grids with production in sectors impacted by the US punitive tariffs or in downstream sectors affected by China's retaliatory tariffs should have a positive exposure in the general equilibrium or in a long-time horizon. To account for this view, we re-weight the product-level tariff according to:

$$\Delta USTariff_{it}^{All} = \sum_{k} \frac{X_{ik0}}{X_{i0}} \Delta ExportTariff_{kt}^{US},$$

$$\text{and} \quad \Delta CHNInputTariff_{it}^{All} = \sum_{k \in \mathcal{K}} \frac{M_{ik0}}{M_{i\mathcal{K}0}} \Delta ImportTariff_{kt}^{US},$$

where X_{ik0}/X_{i0} (respectively, M_{ik0}/M_{i0}) is the export from (respectively, import by) grid i of product k to all destinations (respectively, from all origins) as a share of total grid-level exports (respectively, imports) in 2016.

The validity of the regression model in (1) for identifying the causal effect of the tariff shocks rests on the extent to which the measures in (2) and (3) capture sources of variation in local exposure to the tariffs that are exogenous with respect to the night lights outcome variable. Drawing on the recent literature that has clarified the conditions required for the implementation of a Bartik empirical strategy, one would need to be reassured that, conditional on the set of included controls, the u_{it}'s are uncorrelated with either: (i) the initial export/import structure of the grid cell (Goldsmith-Pinkham et al., 2020); or (ii) the product-specific tariff shocks experienced at the national level (Borusyak et al., 2022). The latter condition is more challenging to defend in the current context, given the targeted nature of the tariff actions. For example, the Section 201 and Section 232 tariffs were directed at narrow sets of products, such as solar panels and washing machines. It has also been documented that the early Section 301 rounds imposed tariffs predominantly on intermediate inputs, out of the Trump administration's apparent desire to avoid tariffs on consumption goods that would fall directly on American households (Grossman and Helpman, 2020; Bown and Kolb, 2021). The Section 301 tariffs were moreover ostensibly directed at products from industries deemed to be beneficiaries of China's "Made in China 2025" industrial policy plan (Ju et al., 2020).[18]

We instead view identification in our context as stemming more plausibly from the conditional exogeneity of the initial grid-level trade shares that capture a location's exposure to subsequent tariff changes (i.e., following Goldsmith-Pinkham et al., 2020). More formally, this requires: $E[(X_{ik0}^{US}/X_{i0})u_{it} \mid \mathcal{W}] = 0$ and $E[(M_{ik0}^{US}/M_{i\mathcal{K}0})u_{it} \mid \mathcal{W}] = 0$, where $\mathcal{W} =$

---

[17]See Table D.6 in Appendix D.1.

[18]This is expressly stated too in the "Section 301 Investigation Fact Sheet" released by the United States Trade Representative, available at: https://ustr.gov/about-us/policy-offices/press-office/fact-sheets/2018/june/section-301-investigation-fact-sheet

12

$\{D_{pt}, D_i, W_{i0} \times D_t\}$ is a shorthand for this set of controls on the right hand-side of the regression. At a basic level, it is worth pointing out that the granular 11km-by-11km grids that are our unit of analysis do not systematically coincide with the geographic boundaries of administrative districts or economic zones within China. The orthogonality conditions may nevertheless still be called into question if: (i) there are grid-specific trends in night lights intensity driven by forces other than the tariff shocks, that are nevertheless correlated with the initial grid-level trade shares (i.e., X_{ik0}^{US}/X_{i0} and $M_{ik0}^{US}/M_{i\mathcal{K}0}$); or if (ii) there are other contemporaneous product-level shocks that affect local outcomes through the same mixture of exposure shares.

We take several steps to address concern (i). First, we will confirm that the tariff shocks in (2) and (3) are uncorrelated with pre-trends in night lights growth. Second, it bears repeating that the specification in (1) includes grid fixed effects (D_i), which account for differences in average year-on-year growth in night lights across grids. As we will see, our findings are further robust to controlling for a $D_i \times t$ term – i.e., grid-specific linear time trends in $\Delta \ln(Light_{it})$ – which accommodates even more flexible differences in how night lights might evolve across grids. Third, there remains the concern that the initial export or import structure could be correlated with other location characteristics, that in turn might be the basis for systematic shifts over time in night-time luminosity. Toward this end, we construct additional grid-level base-year variables W_{i0}, namely: log exports per capita and log intermediate imports per capita (to capture overall openness), the shares of exports to and intermediate imports from the US (to capture the importance of the US as a trading partner), and log mean night lights intensity (to capture the overall level of local economic development). In further checks, we will also consider the possible role of initial grid-level trade shares in particular subsets of products, as well as of the importance of state-owned enterprises in grid-level exports. These are each interacted with a full set of year-quarter dummies $(W_{i0} \times D_t)$, to control for trends in local economic activity that might stem from these initial grid-level features.

To address the latter concern in (ii), we will verify that our findings hold even when controlling for Bartik-style variables that seek to directly pick up grid-level exposure to other candidate shocks. These shocks include: product-level adjustments in China's MFN tariffs, in China's value added tax (VAT) rates, and movements in the bilateral exchange rate.

When estimating (1), we use the US tariff shock (respectively, the retaliatory tariff shock) constructed on the basis of Amap geo-coordinates as an instrumental variable (IV) for the corresponding measure constructed using geo-coordinates retrieved from Google Maps. As discussed earlier, the firm geo-location from each source could be subject to inaccuracy, which potentially introduces measurement error in the initial X_{ik0}^{US}/X_{i0} and $M_{ik0}^{US}/M_{i\mathcal{K}0}$ trade shares that we infer for each grid. The IV approach helps to address attenuation bias in the coefficients of interest $(\pi_1$ and $\pi_2)$, insofar as the measurement error associated with the two web-mapping

13

services is uncorrelated.[19]

3.2 Empirical Results

Baseline Results: Table 1 reports our findings on the impact of the tariffs, following the specification in (1); all columns presented control for prefecture-time and grid fixed effects. When entered into the regression model on its own, the US tariff shock ($\Delta USTariff_{i,t-1}$) has a significant negative effect (Column 1). Relative to other locations, a one percentage point increase in a grid location's exposure to these tariffs in the US market reduces growth in night lights by 0.77 log points, indicating that the US tariffs dampened the intensity of local economic activity. (We will translate the estimates into implied magnitudes for economic outcomes such as GDP per capita in Section 4.) Note that the first-stage F-statistics confirm the relevance of the Amap-based tariff shock for explaining variation in the corresponding Google Maps-based variable, a reflection of the positive correlation between the two sets of geo-coordinates. In the analogous regression for $\Delta CHNInputTariff_{i,t-1}$, the estimated coefficient for the retaliatory tariffs on inputs from the US shows a negative effect on night lights growth, but this is not statistically distinguishable from zero (Column 2).

We include in Column 3 both the US tariff and the China input tariff shocks. The coefficient for the US tariff shock resembles that in Column 1, while that for the tariffs on imported inputs remains insignificant. Column 4 further controls for the grid-level initial characteristics W_{i0} – log exports per capita, log intermediate imports per capita, the US share in total exports, the US share in imported intermediates, and log 2016 mean night lights intensity – each interacted with year-quarter dummies. Our identifying assumption is therefore that, conditional on the fixed effects and these grid-specific trends, the profile of grid-level HS 6-digit trade shares is uncorrelated with night lights growth. The results are reassuringly robust, which helps to assuage the concern that the tariff shocks could instead have been picking up underlying trends in night lights intensity related to initial levels of openness to trade or local development. Even with these additional controls, the magnitude of the US tariff shock coefficient is only slightly smaller, with a one percentage point increase in tariff exposure lowering night lights growth by 0.59 log points (holding all else constant). We illustrate the tariff shock effects implied by this Column 4 specification in Figure D.1 in the appendix. The binned scatterplots of residualized changes in night lights against the residualized tariff shock variables confirm how greater exposure to the US tariffs was associated with slower growth in night lights; on the other hand, the China input tariffs did not affect night lights intensity in a distinct way. These relationships do not appear to be driven by particularly influential population bins.

---

[19]Note that this approach does not require us to take a stand on the relative merits of the respective search algorithms underlying each web-mapping service, or on whether one set of geo-coordinates might contain less measurement error than the other.

Table 1: Tariff Shocks and Night Lights Intensity

Dep. Var.: $\Delta \ln(Light_{it})$	(1) 2SLS	(2) 2SLS	(3) 2SLS	(4) 2SLS	(5) OLS-RF	(6) 2SLS	(7) 2SLS
$\Delta USTariff_{i,t-1}$	-0.7702***		-0.7851***	-0.5903**	-0.2523**	-1.1555**	-0.6522**
	(0.2166)		(0.2099)	(0.2673)	(0.1115)	(0.4839)	(0.2556)
$\Delta CHNInputTariff_{i,t-1}$		-0.0619	0.1051	0.5509	0.1631	0.3897	
		(0.3202)	(0.3299)	(0.5555)	(0.1766)	(0.9943)	
$\Delta CHNInputTariff_{i,t-1}^{Low,\,Proc}$							-0.8043†
							(0.5277)
$\Delta CHNInputTariff_{i,t-1}^{High,\,Proc}$							1.9277**
							(0.9435)
Grid FE	Y	Y	Y	Y	Y	Y	Y
Prefecture×Year-Quarter FE	Y	Y	Y	Y	Y	Y	Y
Grid W_{i0}×Year-Quarter FE	N	N	N	Y	Y	Y	Y
Grid FE×Linear Time Trend	N	N	N	N	N	Y	N
Observations	669,845	669,845	669,845	669,845	669,845	669,845	669,845
F-stat	183.8	72.31	37.33	21.22	–	10.92	5.975

Notes: All columns use each respective Amap grid-level tariff shock as an instrumental variable for the corresponding Google Maps grid-level tariff shock. The exception is Column 5, which reports the OLS reduced-form estimates from using the Amap-based tariff shocks directly as explanatory variables. The initial grid characteristics, W_{i0}, whose time-varying effects are included in Columns 4-6 are: the US share in exports, the US share in imports of intermediates, log exports per capita, log intermediate imports per capita, and log 2016 mean night lights intensity; grid-level exports and imports geolocated via Amap are used to construct the first four of these W_{i0} variables. All regressions are weighted by grid population in 2015, with a minimum population of 1 imputed for cells with zero population in the raw data. Standard errors are clustered at the province level. *** p<0.01, ** p<0.05, * p<0.1, † p<0.15.

For comparison, we report in Column 5 an OLS reduced-form regression where the Amap-based tariff shock measures (the instruments in the prior columns) are used directly as explanatory variables. The US tariff shock effect remains significant, though smaller in magnitude relative to the 2SLS results in Column 4, consistent with the IV approach helping to address attenuation bias in this coefficient of interest. Lastly, Column 6 reports a particularly stringent specification in which we further add grid-specific linear time trends to the right-hand side. This does not affect our conclusions on the negative effect of the US tariffs on local economic activity as proxied by night lights, and in fact yields a much larger coefficient (-1.16). In what follows though, we will use the point estimates from Column 4 for what we view as a more conservative benchmark for the impact of the US-China tariff war on China's economy.

A natural question that arises at this juncture is how uniform and persistent the impact of the tariffs has been. To explore this, we estimate a modified version of the Column 4 specification, that: (i) extends the sample period to encompass all 12 quarters from Q1/2018 to Q4/2020; while (ii) allowing for heterogeneous tariff shock effects over time, specifically for each half-year period.[20] Panel A of Figure 2 plots the time-varying coefficients for the US tariff

---

[20]To be clear, we continue to estimate how changes in night light intensity observed in year-quarter t are affected by year-on-year changes in grid-level tariffs with a one-period lag, $\Delta USTariff_{i,t-1}$ and

shock (with 90% confidence interval bands). We obtain negative and significant US tariff effects on grid-level night lights growth in the second half of 2018 and the first half of 2019, coinciding with the large expansion in scope of the Section 301 tariffs in September 2018. Interestingly, the US tariffs continued to exert a negative impact on night lights growth in the first half of 2020, suggesting that this could have been a contributing factor in the overall contraction of local economic activity during the early months of the Covid-19 pandemic.[21] By contrast, the corresponding plot in Panel B does not uncover any significant effects for the China input tariff shock over the period. Although these tariffs would in principle have raised the cost of inputs from the US, this does not appear to have been a significant drag on local economic activity. We explore the reasons in the following.

Figure 2: Effects of Tariffs on Night Lights Intensity in Different Periods
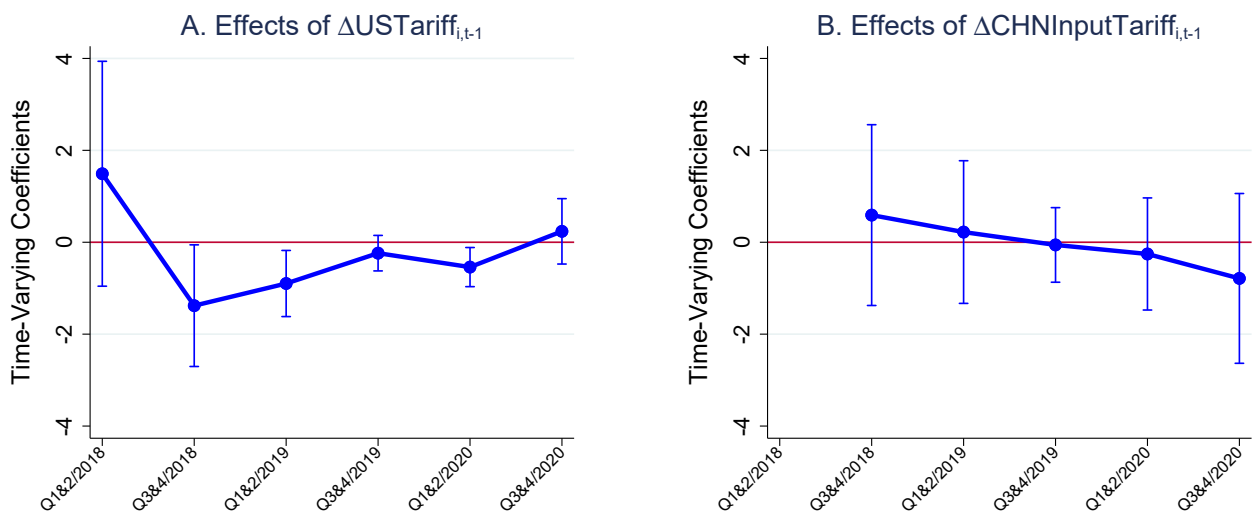
Notes: The figure plots the coefficients of the US tariff and CHN input tariff shock variables respectively, from an extended version of the baseline specification that extends the sample period to cover Q1/2018 through Q4/2020, and incorporates time-varying coefficients for each half-year. The effect of China input tariff exposure for Q1&Q2/2018 is not estimated, as $\Delta CHNInputTariff_{i,t-1}$ is uniformly equal to zero for $t = Q1/2018$ and $t = Q2/2018$. Standard errors are clustered at the province level; error bands show the 90% confidence intervals.

Understanding the Insignificant China Input Tariff Shock Effect: One potential explanation for the insignificant estimated effects of the input tariff shock is that a large portion China's imported inputs enter under the processing trade regime and hence are exempted from tariffs. The dual-trade regimes may serve as a buffer, as producers that previously chose to organize through ordinary trade could switch into processing trade in the face of higher import

---

$\Delta CHNInputTariff_{i,t-1}$. However, the sample period is now $t = Q1/2018, \ldots, Q4/2020$, with separate tariff shock coefficients estimated for $t = Q1\&2/2018, Q3\&4/2018$, etc.

[21]This negative US tariff shock effect in Q1&2/2020 is robust to controlling for the proximity of a grid location to Wuhan, the epicenter of the pandemic, interacted with time fixed effects; see Table D.1 in the appendix.

tariffs. As is revealed in Panel A of Figure 3, the share of imports from the US under process-
ing trade rises sharply following China's retaliatory tariff actions, while the processing import
share remains stable for the ROW.[22] Looking at the trade flows from the US, ordinary imports
decreased sharply, in contrast with the flat trend for processing imports (Panel B). Imports
from the ROW do not display a similar divergence across different trade regimes (Panel C). In
Appendix C.3, based on an event study analysis at the product level, we glean further evidence
for the effects of China's retaliatory tariffs on the reorganization of US-origin imports from
ordinary to processing regime.[23]

Figure 3: Imports Under Different Trade Modes: Ordinary v.s. Non-Ordinary Trade
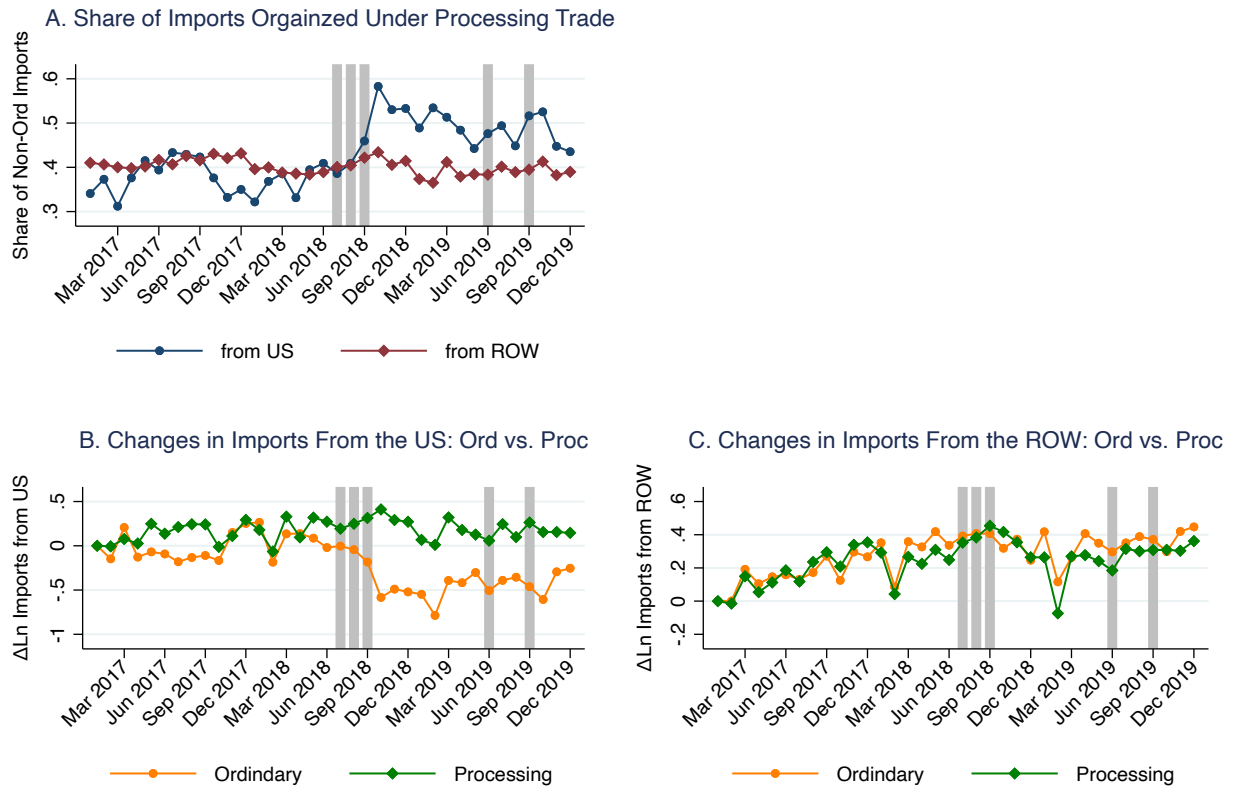
Notes: Panel A plots the shares of imports organized through processing trade from different origins (the US and
the ROW) over time. Panel B presents the change in log imports from the US that is organized through different
trade modes (ordinary v.s. processing), relative to the initial value in January 2017. Panel C is analogous to
Panel B, but focuses on the change in log imports from the ROW. The shaded areas in all panels correspond to
the different phases of China's retaliatory tariff actions, as listed in Table A.2.

To shed lights on the role of processing import intensity in determining the impacts of

---

[22]The monthly bilateral trade data by product and by trade regimes is obtained from China's General
Administration of Customs: http://43.248.49.97.

[23]Our findings mirror the findings in Brandt and Morrow (2017) who show that, following China's accession
to the WTO, lowered import tariffs induce firms to switch from processing to ordinary trade.

input tariff shocks on local economic activities, we proceed as follows. First, we rank HS 6-digit products based on the share of processing imports in total imports from the ROW in 2017. Second, two separate measures of input tariff shocks with different processing import intensities are constructed according to:

$$\Delta CHNInputTariff_{it}^{Low,Proc} = \sum_{k \in \mathcal{K}^{\mathcal{L}}} \frac{M_{ik0}^{US}}{M_{i\mathcal{K}0}} \Delta CHNTariff_{kt}$$

$$\text{and} \quad \Delta CHNInputTariff_{it}^{High,Proc} = \sum_{k \in \mathcal{K}^{\mathcal{H}}} \frac{M_{ik0}^{US}}{M_{i\mathcal{K}0}} \Delta CHNTariff_{kt},$$

where $\mathcal{K}^{\mathcal{L}}$ (respectively, $\mathcal{K}^{\mathcal{H}}$) denotes the set of HS 6-digit products classified as inputs or capital goods and with the share of imports from the ROW organized through processing trade below (respectively, above) the median. Column 7 of Table 1 shows that $\Delta CHNInputTariff_{it}^{Low,Proc}$ has a negative impact on night light intensity, although the estimate is imprecise with a p-value of 0.138. In contrast, the estimated coefficient for $\Delta CHNInputTariff_{it}^{High,Proc}$ is significantly positive. The finding that the adverse effect is more pronounced where processing imports is less relevant is reassuring. The positive effect of input tariff shock where processing imports take a more prominent place suggests that there may be reallocations of production from ordinary to processing regime when China raises import tariffs.

At the same time, we note that there could be other channels through which the adverse impact of higher input tariffs could be counteracted. For example, China cut its MFN tariffs during the trade war which could have helped to dampen the rise in the cost of imports. Moreover, Chinese producers could be able to switch to alternative third-country sources of inputs. The product-level trade responses we study using data from Trade Map in Appendix C (and that are illustrated in Figure C.1) indicate that both of these explanations are potentially relevant. It is plausible too that some substitution with domestic inputs may have occurred, although we lack data on such domestic purchases to verify the extent of this.[24]

Robustness and Additional Results: We have performed a series of checks to establish the robustness of our findings and to validate our Bartik empirical strategy. These results are reported in full in Appendix D, but we provide some key highlights below.

A first set of tests addresses concerns related to pre-existing trends. Table D.2 adapts the Column 4 specification to verify that the time-$(t-1)$ US and China tariff shocks are uncorrelated with night lights growth in earlier periods; there thus do not appear to be pre-

---

[24]Table D.6 in the appendix explores whether there might be indirect evidence of such domestic substitution, by asking if there was an intensification of night lights in grid locations within China that were initially specializing in and exporting products that were subsequently subject to the retaliatory tariffs on inputs; the estimated effect though is not statistically significant. In Appendix D.1, we consider alternative measures of input tariff shocks and ensure that the lack of significance is not a result of measurement issues.

trends or anticipation effects in observed night lights. We next show in Table D.3 that our coefficient estimates are stable, even when we expand the set of initial grid-level characteristics for which we control for associated time trends. We consider additional $W_{i0} \times D_t$ terms for log grid population, the state-owned enterprise share of grid-level exports, as well as grid-level trade shares for each of 15 HS sections. In particular, this helps to account for the potential effects of any explicit or implicit policies, such as over the allocation of bank credit, that might have benefited state-owned relative to private enterprises. This check moreover implies that the negative US tariff shock effect we have identified stems from variation across grids in export composition at the 6-digit level (e.g., Men's or boy's shirts, of cotton), rather than from forces that are affecting broader HS sections (e.g., Textiles and Textile Articles).[25]

Table D.4 turns to a set of checks related to our preferred empirical specification. Among other tests here, we estimate the regression model in levels as in equation (D.1), rather than in time-differenced changes. We also explore: (i) interchanging the roles of the Google Maps and Amap-based measures in our IV strategy; (ii) using the VIIR-DNB night lights measure with stray light correction; (iii) dropping all zero-population grid cells (rather than imputing a population value of 1); (iv) replacing prefecture-by-year-quarter fixed effects with province-year-quarter fixed effects; and (v) excluding observations in the five largest prefectures, where headquarters – rather than production facilities – tend to be located. Our headline result of a negative and significant US tariff shock effect, together with an insignificant China input tariff effect, holds throughout.

Table D.5 controls for other contemporaneous shocks that could affect local economic activity similarly through the initial grid composition of exports or imports. We do so through the use of additional Bartik-style variables to capture a grid location's exposure to: (i) adjustments in China's MFN tariffs; (ii) cuts in VAT rates; and (iii) movements in the USD to RMB exchange rate. (Please see Appendix D.1 for more details on the construction of these shock variables.) The grid-level tariff effects estimated in Table D.5 are virtually unchanged, and so our baseline results are unlikely to be picking up the influence of these other forces.

We explore several alternative tariff shock measures in Table D.6. As a falsification test, we construct US and China input tariff shocks using initial product-level shares for a grid location's trade with a set of other high-income countries (instead of the US).[26] These placebo shocks have insignificant effects on growth in night lights, highlighting that it is specifically export exposure to the US market that is driving our findings. On a separate note, while our baseline retaliatory tariff measure focuses on intermediate inputs, we verify that the tariffs raised by China on consumption goods did not affect night lights growth. We also consider an

---

[25]See Appendix D.1 in the appendix for a full list of the 15 HS sections.

[26]This comprises the eight countries used by Autor et al. (2013) to construct their "China shock" instrumental variable, namely: Australia, Denmark, Finland, Germany, Japan, New Zealand, Spain, and Switzerland.

alternative measure of input tariff shock based on China's input-output table for 2017.

Two additional checks are of note. In Figure D.2, we conduct a permutation test, in which we randomly reshuffle product-level tariff shocks across 6-digit products, and then re-build shift-share regressors by combining actual trade shares in 2016 with the placebo product-level shifters. The standard deviation of the estimates derived from 300 placebo samples is smaller than our baseline standard error (for both the US tariff and retaliatory tariff shocks). This relieves the concern that we may be under-stating the standard errors due to an underlying spatial correlation in the trade shares (Adão et al., 2019).[27] Figure D.3 provides further reassurance on the statistical significance of our results, by alternatively reshuffling the export and import trade shares across grids within each prefecture. Lastly, in Table D.7, we adapt the estimator proposed by de Chaisemartin and D'Haultfoeuille (2020); this guards against concerns that the average treatment effect could be mis-estimated in two-way fixed effects regressions, when the treatment timing differs across grids and treatment effects vary across grids and time.

4   Mapping Night Lights Intensity to Economic Outcomes

Thus far, we have demonstrated that tariff shocks, in particular the higher US tariffs faced by Chinese exporters, adversely affected night-time luminosity. In this section, we examine quantitatively the implications of this finding for China's economic performance. We proceed in two steps. First, drawing on the literature that has exploited night lights data to study economic development, we estimate a structural elasticity between observed night lights intensity and local economic outcomes for China. For this purpose, we use prefecture-level GDP per capita and manufacturing employment data for a pre-tariff war window, from the China City Statistical Yearbooks. Second, we combine this structural elasticity with the earlier estimates from Section 3.2 on the effects of the tariff shocks on night lights growth, in order to assess how much the tariffs impacted these income and employment outcomes within China.

4.1   Statistical Framework

Following Henderson et al. (2012), we specify a statistical framework that relates measured night lights to log GDP per capita (respectively, manufacturing employment). This will discipline the manner in which we back out a structural elasticity that can then be used to map observed

---

[27]As is discussed in Adão et al. (2019), the spatial correlation of regression residuals induced by similarity in sectoral composition is less of a concern when: (i) the number of industries/products in the Bartik measure is large; and (ii) when there is no shift-share structure with similar share weights left in the regression residuals. For the second condition, the standard errors remain remarkably stable when we control for grid-level trade shares for each of 15 HS sections interacted with time dummies (Table D.3), as well as for other shift-share variables that pick up contemporaneous policy shocks (Table D.5).

changes in night lights intensity to more tangible economic outcomes.

In this framework, the true value of log GDP per capita y_{js} for each Chinese prefecture j in year s is reported with measurement error:

$$z_{js} = y_{js} + \varepsilon_{z,js}. \tag{4}$$

Here, z_{js} denotes the measured value of log GDP per capita, with error term $\varepsilon_{z,js}$; the latter is assumed to be independent and identically distributed (iid) with variance σ_z^2.

The intensity of observed night lights, x_{js}, are in turn a function of the true underlying level of per capita income, given by:

$$x_{js} = \beta y_{js} + \varepsilon_{x,js}. \tag{5}$$

The $\varepsilon_{x,js}$ is a classical measurement error term, which arises in particular from idiosyncratic climatic and atmospheric conditions as the daily satellite readings are being taken. We thus assume these are iid with associated variance σ_x^2, and moreover that these are uncorrelated with the measurement error inherent in the GDP data, i.e., that $cov(\varepsilon_{x,js}, \varepsilon_{z,js'}) = 0$ for any given years s and s'. Our goal is to recover an estimate of $1/\beta$, which will then enable us to map changes in night-time luminosity to actual GDP per capita outcomes. (In what follows, it should be understood that z_{js}, x_{js} and y_{js} refer to the respective variables after conditioning out auxiliary controls, namely prefecture and province-year fixed effects.)

Henderson et al. (2012) show that with the above structure, the implied estimating equation is: $z_{js} = (1/\beta)x_{js} + u_{js}$, where $u_{js} = -(1/\beta)\varepsilon_{x,js} + \varepsilon_{z,js}$. The estimator for $1/\beta$ via OLS is then given by:

$$\widehat{\left(\frac{1}{\beta}\right)} = \frac{1}{\beta}\frac{\beta^2\sigma_y^2}{\beta^2\sigma_y^2 + \sigma_x^2}, \tag{6}$$

where σ_y^2 denotes the variance of the true income variable y_{js}. The naive OLS estimate is thus attenuated with respect to the true value of $1/\beta$ whenever $\sigma_x^2 > 0$, due to the measurement error inherent in the night light readings. Henderson et al. (2012) work around this, by proposing a methodology to bound the magnitude of the signal-to-noise ratio $\sigma_y^2/(\sigma_y^2 + \sigma_z^2)$ in the country income data.

We instead adopt an approach that exploits the panel dimension of the available data on night lights and GDP per capita. We make one additional orthogonality assumption, namely: $cov(\varepsilon_{x,js}, \varepsilon_{x,js-1}) = 0$, so that the measurement error inherent in the night lights data are viewed as serially uncorrelated at the annual frequency. In other words, while there may be measurement error in the satellite readings caused by climatic conditions on any given day, the scientific instruments do not make systematic mistakes for a given location j that are correlated over long averages. Then, we can obtain a consistent estimate of the elasticity of

interest by running a regression of log GDP per capita, z_{js}, on observed night lights, x_{js}, while instrumenting for the latter with its lagged value, x_{js-1}. Specifically, the IV estimation yields an estimator of $1/\beta$ as follows:

$$\frac{cov(z_{js}, x_{js-1})}{cov(x_{js}, x_{js-1})} = \frac{cov(\frac{1}{\beta}x_{js} + u_{js}, x_{js-1})}{cov(x_{js}, x_{js-1})} = \frac{1}{\beta} + \frac{cov(-\frac{1}{\beta}\varepsilon_{x,js} + \varepsilon_{z,js}, \beta y_{js-1} + \varepsilon_{x,js-1})}{cov(x_{js}, x_{js-1})} = \frac{1}{\beta},$$

where the last step makes use of: $cov(\varepsilon_{x,js}, \varepsilon_{x,js-1}) = 0$ and $cov(\varepsilon_{z,js}, \varepsilon_{x,js-1}) = 0$. Notice moreover that this approach only requires that the noise term in the night lights data be serially uncorrelated. The procedure remains valid even if observed GDP per capita z_{js} exhibits serial correlation, which is a more distinct possibility should there be persistent errors or reporting biases in this data series.

4.2 Estimating the Inverse Elasticity of Night Lights Intensity

We implement the above IV approach to recover estimates of the inverse elasticity of night lights with respect to two outcomes, GDP per capita and manufacturing employment. These latter variables are taken from the China City Statistical Yearbooks, where they are reported at a lower frequency (on an annual basis) and at a more aggregate geography (prefectures) than the night lights data. We will combine the inverse elasticity of night lights estimated from this prefecture-level data with the earlier findings in Section 3.2 on the effects of tariff shocks on observed night lights, in order to infer the impact of the US-China tariff war on economic outcomes within China. A natural caveat applies, which is that this assessment will be valid to the extent that the structural parameter $(1/\beta)$ is stable across different levels of geographic aggregation and observation frequency. In Appendix D.2, we examine the sensitivity of the estimate of $1/\beta$ using different datasets with geographic units defined at the county or province level. The alternative approaches entail estimates statistically similar to those obtained from the prefecture-level data.

Using the prefecture-level data from 2013-2016, we estimate the following:

$$\ln(GDPpc_{js}) = (1/\beta)\ln(Light_{js}) + D_j + D_{ps} + \nu_{js}, \tag{7}$$

where $GDPpc_{js}$ is the GDP per capita of prefecture j in year s, and $Light_{js}$ is the mean night lights reading in that year over all grid cells whose centroids are in prefecture j. The D_j and D_{ps} denote prefecture and province-year fixed effects respectively; standard errors reported are clustered by province.

Panel A of Table 2 presents these results, starting with more basic OLS specifications in Columns 1-3. We use all the available data in Column 1, which cover about 280 of China's 333

prefectures. As the residualized scatterplots in Figure D.4 show, there are a number of outliers that are associated with very (almost implausibly) large year-to-year swings in prefecture income per capita. Column 2 (respectively, Column 3) therefore trims out data points for which the change in log GDP per capita over the prior year lies in the tail 1% (respectively, 5%) of values across all prefectures for that given year. We obtain positive and significant estimates for the inverse elasticity of night lights, with a magnitude ranging from 0.16 to 0.22. As we have argued above, these OLS estimates would be downward-biased relative to the true value of $1/\beta$, if there is measurement error in the night lights data. Columns 4-7 turn then to two-stage least squares (2SLS) estimation, where we use the one-year lag, $\ln(Light_{j,s-1})$, as the IV.[28] Columns 4-6 report the 2SLS analogues of the specifications in Columns 1-3. These deliver larger coefficient estimates, which associate a 1% increase in night lights intensity with a 0.41-0.47% increase in GDP per capita. Lastly, Column 7 re-runs Column 6 using prefecture-level population as observation weights; this once again yields a significant positively-sloped relationship. Moving forward, we will use the elasticity recovered from the unweighted specification in Column 6, which implies a more conservative range of GDP per capita effects.[29]

It is helpful to benchmark the elasticity estimates in Table 2 against what has been found elsewhere in the night lights literature. These comparisons necessarily come with caveats, as there are differences in the datasets and methodologies across studies. Most existing papers focus on countries as the unit of analysis, and are based on the DMSP-OLS satellite data (the VIIR-DNB's precursor); also, studies often estimate the relationship between night lights and GDP, rather than GDP per capita. Be that as it may, our estimated value of $1/\beta = 0.47$ for China is generally smaller than what has been found in cross-country studies. For example, the findings reported in Table 5 of Henderson et al. (2012) imply a range of values for the inverse elasticity with respect to GDP between 0.58 and 0.97, while the more recent work of Hu and Yao (2022) has a central estimate of $1/1.317 = 0.76$. (Appendix D.2 briefly describes their respective methodologies and how these deliver implied values of $1/\beta$.) On the other hand, Storeygard (2016) reports a night lights coefficient of 0.25 when running a long-difference regression using Chinese prefecture-level GDP data over 1992-2005 (see his Table 1), which is similar in magnitude to our OLS estimates in Panel A of Table 2.

Given that we propose a novel approach for uncovering $1/\beta$, it is useful too to benchmark our estimated elasticity against what we obtain when we apply this panel IV procedure –

---

[28] As the VIIR-DNB commences in April 2012, the mean night lights values for 2012 are computed using fewer months of available data. This could introduce noise to these observations, but as these are only used in the first stage as part of the IV, the 2SLS coefficient in principle continues to yield an unbiased estimate of the elasticity ($1/\beta$).

[29] In lieu of computing Huber-White cluster-robust standard errors, we have obtained very comparable results via a province-block bootstrap procedure. For the Column 6 specification, the standard error implied from 500 bootstrap samples is 0.1683 (versus 0.1536 in Table 2); the corresponding block bootstrap standard error in the Column 13 specification for manufacturing employment is 0.1146 (versus 0.1242 in the table).

Table 2: GDP, Employment and Night Lights Intensity

Panel A.			Dep. Var.: $\ln(GDPpc_{jt})$				
	(1) OLS	(2) OLS	(3) OLS	(4) 2SLS	(5) 2SLS	(6) 2SLS	(7) 2SLS
$\ln(Light_{js})$	0.2238***	0.1955***	0.1563***	0.4104*	0.4667**	0.4698***	0.5534***
	(0.0601)	(0.0518)	(0.0343)	(0.2273)	(0.1821)	(0.1536)	(0.1935)
Observations	1,133	1,115	1,018	1,133	1,115	1,018	1,018
R-squared	0.9772	0.9839	0.9909	—	—	—	—
F-stat	—	—	—	54.43	41.18	29.80	28.48
Panel B.			Dep. Var.: $\ln(Emp_{jt})$				
	(8) OLS	(9) OLS	(10) OLS	(11) 2SLS	(12) 2SLS	(13) 2SLS	(14) 2SLS
$\ln(Light_{js})$	0.0895*	0.0748**	0.0820**	0.4704**	0.2708***	0.3021**	0.3014**
	(0.0523)	(0.0281)	(0.0355)	(0.1922)	(0.0918)	(0.1242)	(0.1182)
Observations	1,133	1,116	1,013	1,133	1,116	1,013	1,013
R-squared	0.9853	0.9926	0.9949	—	—	—	—
F-stat	—	—	—	54.43	48.44	47.58	67.37
Province×Year FE	Y	Y	Y	Y	Y	Y	Y
Prefecture FE	Y	Y	Y	Y	Y	Y	Y
Trimmed	N	Tail 1%	Tail 5%	N	Tail 1%	Tail 5%	Tail 5%
Weighted by population	N	N	N	N	N	N	Y

Notes: The dependent variables are log prefecture GDP per capita (Panel A) and log employment (Panel B) respectively. In each panel, Columns 1-3 report OLS regressions, while Columns 4-7 perform 2SLS regressions in which the lagged night lights variable, $\ln(Light_{j,s-1})$ is used as an IV. Columns 2 and 5 drop observations where the annual change in log prefecture GDP per capita (respectively, log employment) between years $t-1$ and t is below the 1st percentile or above the 99th percentile values of its distribution in that year. Columns 3, 6 and 7 further drop observations where the annual change in the dependent variable is below the 5th percentile or above the 95th percentile of its distribution in each given year. Column 7 weights the observations by initial prefecture population in 2015. Standard errors are clustered at the province level. *** p<0.01, ** p<0.05, * p<0.1.

based on the regression model in (7) – on a standard cross-country dataset. Table D.8 in the appendix provides this point of reference, using the dataset on DSMP-OLS night lights and GDP per capita for 1993-2010 from Pinkovskiy and Sala-i-Martin (2016). The 2SLS estimates of the inverse elasticity of night lights to income per capita range from 0.37 to 0.41, which is comparable with the values we have just reported for the Chinese prefecture-level data.

Turning to Panel B of Table 2, we run a parallel set of regressions focusing on prefectures' manufacturing sector employment as the outcome variable.[30] We obtain OLS estimates of the inverse elasticity of night lights to manufacturing employment that are in the neighborhood of 0.08 (Columns 8-10). These once again are biased downward relative to the 2SLS estimates in Columns 11-14, which range from 0.27 to 0.47. We will use the Column 13 estimate of 0.30 in what follows, particularly since the trimming of tail observations associated with large changes

---

[30]The employment data from the China City Statistical Yearbooks covers only workers with residency status (hukou). Information on non-hukou workers is reported in the population census, but these are available only every five years when a census or mini-census is conducted.

in manufacturing employment appears to moderate the influence of potential outliers on the magnitude of the elasticity.

4.3 Sizing Up the Effects on GDP per capita and Employment across Locations

We explore now the implications of the US tariffs for local economic outcomes within China. To fix ideas, consider first a one percentage point increase in a grid location's exposure to these tariffs on Chinese exports to the US. Our preferred estimate in Column 4 of Table 1 indicates that this reduces night lights intensity by 0.59 percent relative to other locations. Combining these with the inverse night lights elasticities obtained in the previous subsection, this translates to a decrease in income per capita of $0.59 \times 0.47 = 0.28\%$ and a fall in manufacturing employment of $0.59 \times 0.30 = 0.18\%$.

In practice, there was substantial skew across grids in the severity of exposure to the US tariffs, and the most negatively affected locations saw a cumulative tariff shock well in excess of one percentage point. To illustrate this, we sort mainland China's population into percentile bins in ascending order of the increase in $USTariff_i$ between Q4/2017-Q4/2019. The direct exposure of the median individual to the US tariffs is zero, and this remains relatively small even up to the 70th population percentile bin, which had a cumulative US tariff shock over the two-year period of 0.6 percentage points. On the other hand, the tail 2.5% of China's population in the most exposed grids experienced a US tariff shock of 9.1 percentage points. These latter grids are geographically spread out across China, with 203 prefectures having at least one grid cell in this right tail.

This dispersion in tariff exposure translates into highly heterogenous impacts on observed night lights, income per capita, and manufacturing employment. We compute these implied effects at various percentiles using the same tariff shock and night lights coefficients (0.59, 0.47, and 0.30) that were applied above; Figure 4 presents these together with 90% confidence intervals (based on Monte Carlo draws from the underlying distributions of the estimated coefficients). The implied effects at the 70th population-weighted percentile bin are -0.16% for GDP per capita and -0.10% for manufacturing employment. For the 97.5th percentile, the negative hit is much more sizeable at -2.52% for income per capita and -1.62% for manufacturing employment, holding all else constant. [31] These latter effects are economically meaningful, even bearing in mind that they are spread out over 24 months; as a point of reference, the annual growth rate of GDP per capita for China as a whole was 11.7% in 2017-2018 and 2.4% in

---

[31]The grid cells in the top 2.5 percentiles tend to be more developed. The average night light intensity in these grid cells is 1.97, compared to 0.41 in the other grids. We can sum up the night lights in China, and calculate the share of lights emanating from the top 2.5 percentile. It turns out the top grid contributes 2.68% of the total night lights in China.

Figure 4: Relative Effects of Export Tariff Shock
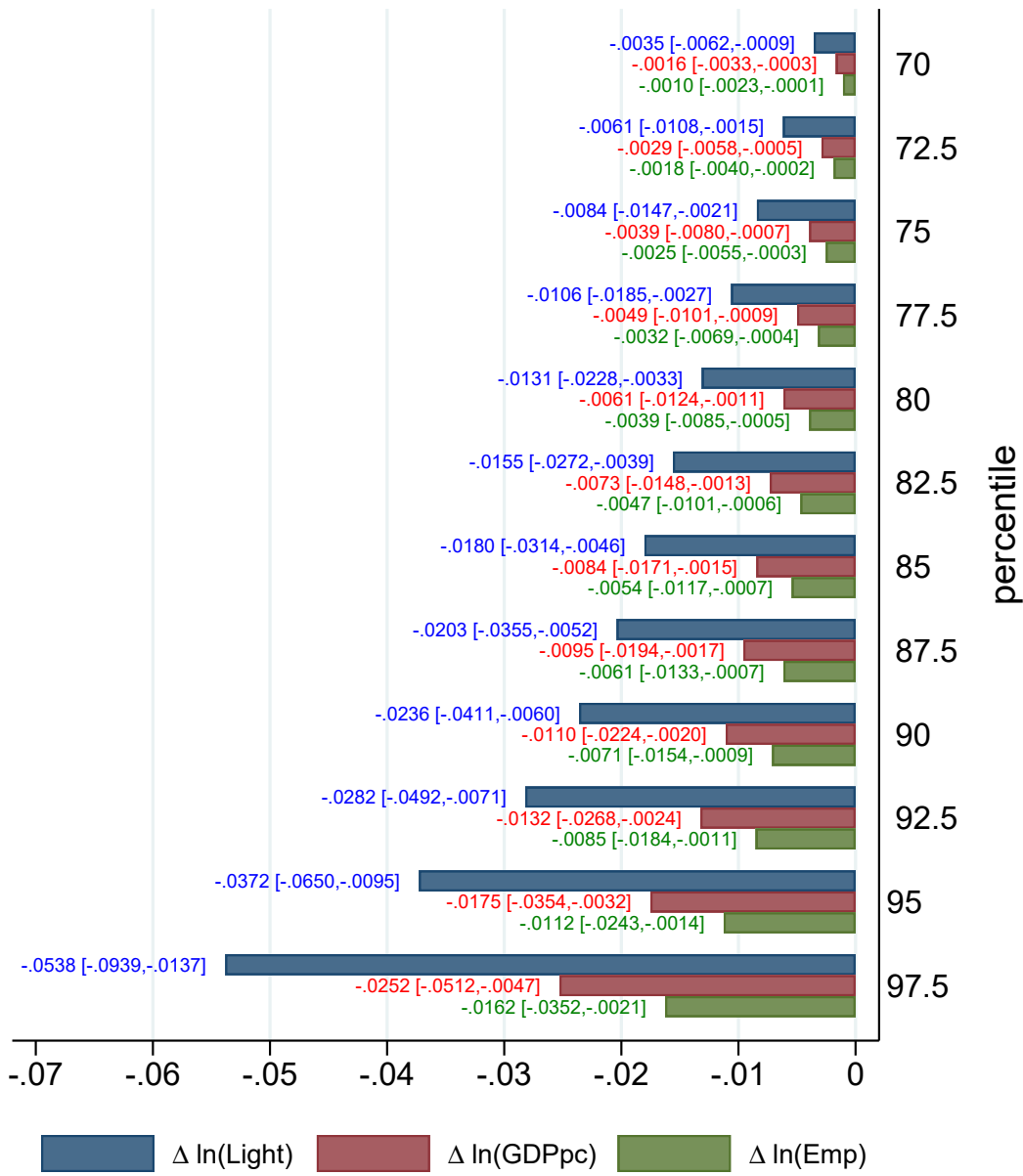
Notes: The vertical axis indicates grid-level percentiles of cumulative exposure to the US tariffs between Q4/2017 and Q4/2019; the percentiles are weighted by grid population, so that each successive percentile contains an equal share of total population. The figure illustrates the implied grid-level impact of the US tariffs on night lights, GDP per capita, and employment respectively, based on the methodology described in Section 4. Point estimates of each implied effect are reported. For night lights, the 90% confidence intervals reported are based on the distribution of the regression coefficient on the US grid-level tariff shock variable in Column 4 of Table 1; for GDP per capita (respectively, employment), the 90% confidence intervals are computed based on 10,000 sets of Monte Carlo draws from the distribution of the aforementioned US tariff shock coefficient and the distribution of the estimated elasticity between GDP per capita (respectively, employment) and night lights from Column 6 (respectively, Column 13) of Table 2.

2018-2019.[32]

4.4   Spillovers and Reallocation

The difference-in-differences nature of our regression models means that the implied impacts we have just computed should be interpreted as partial equilibrium effects. The fixed effects structure in (1) absorbs the average change across all grids in night lights that might be induced by the US-China tariff war, leaving us with variation that speaks to the differential impact when one location suffers a more severe shock relative to another. In addition, although the analysis at the granular grid cell level renders rich data variation and statistical power for identification, the geographic spillover effects of tariff shocks across grids may bias our difference-in-differences estimates. The sign of the bias is *a priori* ambiguous. On the one hand, the depressed labor demand in one grid cell may induce labor reallocation towards other grid cells which biases our estimate downward away from zero (i.e., overstates the full effect of the labor demand shock). This labor supply response could be mediated by commuting patterns across regions. On the other hand, the lowered income induced by tariff shocks in one grid cell may lower demand for goods from elsewhere through spatial input-output linkages, which biases our estimate upwards to zero.

To what extent can we make further inferences about the direction and magnitude of the full impact of the US tariffs, that takes into account these spatial spillovers and general equilibrium effects as well? We address this question via three approaches. First, based on the summary statistic approach in Monte et al. (2018), we explore the spillovers along linkages in commuting networks which reveal the spatial general equilibrium effect of the tariff shocks. Second, with the insights from Adão et al. (2020), we capture the spatial equilibrium linkages by including various measures of non-local tariff shocks into the regression model. Third, we aggregate the data and carry out the analysis at the prefecture level, which relates our findings more directly to the "local labor market approach" (Campante et al., 2019). It may also reveal the general equilibrium effect operating at the prefecture level.[33]

4.4.1   Spillovers Across Grid Cells: Commuting Flows

As is shown in Monte et al. (2018), the general equilibrium elasticity of local employment to a labor demand shock is heterogeneous depending on the commuting flows across locations. Since our baseline analysis focuses on the outcomes across granular grid cells, trade shocks may easily

---

[32]Based on GDP per capita in local currency units, from the World Bank.

[33]Relatedly, in Table D.3, we consider an alternative specification that replaces prefecture-by-year-quarter fixed effects with province-year-quarter fixed effects, which lessens the concern that the baseline findings are severely biased by spatial spillovers across geographically nearby grid cells within prefectures.

propagate across the boundaries through commuting flows.[34,35] To account for such spillovers, we adopt the approach suggested by Monte et al. (2018). Specifically, their quantitative spatial model highlights that initial commuting openness can be included in reduced-form regressions as a summary statistic to back out the heterogeneous GE employment elasticities that embeds the cross-boundary spillover effects. Intuitively, the employment responses are larger in locations with a larger commuting openness.

The measure of commuting openness comes from a 10% subsample of the *1% Population Sampling Survey of China* (mini census) in 2015. The mini census contains information on residence-workplace commuting patterns within or across county boundaries for workers residing in prefectures with urban districts.[36] As with Monte et al. (2018), we calculate for each county the share of residents that work locally (λ_{cc}^R), and the commuting openness is defined accordingly as $1 - \lambda_{cc}^R$. As a robustness check, we also proxy for the commuting openness by $1 - \lambda_{cc}^L$, where λ_{cc}^L is the share of workers that reside locally. We assign to each grid the commuting openness of the county that it locates in, and then rank the grids based on the measure to alleviate the potential measurement error.

Table 3 reports the results for the heterogeneity analysis. Column 1 re-estimates the baseline regression but restricts the sample to grids with information on commuting openness (i.e., grids within prefectures with urban districts). Column 2 finds larger decreases in night light intensity in response to the US tariff shock in grid cells with commuting openness ($1 - \lambda_{cc}^R$) above the median. Columns 3 repeats the analysis but uses $1 - \lambda_{cc}^L$ as a proxy for openness to commuting, and obtains consistent findings. A potential concern is that the responses of local economic activities to tariff shocks could vary with other location characteristics which are correlated with initial commuting openness, and hence the interaction effects detected in Columns 2 and 3 could be spurious. To mitigate this concern, in Columns 4 and 5, we include interaction terms of $\Delta USTariff_{i,t-1}$ (respectively, $\Delta CHNInputTariff_{i,t-1}$) with characteristics of the county in which the grid cell locates and those of neighboring countries within 100km. Following Monte et al. (2018), the set of location characteristics includes log employment, log land area and share of population with high school education or above. (All these variables are demeaned.) The estimated differential effects along the dimension of initial commuting openness change little to the inclusion of these additional controls.

---

[34]The median and average one-way residence-workplace-commuting distance is 3.3 km and 7.1 km, respectively. We calculate these statistics based on the information on commuting time and commuting modes from the *1% Population Sampling Survey of China* in 2015.

[35]For the prefecture-level analysis reported in Section 4.4.3, the cross-boundary spillovers are unlikely to be driven by commuting flows given that the share of workers commuting across prefecture boundary is close to zero.

[36]92% of the observations in the 2015 mini census reside in prefectures with urban districts. These prefectures may comprise of urban districts, rural counties and county-level cities.

Table 3: Spillovers Aross Grid Cells by Commuting Openness, 2SLS

Dep. Var.: $\Delta \ln(Light_{it})$ Measure of Commuting Openness:	(1)	(2) $1 - \lambda^R_{cc\|c}$	(3) $1 - \lambda^L_{cc\|c}$	(4) $1 - \lambda^R_{cc\|c}$	(5) $1 - \lambda^L_{cc\|c}$
$\Delta USTariff_{i,t-1}$	-0.6320**				
	(0.2709)				
$\Delta USTariff_{i,t-1} \times$:					
Commuting Openness$_c$: above median		-0.7580***	-0.7606**	-0.7632*	-0.7723*
		(0.2698)	(0.2801)	(0.3814)	(0.4073)
Commuting Openness$_c$: below median		-0.1094	-0.2016	-0.1007	-0.1392
		(0.3685)	(0.3033)	(0.3994)	(0.3116)
$\Delta CHNInputTariff_{i,t-1}$	0.4071				
	(0.5401)				
$\Delta CHNInputTariff_{i,t-1} \times$:					
Commuting Openness$_c$: above median		0.5111	0.7876	0.4616	0.8543
		(0.4846)	(0.4866)	(0.5736)	(0.6077)
Commuting Openness$_c$: below median		-0.1491	-0.9812	-0.5975	-1.4617
		(1.6032)	(1.0468)	(1.7425)	(1.1516)
Grid FE	Y	Y	Y	Y	Y
Prefecture×Year-Quarter FE	Y	Y	Y	Y	Y
Grid W_{i0}×Year-Quarter FE	Y	Y	Y	Y	Y
Location Characteristics×Tariff Shocks	N	N	N	Y	Y
Observations	343,222	343,222	343,222	343,222	343,222
F-stat	27.18	16.80	14.05	3.697	2.288

Notes: All columns report 2SLS estimates, using the respective Amap grid-level and nonlocal tariff shocks as instrumental variables for the corresponding Google Maps grid-level and nonlocal tariff shocks. The initial grid characteristics, W_{i0}, whose time-varying effects are included in all columns are: the US share in exports, the US share in imports of intermediates, log exports per capita, log intermediate imports per capita, and log 2016 mean night lights intensity; grid-level exports and imports geolocated via Amap are used to construct the first four of these W_{i0} variables. Columns (3) and (4) further control for (demeaned) characteristics of the local county and the neighboring counties (within 100km) interacted respectively with $\Delta USTariff_{i,t-1}$ and $\Delta USTariff_{i,t-1}$, including log county employment, log land area, and share of population with high school education or above. All regressions are weighted by grid population in 2015, with a minimum population of 1 imputed for cells with zero population in the raw data. Standard errors are clustered at the province level. *** p<0.01, ** p<0.05, * p<0.1.

4.4.2 Effects of Non-local Tariff Shocks

To account for spatial spillovers via spatial input-output linkages and migration, we take guidance from the quantitative spatial model developed by Adão et al. (2020). In their framework, locations are linked both through trade flows and labor mobility. Under fairly minimal parametric assumptions, they derive a model-implied expression that traces out how external trade shocks affect local economic outcomes; this comprises a partial equilibrium effect – capturing the differential impact of a location's own exposure to the trade shock – and a general equilibrium effect – reflecting the overall impact of the shock. The empirical implementation in Adão et al. (2020) then proceeds to capture the full effect of the trade shock through a specification

that includes: (i) a Bartik variable to capture a location's own-exposure, arising from the initial sectoral composition of its trade-exposed activities (as in Autor et al., 2013), and (ii) a novel nonlocal exposure term, that is a weighted average of the Bartik variables across all other locations. Standard economic intuition would suggest that the nonlocal exposure effects in (ii) could run in either direction: A negative US tariff shock in neighboring locations could depress demand for firms in a given grid, if the neighboring firms tend to be downstream buyers of inputs produced by local firms. On the other hand, if the neighboring firms tend instead to be upstream suppliers, then the US tariffs on their exports could end up lowering input prices to the benefit of domestic firms. The net effect of nonlocal exposure thus ultimately needs to be pinned down empirically. The estimates obtained from regressions of the form just described can then inform whether indirect effects through spatial general equilibrium responses reinforce (or not) the impact of local exposure to tariff shocks.

In our empirical setting, we are unable to implement the full structural approach in Adão et al. (2020), given the absence of data on cross-location trade and labor flows at the granular grid level. That said, we can nevertheless run regressions of the form they recommend, that would speak in principle to the full effect of the US tariff shocks when interpreted through the lens of their model. To do so, we augment the regression model in (1) as follows:

$$
\begin{aligned}
\Delta \ln(Light_{it}) \quad = \quad & \pi_1 \Delta USTariff_{i,t-1} + \pi_2 \Delta CHNInputTariff_{i,t-1} \\
& + \rho_1 \Delta NonLocalUSTariff_{i,t-1} + \rho_2 \Delta NonLocalCHNInputTariff_{i,t-1} \\
& + D_{pt} + D_i + W_{i0} \times D_t + u_{it},
\end{aligned}
\tag{8}
$$

where the nonlocal US and China input tariff shocks seek to account for general equilibrium forces. In particular, the signs of ρ_1 and ρ_2 will be informative of whether these forces reinforce or offset the direct effect of a location's own exposure to the tariff war.

We have worked with several potential specifications for capturing the nonlocal tariff shock terms (see Appendix D.3 for details on the construction of these variables). In Table D.9, we include population weighted-average tariff shocks in grid cells that are located within rings that are of increasing distance from a grid location (specifically, <15km, 15-30km, 30-50km, 50-100km). Whenever statistically significant, these spatial spillover effects from either the US tariffs or the China input tariffs have a negative sign. In Table D.10, we further aggregate these neighboring ring tariff shocks with weights that reflect both the local population size and bilateral distance, as would be implied by a standard gravity model (following in particular Adão et al., 2020). This yields a negative and significant estimate of the nonlocal impact of the US tariff shock within 100km, though this effect is sensitive to whether or not we control for grid-specific time trends. One drawback of this last approach is that it considers only spillovers within a given radius. We have therefore also experimented with an alternative construction in

which we compute the tariff shocks at the prefecture level, and then take a distance-adjusted weighted-average of all prefecture tariff shocks for each grid location. We once again obtain negative coefficient estimates for the nonlocal US tariff shock as proxied in this manner, though none of these effects is statistically significant. Importantly, across all of Tables D.9 and D.10, controlling for the role of nonlocal tariff shocks does not affect the stability of the negative effect we have already seen in a location's own direct exposure to the US tariffs. The evidence on the nonlocal tariff shocks moreover points us toward the conclusion that general equilibrium forces are likely pushing in the same direction of reducing observed night lights. This suggests that the implied effects that we have recovered in Figure 4 are likely lower bounds on the full negative impact of the tariff shocks on the Chinese economy.

4.4.3 Prefecture-Level Analysis

In Table 4, we carry out a prefecture-level analysis.[37] The measurements are analogous to equations (2) and (3) and the regression specification is parallel to equation (1). The difference is that in the China customs data, we directly observe firms' locations at the prefecture level, and hence the tariff shocks to prefecture j, $\Delta USTariff_{j,t-1}$ and $\Delta CHNInputTariff_{j,t-1}$, are not subject to the measurement errors as the corresponding grid-level measures. Throughout the prefecture-level analysis, we adopt the OLS regression model. The standard errors are clustered at the province level. Again, the identification stems from the exogeneity of initial export and import shares at the prefecture-level conditional on prefecture fixed effects, province-by-year-quarter fixed effects, and time-varying effects of initial prefecture characteristics ($W_{j0} \times D_t$). Here, the vector W_{j0} includes prefecture-level controls including: the US share in exports, the US share in imports of intermediates, log exports per capita, log intermediate imports per capita, and log 2016 mean night lights intensity. We winsorize the $\Delta \ln(Light_{it})$ observations that are above the 97.5th percentile or below the 2.5th percentile within each period t to reduce the influence of outliers.

Column 1 finds that the estimated coefficient for the US tariff shock has a larger magnitude but is statistically similar to that obtained from the corresponding grid-level specification (-0.77 v.s. -0.59). As is expected, given the noise contained in the measure of night lights growth, the prefecture-level analysis has a weaker statistical power due to a smaller sample size, and hence the estimates are less precise. Again, the estimate for the input tariff shock is statistically insignificant. The similarity in the prefecture- and grid-level findings alleviates the concern that the difference-in-differences estimates obtained from the grid-level analysis might overstate the impacts of the tariff shocks if it reflects both the negative effect in the high-exposure grid cells and positive spillovers to the low-exposure grid cells. Column 2 includes

---

[37]In Appendix D.4, we present the county-level evidence. The results are similar.

neighboring-prefecture weighted-average measure of tariff shocks, while Column 3 accounts for inverse-distance weighted average of tariff shocks across all non-local prefectures. The results indicate that the local US tariff shock remains important for explaining the night lights growth in prefecture j itself, even when we account for spillovers from non-local economies.

Table 4: Tariff Shocks and Night Lights Intensity: Prefecture-Level Analyses

| | | Measure of Non-local Shocks | |
| | | Neighbors | Dist. Wtg. |
Dep. Var.: $\Delta \ln(Light_{jt})$	(1)	(2)	(3)
$\Delta USTariff_{j,t-1}$	-0.7664*	-0.8773*	-0.7899*
	(0.4271)	(0.4717)	(0.4294)
$\Delta CHNInputTariff_{j,t-1}$	0.0012	0.0887	0.0500
	(0.3055)	(0.3469)	(0.3340)
Non-local $\Delta USTariff_{j,t-1}$		-2.0048*	0.3023
		(0.9754)	(0.4742)
Non-local $\Delta CHNInputTariff_{j,t-1}$		1.1408	1.0027
		(0.7720)	(0.9158)
Prefecture FE	Y	Y	Y
Province FE	Y	Y	Y
$W_{j0} \times$ Year-Quarter FE	Y	Y	Y
Observations	2,259	2,259	2,259
R-squared	0.6366	0.6383	0.6372

Notes: All columns report the OLS estimation results for the prefecture-level analysis. The initial prefecture characteristics, W_{j0}, whose time-varying effects are included across all regressions are: the US share in exports, the US share in imports of intermediates, log exports per capita, log intermediate imports per capita, and log 2016 mean night lights intensity. Prefecture-level exports and imports are inferred directly from the geolocation information available in the customs data, which are employed to construct the first four of these W_{i0} variables. All regressions are weighted by prefecture population in 2010. Standard errors are clustered at the province level. *** p<0.01, ** p<0.05, * p<0.1.

5 Conclusion

We present evidence that the US-China tariff war had an adverse impact on China's economy. We circumvent constraints on the availability and reliability of official data by using satellite readings on night-time luminosity, drawing on a recent body of work that has used such measures to infer economic performance. The granularity of the satellite readings allows us to work with grid locations as our unit of analysis. We combine this with customs-level information on the

initial profile of Chinese firms' exports and imports, together with geo-located firm coordinates, to implement a Bartik identification strategy that uncovers the local impact of the tariffs. Our central finding is that night-time luminosity was dimmer in grids that were more exposed to the US tariffs on Chinese exports, implying worse income per capita and manufacturing employment outcomes in these locations. These effects were particularly concentrated on the 30% of China's population in the most tariff-exposed grids. By contrast, the retaliatory tariffs enacted by China on imports from the US did not exhibit a significant effect.

Our findings contribute towards a better understanding and quantitative assessment of the impact of the tariff war on China's economy. The effects we have identified speak to the usefulness of satellite data for uncovering shifts in economic activity in data-scarce polities such as China. We view this as a useful first step, and would welcome future work that seeks to validate these findings using direct regional or even firm-level data, as and when these might become available for the tariff war and Covid-19 pandemic periods. Moreover, it remains an open question to assess what the full long-term impact of the tariff war will be, bearing in mind that the increase in business uncertainty induced by the tariffs has likely led Chinese firms to hold back on investment in production capacity (Altig et al., 2018).

References

Adão, Rodrigo, Michal Kolesàr, and Eduardo Morales. 2019. "Shift-Share Design: Theory and Inference." *Quarterly Journal of Economics*, 134(4): 1949-2010.

Adão, Rodrigo, Costas Arkolakis, and Federico Esposito. 2020. "General Equilibrium Effects in Space: Theory and Measurement." NBER Working Paper.

Ahn, JaeBin, Amit K. Khandelwal, and Shang-Jin Wei. 2011. "The Role of Intermediaries in Facilitating Trade." *Journal of International Economics*, 84(1): 73-85.

Altig, David, Nick Bloom, Steven J. Davis, Brent Meyer, and Nick Parker. 2018. "Are Tariff Worries Cutting Into Business Investment?" Federal Reserve of Atlanta Blog.

Amiti, Mary, and Jozef Konings. 2007. "Trade Liberalization, Intermediate Inputs, and Productivity: Evidence from Indonesia." *American Economic Review*, 97(5): 1611-1638.

Amiti, Mary, Stephen J. Redding, and David Weinstein. 2019. "The Impact of the 2018 Trade War on U.S. Prices and Welfare." *Journal of Economic Perspectives*, 33(4): 187-210.

Amiti, Mary, Sang Hoon Kong, and David Weinstein. 2020. "The Effect of the U.S.–China Trade War on U.S. Investment." NBER Working Paper.

Angrist, Joshua D. and Jörn-Steffen Pischke. 2009. 'Mostly Harmless Econometrics." Princeton, New Jersey: Princeton University Press.

Autor, David, David Dorn, and Gordon Hanson. 2013. "The China Syndrome: Local Labor effects of Import Competition in the United States." *American Economic Review*, 103(6): 2121-2168.

Benguria, Felipe, and Felipe Saffie. 2020. "The Impact of the 2018-2019 Trade War on U.S. Local Labor Markets." Mimeo.

Benguria, Felipe, Jaerim Choi, Deborah L. Swenson, and Mingzhi Xu. 2022. "Anxiety or Pain? The Impact of Tariffs and Uncertainty on Chinese Firms in the Trade War." *Journal of International Economics*, 137: 103608.

Bown, Chad P., Euijin Jung, and Eva Zhang. 2019. "Trump Has Gotten China to Lower Its Tariffs. Just Toward Everyone Else." Peterson Institute for International Economics.

Bown, Chad P. 2021. "The US–China Trade War and Phase One Agreement." Peterson Institute for International Economics, Working Paper 21-2.

Bown, Chad P., and Melina Kolb. 2021. "Trump's Trade War Timeline: An Up-to-Date Guide." Peterson Institute for International Economics.

Blanchard, Emily J., Chad P. Bown, and Davin Chor. 2019. "Did Trump's Trade War Impact the 2018 Election?" NBER Working Paper.

Bleakley, Hoyt, and Jeffrey Lin. 2012. "Portage and Path Dependence." *Quarterly Journal of Economics*, 127(2): 587-644.

Bluhm, Richard, and Melanie Krause. 2022. 'Top Lights: Bright Cities and Their Contribution to Economic Development." *Journal of Development Economics*, 157: 102880.

Borusyak, Kirill, Peter Hull, and Xavier Jaravel. 2022. "Quasi-Experimental Shift-Share Research Designs." *Review of Economic Studies*, 89(1): 181-213.

Brandt, Loren, and Peter M. Morrow. 2017. "Tariffs and the Organization of Trade in China." *Journal of International Economics*, 104: 85-103.

Brandt, Loren, Johannes Van Biesebbroeck, Luhang Wang, and Yifan Zhang. 2017. "WTO Accession and Performance of Chinese Manufacturing Firms." *American Economic Review*, 107(9): 2784-2820.

Caliendo, Lorenzo, and Fernando Parro. 2015. "Estimates of the Trade and Welfare Effects of NAFTA." *Review of Economic Studies*, 82(1): 1-44.

Campante, Filipe R., Davin Chor, and Bingjing Li. 2019. "The Political Economy Consequences of China's Export Slowdown." NBER Working Paper.

Cavallo, Alberto, Gita Gopinath, Brent Neiman, and Jenny Tang. 2021. "Tariff Pass-Through at the Border and at the Store: Evidence from US Trade Policy." *American Economic Review: Insights*, 3(1): 19-34.

Chen, Wei, Xilu Chen, Chang-Tai Hsieh, and Zheng Song. 2019. "A Forensic Examination of China's National Accounts." *Brookings Papers on Economic Activity*, 2019(1): 77-141.

Chen, Xi, and William D. Nordhaus. 2012. "Using Luminosity Data as a Proxy for Economic Statistics." *Proceedings of the National Academic of Sciences*, 108(21): 8589-8594.

Chen, Tuo, Chang-Tai Hsieh, and Zheng (Michael) Song. 2022. "Non-Tariff Trade Barriers in the U.S.-China Trade War." NBER Working Paper No. 30318.

Chodorow-Reich, Gabriel, Gita Gopinath, Prachi Mishra, and Abhinav Narayanan. 2019. "Cash and the Economy: Evidence from India's Demonetization." *Quarterly Journal of Economics*, 135(1): 57-103.

Cui, Chuantao, and Leona Shao-Zhi Li. 2021. "The Effect of the US-China Trade War on

Chinese New Firm Entry." *Economic Letters*, 203: 109846.

de Chaisemartin, Clément, and Xavier D'Haultfoeuille. 2020. "Two-Way Fixed Effects Estimators with Heterogeneous Treatment Effects." *American Economics Review*, 110(9): 2964-2996.

Donaldson, Dave, and Adam Storeygard. 2016. "The View from Above: Applications of Satellite Data in Economics." *Journal of Economic Perspective*, 30(4): 171-198.

Fajgelbaum, Pablo D., Pinelopi K. Goldberg, Patrick J. Kennedy, and Amit K. Khandelwal. 2020. "The Return to Protectionism." *Quarterly Journal of Economics*, 135(1): 1-55.

Fajgelbaum, Pablo D., and Amit K. Khandelwal. 2021. "The Economic Impacts of the US-China Trade War." *Annual Review of Economics*, Forthcoming.

Ferraro, John K., and Eva Van Leemput. 2019. "Long-Run Effects of Chinese GDP from U.S.-China Tariff Hikes." FEDS Notes. Washington: Board of Governors of the Federal Reserve System, July 15, 2019, https://doi.org/10.17016/2380-7172.2382.

Fetzer, Thiemo, and Carlo Schwarz. 2021. "Tariffs and Politics: Evidence from Trump's Trade Wars." *Economy Journal* 131(636): 1717-1741.

Flaaen, Aaron, Ali Hortaçsu, and Felix Tintelnot. 2019. "The Production, Relocation, and Price Effects of US Trade Policy: The Case of Washing Machines." *American Economic Review*, 110(7): 2103-2127.

Flaaen, Aaron, and Justin Pierce. 2019. "Disentangling the Effects of the 2018-2019 Tariffs on a Globally Connected U.S. Manufacturing Sector." Working Paper.

Garred, Jason. 2018. "The Persistence of Trade Policy in China after WTO Accession." *Journal of International Economics* 144: 130-142.

Goldsmith-Pinkham, Paul, Isaac Sorkin, and Henry Swift. 2020. "Bartik Instruments: What, When, Why, and How." *American Economic Review* 110(8): 2586-2624.

Goswami, Sanjana. 2020. "Employment Consequences of the U.S. Trade Wars." Mimeo.

Gourdon, Julien, Laura Hering, Stephanie Monjon, and Sandra Poncet. 2021. "Estimating the Repercussions from China's Export VAT Rebate Policy." *Scandinavian Journal of Economics*, forthcoming.

Grossman, Gene M., and Elhanan Helpman. 2020. "When Tariffs Disturb Global Supply Chains." NBER Working Paper No. 27722.

Handley, Kyle, Fariha Kamal, and Ryan Monarch. 2020. "Rising Import Tariffs, Falling Export Growth: When Modern Supply Chains Meet Old-Style Protectionism." NBER Working Paper.

He, Chuan, Kasten Mau, and Mingzhi Xu. 2021. "Trade Shocks and Firms Hiring Decisions: Evidence from Vacancy Postings of Chinese Firms in the Trade War." *Labour Economics* 71: Article 102021.

Henderson, J. Vernon, Adam Storeygard, and David N. Weil. 2012. "Measuring Economic Growth from Outer Space." *American Economic Review*, 102(2): 994-1028.

Henderson, J. Vernon, Tim Squires, Adam Storeygard, and David N. Weil. 2017. "The Global Distribution of Economic Activity: Nature, History, and the Role of Trade." *Quarterly Journal of Economics*, 133(1): 357-406.

Hodler, Roland, and Paul A. Raschky. 2014. "Regional Favoritism." *Quarterly Journal of Economics*, 129(2): 995-1033.

Hu, Yingyao, and Jiaxiong Yao. 2022. "Illuminating Economic Growth." *Journal of Econometrics*, 228(2): 359-378.

Huang, Yi, Chen Lin, Sibo Liu, and Heiwai Tang. 2022. "Trade Networks and Firm Value: Evidence from the US-China Trade War." Working Paper.

Jiang, Lingduo, Yi Lu, Hong Song, and Guofeng Zhang. 2022. "Responses of Exporters to Trade Protectionism: Inference from the U.S.-China Trade War." *Journal of International Economics*, forthcoming.

Jiao, Yang, Zhikuo Liu, Zhiwei Tian, and Xiaxin Wang. 2022. "The Impacts of the U.S. Trade War on Chinese Exporters." *Review of Economics and Statistics*, forthcoming.

Ju, Jiandong, Hong Ma, Zi Wang, and Xiaodong Zhu. 2020. "Trade Wars and Industrial Policy along the Global Value Chains." Working Paper.

Liao, Steven, In Song Kim, Sayumi Miyano, and Hao Zhang. 2020. concordance: Product Concordance. R package version 2.0.0. https://CRAN.R-project.org/package=concordance.

Michalopoulos, Stelios, and Elias Papaioannou. 2013. "National Institutions and Subnational Development in Africa." *Quarterly Journal of Economics*, 129(1): 151-213.

Mills, Stephen, Stephanie Weiss, and Calvin Liang. 2013. "VIIRS Day/Night Band (DNB) Stray Light Characterization and Correction." *SPIE Proceedings*, 8866.

Monte, Ferdinando, Stephen J. Redding, and Esteban Rossi-Hansberg. 2018. "Commuting, Migration, and Local Employment Elasticities." *American Economic Review*, 108(12): 3855-3890.

Nakamura, Emi, Jon Steinsson, and Miao Liu. 2016. "Are Chinese Growth and Inflation Too Smooth? Evidence from Engel Curves" *American Economic Journal: Macroeconomics*, 8(3): 113-144.

New York Times. 2019. "China's Economic Growth Slows as Challenges Mount." 17 Oct 2019.

Pinkovskiy, Maxim, and Xavier Sala-i-Martin. 2016. "Lights, Camera ... Income! Illuminating the National Accounts-Household Surveys Debate." *Quarterly Journal of Economics*, 131(2): 579-631.

Rauch, James E. 1999. "Networks versus Markets in International Trade." *Journal of International Economics*, 48(1): 7-35.

Storeygard, Adam. 2016. "Farther on down the Road: Transport Costs, Trade and Urban Growth in Sub-Saharan Africa." *Review of Economic Studies*, 83(3): 1263-1295.

Tian, Wei, Miaojie Yu, and Chunru Zheng. 2022. "China-US Trade Protectionism: The Role of China's Retaliatory Tariffs." CCER Working Paper.

Wong, Dorcas, and Alexander Chipman Koty. 2019. "The US-China Trade War: A Timeline."

Waugh, Michael E.. 2019. "The Consumption Response to Trade Shocks: Evidence from the US-China Trade War." NBER Working Paper.

World Bank. 2017. "Growth Out of the Blue." *South Asia Economic Focus*.

Zhou, Yang. 2020. "The US-China Trade War and Global Value Chains." Mimeo.

Appendix

A The US-China Tariff War and Stylized Facts

In this Appendix, we provide a brief overview and description of the major tariff actions that occurred between the US and China, as the tariff war between the two countries unfolded.[38]

We describe first the tariffs that were initiated by the US, as documented too in Table A.1 below. In early February 2018, the Trump administration invoked Section 201 import protection to place a 28 percent safeguard tariff on solar panels and a 20 percent tariff on washing machines. This was followed by a second set of tariffs in mid-March 2018; a 25 percent tariff on steel imports and a 10 percent tariff on aluminum imports were introduced, under Section 232 of the US Trade Expansion Act of 1962 on national security grounds. These first two sets of tariff actions were not targeted solely at China, and only 0.3% of China's exports (by value in 2017) was directly affected.

The major US tariff actions focused specifically on China commenced in early July 2018, under Section 301 of the Trade Act of 1974 on the grounds of responding to unfair trade practices. List 1 of these Section 301 tariffs targeted $34 billion of US imports from China. This was followed by a List 2 in late August 2018, levied on an additional $16 billion of imports from China. The July-August 2018 actions raised tariff rates by 25 percent, covering around 3% of China's exports. The tariff action with the largest scope occurred in late September 2018, when the List 3 tariffs targeted $200 billion of imports from China, at a tariff rate of 10 percent. This vastly expanded the set of HS 6-digit products covered by US tariffs, while significantly raising the share by value of China's exports that was affected to around 10%. In June 2019, the List 3 tariffs were increased to 25 percent. A further escalation of the tariff war took place in early September 2019: a List 4 of Section 301 tariffs was enacted, with an additional 15 percent tariff on a host of Chinese products valued at $112 billion. The cumulative share of HS6 products and the cumulative share of China's dollar value exports now under US tariff hikes surged to 93.0% and 14.2%, respectively. Comparing the last two columns of Table A.1, a noteworthy feature of the US tariffs was that these fell predominantly on intermediate inputs and capital goods, rather than on consumption goods.

Each round of US tariff increases provoked retaliatory tariff actions from China, as reported in Table A.2. Following the Section 232 tariffs, China raised tariffs on US aluminum waste and several agricultural products in early April 2018, with tariff rates ranging from 15 to 25 percent. When the US enacted the List 1 and List 2 Section 301 tariffs, China retaliated by placing tariffs on an equivalent dollar value of Chinese imports from the US. The counter-actions by China were not as large in scale relative to the corresponding US actions in the subsequent tariff waves. The retaliation against the List 3 Section 301 tariffs covered $60 billion of China's imports from

---

[38]See Wong and Koty (2019) and Bown and Kolb (2021) for up-to-date resources that track the detailed timeline of events for the US-China tariff war.

the US, at rates ranging from 5 to 10 percent. When the US increased its List 3 tariff rates in June 2019, China followed up by raising over half of its List 3 retaliatory tariff rates. In response to the List 4 Section 301 tariffs, China imposed additional tariffs ranging between 5 to 10 percent on $75 billion of imports from the US. By September 2019, the cumulative share of HS6 products and the cumulative share of the 2017 dollar value of China's total imports that were affected by the retaliatory tariffs amounted to 84.3% and 5.6%, respectively.

Two qualifying remarks are in order. First, as mentioned briefly in Section 2, both the US and Chinese authorities granted tariff exemptions on a case-by-case basis to a subset of products after each round of tariff announcements. Second, though this falls outside the core sample period of our analysis, the Phase 1 trade deal signed between the US and China on January 2020 brought a halt to the pattern of tariff escalation. As part of this agreement, the US reduced its List 4 Section 301 tariffs by a half on 14 February 2020, and China reciprocated with reductions in retaliatory tariffs on the same day. We have incorporated the information on tariff exemptions, as listed in Bown (2021), into the summary statistics on tariff coverage reported in Tables A.1 and A.2. Likewise, when our analysis explores the extended period up till end-2020, this takes into account any tariff cuts reported by Bown (2021), including those negotiated under the Phase 1 deal. As of the end of 2019, tariff exemptions or reductions had been granted by the US on 7.9% of HS6 product codes (that accounted for 4.9% of the 2017 dollar value of China's exports); similarly, China had granted exemptions/reductions to 0.9% of HS6 codes (that covered 1.0% of the 2017 value of China's imports). The reach of these tariff exemptions/reductions was even more extensive by the end of 2020, as these now covered 31.9% (respectively, 25.9%) of HS6 codes, that accounted for 9.0% of China's 2017 export value (3.6% of China's 2017 import value).

Last but not least, we also keep track of China's declining MFN tariff rates during 2018-2019, as presented in Table A.3. This information is extracted from the China General Administration of Customs, specifically: (i) its "baseline" MFN tariff schedule, released on January each year; and (ii) periodic revisions released throughout the calendar year.[39] On the latter, MFN tariff cuts on high-tech goods are routinely announced and implemented on 1 July each year; there have also been periodic reductions in MFN tariffs on consumer goods. In 2018, China's MFN tariff cuts became more frequent, and extended to a broader range of products including pharmaceutical, auto-related and industrial goods. By July 2019, the cumulative share of HS6 product codes that had received an MFN tariff cut relative to their early-2017 levels reached 42.1% (or 35.6% by value of China's imports).

Figure A.1 illustrates the above tariff changes as these unfolded over time, respectively for the US tariffs on imports from China (panels a.1 and a.2), for the Chinese tariffs on imports from the US (panels b.1 and b.2), and China's MFN tariffs (panels c.1 and c.2). The latter two sets of tariff changes are illustrated for products classified as intermediates and capital goods

---

[39]In recent years, China has amended MFN tariffs on some products that it designates as interim or temporary rates (Bown et al., 2019). These tariffs typically apply for one year or until they are revoked, and are reported in the "baseline" tariff schedules released in January of each year.

under the UN Broad Economic Categories (BEC), Revision 5, since our baseline measure of the China tariffs focuses on these tariffs levied on inputs. Panels a.1-b.2 reinforce how pervasive and extensive the US-China tariffs became in terms of the share of products that were affected, especially after September 2018 (List 3 of the Section 301 tariffs). Panels c.1-c.2 highlight the non-trivial adjustments to China's MFN tariffs made by the customs authorities, particularly in supplementary lists released in July 2018 and November 2018.

Table A.1: US Tariff Actions, February 7, 2018 – September 1, 2019

Effective Dates	Description of US Tariff Increase	Cumulative Share of HS 6-digit Products	Cumulative 2017 Export Share	
			All Products	Intermediate and Capital goods
February 7, 2018	Section 201 tariffs on solar panels	0.14%	0.09%	0.08%
	Section 201 tariffs on washing machines			
March 23, 2018	Section 232 tariffs on steel	3.80%	0.25%	0.24%
	Section 232 tariffs on aluminum			
July 6, 2018	Section 301 List 1	14.38%	2.92%	2.80%
August 23, 2018	Section 301 List 2	17.48%	3.25%	3.13%
September 24, 2018	Section 301 List 3	72.63%	10.02%	8.79%
June 1, 2019	Additional 15% tariff on Section 301 List 3	72.30%	9.97%	8.74%
September 1, 2019	Section 301 List 4A	93.02%	14.20%	9.99%

Notes: From Bown (2021). The third column reports the cumulative share of HS6 products covered after each set of US tariff actions. The remaining columns report the cumulative share of China's exports subject to US tariff increases, for all products (fourth column) and intermediate and capital goods (fifth column); these are expressed as a share of China's total exports to the world in 2017 (from UN Comtrade).

Table A.2: China's Retaliatory Tariff Actions, April 2, 2018 – September 1, 2019

Effective Dates	Description of China's Tariff Increase	Cumulative Share of HS 6-digit Products	Cumulative 2017 Import Share	
			All Products	Intermediate and Capital goods
April 2, 2018	Retaliation to US Section 232 tariffs	1.71%	0.16%	0.05%
July 6, 2018	Retaliation to US Section 301 List 1	7.20%	1.96%	1.77%
August 23, 2018	Retaliation to US Section 301 List 2	10.38%	2.75%	2.54%
September 24, 2018	Retaliation to US Section 301 List 3	80.38%	6.10%	5.70%
January 1, 2019	Suspension of retaliatory tariffs on auto and parts	79.86%	5.31%	4.91%
June 1, 2019	Increase in retaliatory tariffs on some products	79.86%	5.31%	4.91%
September 1, 2019	Retaliation to US Section 301 List 4	84.33%	5.55%	5.15%

Notes: From Bown (2021) and Ministry of Finance of China. The third column reports the cumulative share of HS6 products covered after each set of China's tariff actions. The remaining columns report the cumulative share of China's imports subject to tariff increases, for all products (fourth column) and intermediate and capital goods (fifth column); these are expressed as a share of China's total imports from the world in 2017 (from UN Comtrade).

Table A.3: Changes to China's MFN tariffs, January 1, 2017 – July 1, 2019

Effective Dates	Description of MFN Tariff Reduction	Cumulative Share of HS 6-digit Products	Cumulative 2017 Import Share	
			All Products	Intermediate and Capital goods
July 1, 2017	Information Technology Agreement tariff cut	3.06%	20.92%	20.38%
December 1, 2017	Tariff cut on consumer goods	5.68%	23.01%	21.41%
January 1, 2018	Interim MFN rates for 2018	6.01%	23.89%	22.29%
May 1, 2018	Tariff cut on pharmaceuticals	6.03%	23.91%	22.31%
July 1, 2018	Tariff cut on broken rice	22.72%	29.84%	26.93%
	Information Technology Agreement tariff cut			
	Tariff cut on consumer goods			
	Tariff cut on autos and auto parts			
November 1, 2018	Tariff cut on industrial goods	41.69%	34.62%	31.70%
January 1, 2019	Interim MFN rates for 2019	41.96%	34.70%	31.76%
July 1, 2019	Information Technology Agreement tariff cut	42.08%	35.58%	32.64%

Notes: From Bown (2021) and General Administration of Customs, China. The third column reports the cumulative share of HS6 products covered after each set of China's MFN tariff rate cuts. The remaining columns report the cumulative share of China's imports subject to MFN tariff reductions, for all products (fourth column) and intermediate and capital goods (fifth column); these are expressed as a share of China's total imports from the world in 2017 (from UN Comtrade).

Figure A.1: Tariff Changes During the US-China Trade War

(a.1) Δ US Tariff on CHN (unweighted)
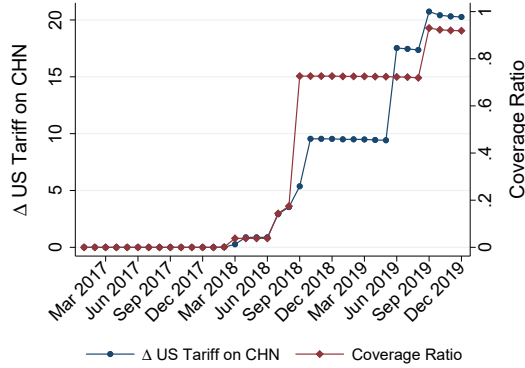
(a.2) Δ US Tariff on CHN (weighted)
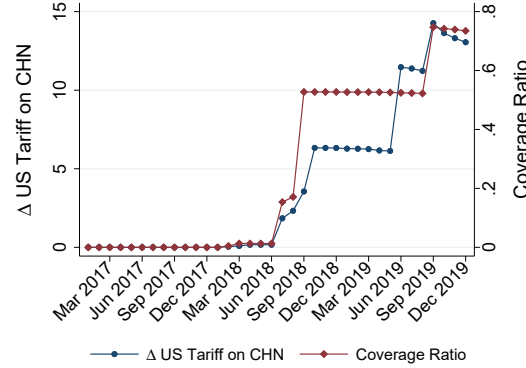
(b.1) Δ CHN Tariff on US (unweighted)
Intermediate and Capital Goods
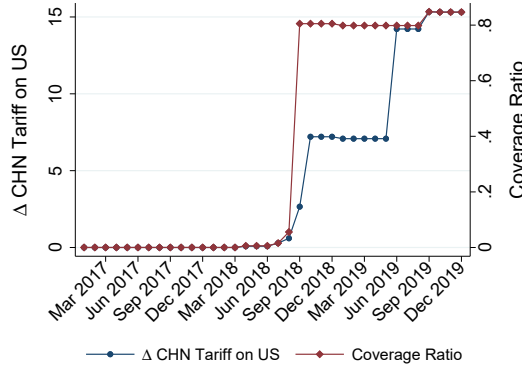
(b.2) Δ CHN Tariff on US (weighted)
Intermediate and Capital Goods
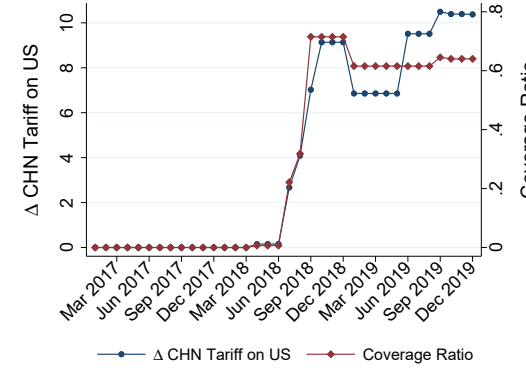
(c.1) Δ CHN MFN Tariff (unweighted)
Intermediate and Capital Goods
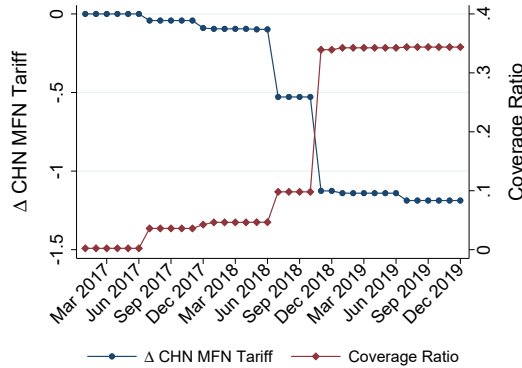
(c.2) Δ CHN MFN Tariff (weighted)
Intermediate and Capital Goods
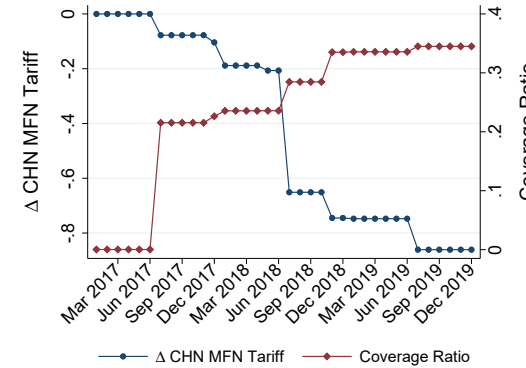
Notes: The first row illustrates the share of HS 6-digit codes affected and the average tariff imposed by the US on China (over all products); panel a.1 presents unweighted shares/averages, while panel a.2 weights these by each HS 6-digit product's share in China's exports to the US in 2017. The second row illustrates the share of HS 6-digit codes affected and the average retaliatory tariff imposed by China on the US (over all intermediate and capital goods); panel b.1 presents unweighted shares/averages, while panel b.2 weights these by each HS 6-digit product's share in China's total imports of intermediate and capital goods from the US in 2017. The third row illustrates the share of HS 6-digit codes affected and the average MFN tariff reduction by China (over all intermediate and capital goods); panel c.1 presents unweighted shares/averages, while panel c.2 weights these by each HS 6-digit product's share in China's total imports of intermediate and capital goods from the world.

B   Data Appendix

B.1   Geo-coordinates from Google Maps and Amap

From the 2016 China customs data, we identified 283,057 firms that are not intermediary trading firms. As reported in Table B.1, we can locate the geo-coordinates of 271,565 (respectively, 226,039) of these firms from Google Maps (respectively, Amap). The average latitude and the average longitude from Google Maps (respectively, Amap) are 30.619°N and 117.680°E (respectively, 30.334°N and 117.489°E). The correlation of latitudes (respectively, longitudes) from the two sources is 0.986 (respectively, 0.956). The median distance between geo-locations identified by the two web-mapping services is 5.24km. Note that the grids in our analysis have a physical distance of approximately 11.13km. For more than 50% of the cases, Google Maps and Amap imply the same mapping of firms to grids. Note though that the distribution of the distance between geo-locations identified by the sources has a long right tail: The mean distance is 31.90km, which is much larger than the median distance, and moreover is larger than the dimensions of a grid cell. This points to the geo-information from Google Maps and/or Amap containing measurement error. As long as the measurement error inherent in the Google Maps geo-coordinates is independent from that in Amap, we can employ tariff shock measures constructed from one source as an instrumental variable for the measures constructed from the other source, to address attenuation bias in the regressions.

B.2   Other Data

Product-level Bilateral Trade Flows: We obtain monthly bilateral trade data at the HS 6-digit level between China and other countries from Trade Map, a database developed by the International Trade Centre of UNCTAD/WTO (ITC). According to the ITC's documentation, the underlying data is reported by the General Customs Administration of China.

Panel A of Figure B.1 plots the year-on-year change in log export value from China to the US and to the other countries in the world (ROW), respectively. The shaded vertical bars indicate the onset of different phases of the US Section 301 tariff actions, namely the implementation of each of Lists 1-4, as well as the increase in List 3 tariffs in July 2019. The year-on-year growth of exports to the US is on average 11 log points over the period 01/2017-06/2018. The average growth slowed down to 9.4 log points in the second half of 2018 (07/2018-12/2018) when the Section 301 tariffs were implemented, and further slid down to -9.6 log points in the first half of 2019 (01/2019-06/2019) and -17.9 log points in the second half of 2019 (07/2019-12/2019). There is no evident export re-direction until late 2019: Exports to the ROW appear to fall in tandem with exports to the US until mid-2019, with the average year-on-year change in exports to the ROW equal to 7.9, 7.7, and 1.1 log points during 01/2017-06/2018, 07/2018-12/2018, and 01/2019-06/2019, respectively. Export growth to the ROW diverged somewhat from that to the US, with an average growth of 4.2 log points over 07/2019-12/2019, even as exports to

the US continued to fall.

Panel B displays the year-on-year changes in log imports from the US and from the ROW, respectively. The shaded vertical bars indicate the onset of different phases of China's retaliatory tariff actions against the US Section 301 tariffs. The average year-on-year growth in imports plunged from 13 log points over 01/2017-06/2018, to -9.7 log points over 07/2018-12/2018, and further down to -35 log points in the first half of 2019 and -11.2 log points in the second half of 2019. We do not detect clear patterns of import diversion from this aggregate data. The average year-on-year change in log imports from the ROW is 17.3, 14.6, -1.8 and -1 for the periods 01/2017-06/2018, 07/2018-12/2018, 01/2019-06/2019, and 07/2019-12/2019, respectively.

Grid-Level Population Data: These are taken from the fourth version of the Gridded Population of the World (GPWv4) dataset, which has a grid resolution of 30 arc-seconds (about 1km). We use the population estimates for 2015, and aggregate the data to the night-light grids.[40] In the raw data, 0.52% of the night-light grids have zero population. We impute a minimum population of 1 for these grids. As is shown in Table D.4, the baseline findings are unchanged without this imputation.

Exchange Rates: The quarterly nominal exchange rate data are obtained from the IMF's International Financial Statistics (IFS). Figure B.2 shows the change in the exchange rate of the RMB against the USD, relative to its January 2017 level. We measure the exchange rate as the amount of foreign currency purchased by one unit of RMB, so an increase in the exchange rate corresponds to an appreciation of the RMB against the foreign currency. Against the USD, the RMB depreciated 12.9 log points from its peak in March 2018 to its trough in August 2019, while rebounding slightly afterwards. The RMB also depreciated against a weighted-average of currencies in the ROW during this period; this is true for both an export-weighted and an import-weighted average.

Value Added Tax Rates (VAT): The structure and rates of China's VAT changed over the sample period under study. Prior to the tariff war in early 2017, VAT rates varied across products with four distinct levels: 17 percent, 13 percent, 11 percent, and 6 percent. In July 2017, products that were originally subject to the VAT rate of 13 percent received a tax cut to 11 percent. As a result, the VAT system was simplified from four tiers to three tiers. In May 2018, the 17 percent and 11 percent VAT rates were each adjusted to 16 percent and 10 percent respectively. China implemented another round of large-scale tax cuts in April 2019, seeking to reduce costs for businesses amid a slowing economy and the tariff dispute with the US. The headline VAT rate was lowered from 16 percent to 13 percent, together with a reduction of its 10 percent VAT rate to 9 percent.

We obtain the HS 10-digit product-level VAT rates from the Ministry of Commerce of China.

---

[40]For GPWv4, population input data are collected at the most detailed spatial resolution available from the results of the 2010 round of Population and Housing Censuses, which occurred between 2005 and 2014. The input data are extrapolated to produce population estimates for 2015.

As with the external tariff data, we aggregate the VAT data to the 6-digit level by taking the simple average across the corresponding tax rates. As shown in Figure B.3, a simple average of the product-level VAT tax rates declined from 16.9 percent in early 2017 to 12.8 percent by June 2019.

Other Prefecture-level Data: We collected a set of economic outcome variables at the prefecture level from the China City Statistical Yearbooks, including GDP per capita and manufacturing employment. The data is at the annual frequency and covers the pre-tariff war period, 2013-2016.

B.3 Summary Statistics of the Grid-Level Tariff Shocks

Table B.2 reports summary statistics for the grid-level measures of tariff shocks and changes in night lights. (For ease of presentation, the tariff shock measures are multiplied by 100.) Panel A shows that as the US-China tariff war escalated, the year-on-year change in US tariff rates at the grid level also increased. The mean US tariff shock (weighted by grid population) rose from 0.01 during Q1/2017-Q1/2018 to 0.88 percent during Q3/2018-Q3/2019. By Q3/2019, grid-level tariffs on exports to the US had increased by 1.15 percent from their level at the start of 2017. Moreover, there is substantial variation in US tariff exposure, with a cross-grid standard deviation of 2.76 percent. Panel B shows that tariffs on inputs imported from the US also rose as a result of China's retaliatory tariff actions, but to a lesser extent compared to the US tariff shock. By Q3/2019, the grid-level China input tariff had increased on average by 0.55 percent from Q1/2017; the associated cross-grid standard deviation was 2.23 percent. From Panel C, we see that the mean change in grid-level MFN tariffs on inputs was a decline of 0.28 percent over the period Q1/2017-Q3/2019. This offsets (on average) one-half of the contemporaneous increase in tariffs levied by China on imported inputs from the US.

Last but not least, Panel D presents the summary statistics on year-on-year changes in grid-level night lights intensity. Night lights dimmed starting in Q3/2018 (relative to a year ago), coinciding with the first round of Section 301 tariffs by the US (in July 2018). The year-on-year decrease in mean night lights intensity continued through Q1/2019. Over the sample period Q2/2017-Q4 2019, night-light intensity increased by 18.9 log points, though this masks a lot of heterogeneity across grids (the standard deviation was 28.4 log points). Bear in mind too that our regression specifications will ultimately focus on within-grid (rather than cross-grid) changes in night lights intensity, to investigate whether this is linked to variation over time in grid-level tariff shocks.

Table B.1: Summary Statistics: Firm Geo-coordinates from Google Maps and Amap

	Google Maps	Amap	Overlap/Correlation				
Number of firms geo-located	271,565	226,039	220,919				
Latitude	30.619	30.334	0.986				
Longitude	117.680	117.489	0.956				
			mean	std	p25	p50	p75
Distance of Google Maps and Amap locations (km)			31.901	156.704	0.032	5.243	20.945

Table B.2: Summary Statistics: Grid-Level Measures

	mean	std	5th	25th	50th	75th	95th
Panel A: Exposure to US Tariff Shocks							
Q1 2017-Q1 2018	0.009	0.158	0.000	0.000	0.000	0.000	0.004
Q2 2017-Q2 2018	0.028	0.378	0.000	0.000	0.000	0.000	0.020
Q3 2017-Q3 2018	0.269	1.158	0.000	0.000	0.000	0.084	1.147
Q4 2017-Q4 2018	0.614	1.675	0.000	0.000	0.000	0.422	3.164
Q1 2018-Q1 2019	0.599	1.626	0.000	0.000	0.000	0.415	2.998
Q2 2018-Q2 2019	0.729	1.907	0.000	0.000	0.000	0.530	3.749
Q3 2018-Q3 2019	0.880	2.372	0.000	0.000	0.000	0.755	4.533
Q1 2017-Q3 2019	1.149	2.762	0.000	0.000	0.000	1.169	5.591
Panel B: Exposure to China's Retaliatory Tariff Shocks							
Q1 2017-Q1 2018	0.000	0.000	0.000	0.000	0.000	0.000	0.000
Q2 2017-Q2 2018	0.008	0.293	0.000	0.000	0.000	0.000	0.000
Q3 2017-Q3 2018	0.118	0.971	0.000	0.000	0.000	0.002	0.292
Q4 2017-Q4 2018	0.352	1.552	0.000	0.000	0.000	0.025	1.406
Q1 2018-Q1 2019	0.335	1.513	0.000	0.000	0.000	0.023	1.331
Q2 2018-Q2 2019	0.393	1.630	0.000	0.000	0.000	0.030	1.672
Q3 2018-Q3 2019	0.427	1.836	0.000	0.000	0.000	0.031	1.914
Q1 2017-Q3 2019	0.545	2.228	0.000	0.000	0.000	0.044	2.311
Panel C: Exposure to China's MFN Tariff Changes							
Q1 2017-Q1 2018	-0.034	0.138	-0.221	-0.000	0.000	0.000	0.000
Q2 2017-Q2 2018	-0.036	0.152	-0.223	-0.000	0.000	0.000	0.000
Q3 2017-Q3 2018	-0.125	0.676	-0.560	-0.004	0.000	0.000	0.000
Q4 2017-Q4 2018	-0.198	0.738	-1.007	-0.077	0.000	0.000	0.000
Q1 2018-Q1 2019	-0.220	0.794	-1.153	-0.088	0.000	0.000	0.000
Q2 2018-Q2 2019	-0.218	0.793	-1.136	-0.088	0.000	0.000	0.000
Q3 2018-Q3 2019	-0.136	0.428	-0.659	-0.065	0.000	0.000	0.000
Q1 2017-Q3 2019	-0.278	0.844	-1.438	-0.132	0.000	0.000	0.000
Panel D: Growth in Night Lights							
Q2 2017-Q2 2018	0.053	0.221	-0.302	-0.052	0.049	0.159	0.427
Q3 2017-Q3 2018	-0.040	0.196	-0.353	-0.147	-0.035	0.072	0.299
Q4 2017-Q4 2018	-0.023	0.181	-0.347	-0.122	-0.002	0.084	0.256
Q1 2018-Q1 2019	-0.045	0.203	-0.419	-0.156	-0.029	0.085	0.256
Q2 2018-Q2 2019	0.052	0.203	-0.264	-0.051	0.045	0.153	0.384
Q3 2018-Q3 2019	0.070	0.191	-0.234	-0.032	0.068	0.165	0.385
Q4 2018-Q4 2019	0.130	0.160	-0.105	0.032	0.118	0.209	0.428
Q2 2017-Q4 2019	0.189	0.284	-0.268	0.033	0.177	0.333	0.675

*Notes:* The summary statistics reported are for $100 \times \Delta USTariff_{it}$ (Panel A), $100 \times \Delta CHNInputTariff_{it}$ (Panel B), and $100 \times \Delta CHNMFNInputTariff_{it}$ (Panel C), over the respective time periods, based on the Google Maps geolocated coordinates. The summary statistics reported in Panel D are for the log grid-level night lights intensity measure, $\Delta \ln(Light)_{it}$.

Figure B.1: Changes in Trade Flows During the US-China Trade War
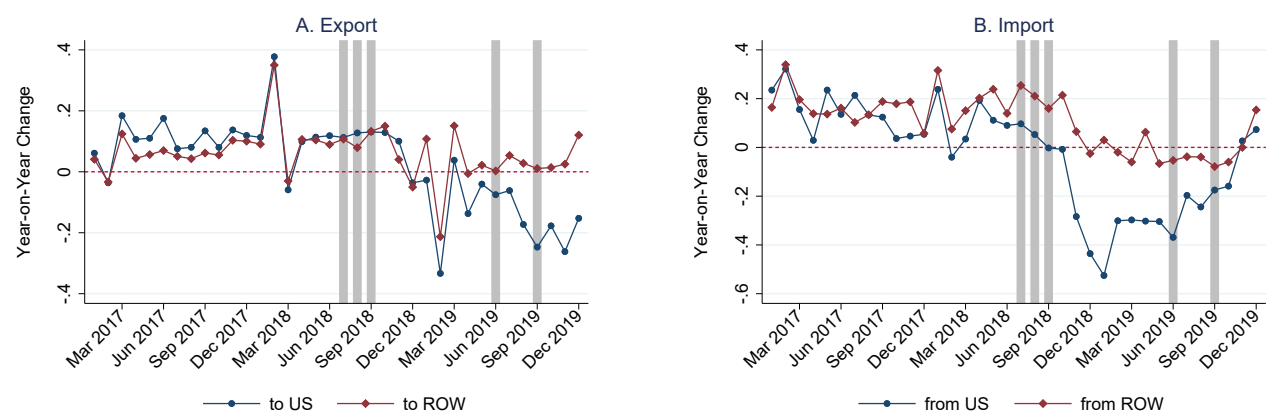
Notes: The figure plots the year-on-year changes (i.e., over the preceding twelve-month period) in China's log exports to the US and to the rest of the world (Panel A), and in China's log imports from the US and from the rest of the world (Panel B). The shaded areas in Panel A correspond to the onsets of the different phases of the US Section 301 tariff actions, as listed in Table A.1. The shaded areas in Panel B correspond to the different phases of China's retaliatory tariff actions, as listed in Table A.2.

Figure B.2: Changes in Exchange Rate During the US-China Trade War
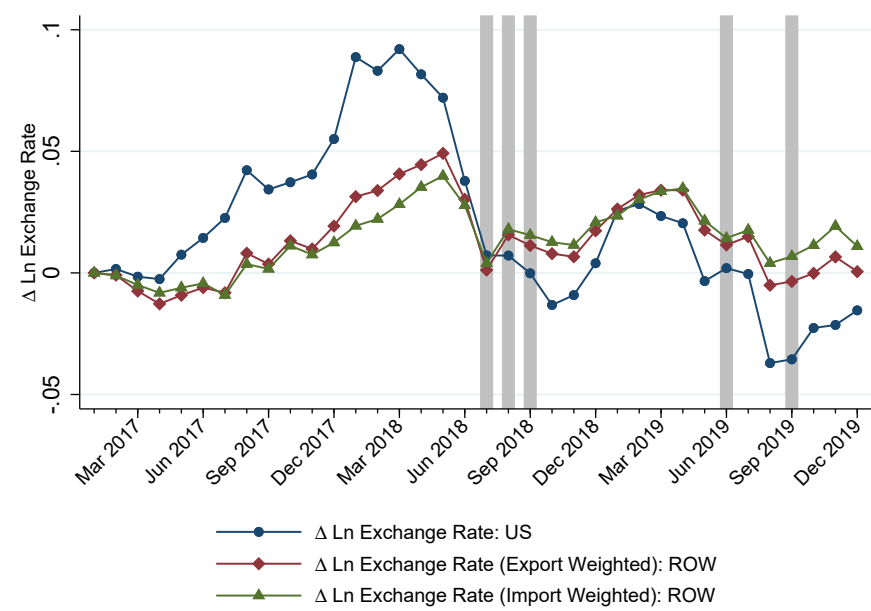
Notes: The figure plots movements in the strength of the RMB, relative to its initial value in January 2017. This is illustrated for: (i) the log USD per RMB exchange rate; (ii) an export-weighted rest-of-the-world log exchange rate (i.e., excluding the USD) per RMB; and (iii) an import-weighted rest-of-the-world log exchange rate per RMB. For (ii) and (iii), the weights used are drawn from UN Comtrade data for 2017. The shaded areas correspond to the onsets of the different phases of the US Section 301 tariff actions, as listed in Table A.1.

Figure B.3: Changes in Value Added Tax During the US-China Trade War
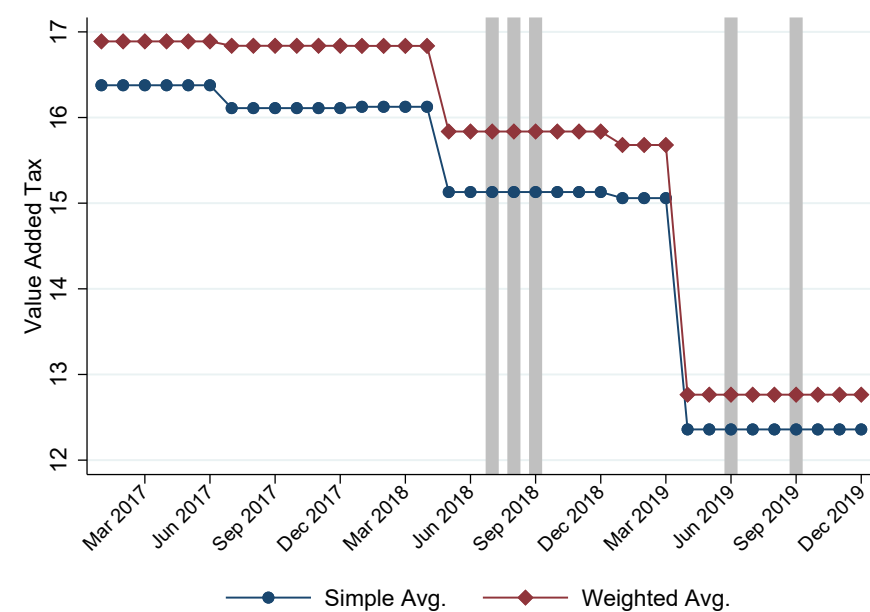
Notes: The figure plots China's value added tax rate starting from January 2017; both a simple average and a weighted-average of the tax rates for HS 6-digit products are illustrated, where the weights for the latter are UN Comtrade export flows in 2017. The shaded areas correspond to the onsets of the different phases of the US Section 301 tariff actions, as listed in Table A.1.

C Product-level Analysis: Tariff Shocks, Trade Flows, and Night Lights Intensity

Our empirical work in the main paper focuses on grid cells as the unit of observation, given our primary interest in understanding the impact of the US-China tariff war across different geographic locations within China. As the tariffs are levied on products though, one should also expect to observe direct responses in product-level outcomes such as in trade flows. We perform this product-level analysis in this appendix using information on trade flows downloaded from the Trade Map database, as a complement to our grid-level findings in the main paper. We establish that the US-China tariff increases were associated with: (i) a decrease in HS 6-digit trade flows between the US and China; and (ii) a decrease in night-time luminosity when this measure is suitably recast to the product level. Employing the monthly bilateral trade by product and by trade regimes from China's General Administration of Customs, we show that China's retaliatory tariffs induce reorganization of US-origin imports from ordinary to processing trade.

C.1 Changes in Trade Flows and Tariff Shocks

We assess the response of product-level trade flows using the following flexible lead-lag regression model, which we run on monthly data:

$$\Delta \ln X_{km} = \sum_{\tau=-6}^{\tau=6} \varphi^\tau \Delta USTariff_{k,m+\tau} + D_k + D_{sm} + \varepsilon_{km}^X. \tag{C.1}$$

Here, $\Delta \ln X_{km}$ denotes the year-on-year change in the log export value of HS 6-digit product k, i.e., $\ln(X_{km}/X_{k,m-12})$, where m indexes months; $\Delta USTariff_{km}$ measures the change in tariff imposed by the US on China's exports of product k over the same twelve-month period; the D_k's are HS 6-digit fixed effects, which capture product-specific linear time trends in $\ln X_{km}$; and the D_{sm}'s are HS-section-by-month fixed effects, which flexibly control for unobserved shocks within each of the 15 broader HS sections.[41] We separately investigate how the US tariffs affected China's exports to the US ($\Delta \ln X_{km}^{US}$), and China's exports to other countries excluding the US ($\Delta \ln X_{km}^{ROW}$). We winsorize observations with $\Delta \ln X_{km}^{US}$ values (respectively, $\Delta \ln X_{km}^{ROW}$ values) greater than the 99th percentile or smaller than the 1st percentile within each year-month, to trim potential outliers.

Panel I.A of Figure C.1 reports the cumulative estimated coefficients $\sum_{\tau=-6}^{\tau=t} \hat{\varphi}^\tau$; these are illustrated together with the associated 90% confidence intervals, based on standard errors

---

[41]The HS sections are: (i) Animal & Animal Products; (ii) Vegetable Products; (iii) Foodstuffs; (iv) Mineral Products; (v) Chemical & Allied Industries; (vi) Plastics/Rubbers; (vii) Raw Hides, Skins, Leather & Furs; (viii) Wood & Wood Products; (ix) Textiles; (x) Footwear/Headgear; (xi) Stone/Glass; (xii) Metals; (xiii) Machinery/Electrical; (xiv) Transportation; and (xv) Miscellaneous.

clustered at the HS 2-digit level. The results reveal no quantitatively large patterns of tariff anticipation leading up to the implementation of tariffs ($\tau = 0$). What is clear is that the tariffs had an adverse impact on China's product-level exports to the US upon implementation, and that the cumulative negative effect grew over time. For China's exports to the rest of the world (ROW), Panel I.B indicates a modest amount of trade diversion (i.e., China's exports being diverted to other destination markets), with the cumulative effect being positive and significant in the fifth month after tariff implementation. The size of this effect is small though in comparison to the decrease in China's exports to the US seen in Panel I.A.

Analogously, we investigate the effects of China's retaliatory tariffs and the contemporaneous changes in China's MFN tariffs by estimating the following:

$$\Delta \ln M_{km} = \sum_{\tau=-6}^{\tau=6} \theta_1^\tau \Delta CHNInputTariff_{k,m+\tau} + \sum_{\tau=-6}^{\tau=6} \theta_2^\tau \Delta CHNMFNInputTariff_{k,m+\tau}$$
$$+ D_k + D_{sm} + \varepsilon_{km}^M, \tag{C.2}$$

where $\Delta \ln M_{km}$ denotes the year-on-year change in China's log imports of HS 6-digit product k, i.e., $\ln(M_{km}/M_{k,m-12})$. $\Delta CHNInputTariff_{km}$ and $\Delta CHNMFNInputTariff_{km}$ are respectively the change in tariff imposed by China on goods from the US, and the change in China's MFN tariff, over the same twelve-month period. We restrict the sample to products $k \in \mathcal{K}$, where $\mathcal{K}$ is the set of intermediate and capital goods as designated by the UN BEC, Revision 5; this is the same set of imported products we focus on in the main paper. The empirical specification once again controls for product and HS-section-by-month fixed effects. We examine separately how the tariffs affected China's imports from the US ($\Delta \ln M_{km}^{US}$), and China's imports from the rest of the world ($\Delta \ln X_{km}^{ROW}$), while winsorizing the tail 1% of observations in each year-month for each respective dependent variable.

The cumulative effects of China's retaliatory tariffs and China's adjustments to MFN tariffs (i.e., $\sum_{\tau=-6}^{\tau=t} \hat{\theta}_1^\tau$ and $\sum_{\tau=-6}^{\tau=t} \hat{\theta}_2^\tau$) are displayed in Panel II. Panel II.A reveals: (i) a slight increase in imports of inputs from the US in the month immediately prior to the implementation of retaliatory tariffs ($\tau = -1$), suggesting some anticipation effects; and (ii) a significant negative cumulative effect upon implementation of the tariff retaliation, that gets stronger in magnitude over time. On the other hand, the retaliatory tariffs have only a slight effect on China's imports from the ROW (Panel II.B); there is a marginally significant cumulative positive effect in the third month after tariff implementation, suggesting a small amount of trade diversion (i.e., purchasing inputs from other source countries).

Turning to China's adjustments to its MFN tariff rates, the patterns in Panels II.C and II.D are consistent with the reduction in MFN tariffs raising imports of inputs from both the US and the ROW, though the effect is imprecisely estimated for imports from the ROW. It appears then that the contemporaneous cuts in MFN tariff rates offset some of the negative effect that the retaliatory tariffs had on Chinese firms' imports of inputs from the US.

C.2 Changes in Product-Level Night Lights and Tariff Shocks

We next examine if the product-level tariff shocks impacted night-time luminosity. We do so by recasting the observed grid-level changes in night lights intensity to the product level, following Borusyak et al. (2022). This enables us to see if larger product-level tariff hikes were associated with slower growth in night lights intensity across locations that tend to host the product's exports to the US (or respectively, imports from the US).

We construct the product-level analogue, y_{km}, of the grid-level outcome variable, $y_{im} = \Delta \ln(Light_{im})$, according to:

$$y_{km} = \frac{\sum_i e_i s_{ik} y_{im}}{\sum_i e_i s_{ik}}, \tag{C.3}$$

where s_{ik} measures the exposure of location i to the product-level tariff shock g_{km}, and e_i is the population of the location. As demonstrated by Borusyak et al. (2022), a product-level regression of y_{km} on the tariff shock g_{km} in which the observations are weighted by $s_k = \sum_i e_i s_{ik}$ will yield a tariff shock coefficient that is equivalent to that in a grid-level regression of y_{im} on the Bartik measure $\sum_k s_{ik} g_{km}$ in which the observations are weighted by e_i.

Consider first the US tariff shocks faced by Chinese exporters. In our context, the s_{ik}'s associated with the US tariff shocks are the X_{ik0}^{US}/X_{i0}'s, these being the initial shares used in the construction of the Bartik measure of US tariff exposure in (2). Let $\Delta \ln(Light_{km}^X)$ denote the product-level analogue constructed based on (C.3) of night lights intensity. We relate this product-level outcome measure to the US tariff shock in a regression model similar to that in (C.1):

$$\Delta \ln(Light_{km}^X) = \sum_{\tau=-6}^{\tau=6} \delta^\tau \Delta USTariff_{k,m+\tau} + D_k + D_{sm} + \nu_{km}^X. \tag{C.4}$$

This explores how the US product-level tariff shocks affected night lights intensity in a lead-lag window from six months prior to six months after tariff implementation, while controlling for product and HS-section-by-month fixed effects. To reduce the influence of outliers on the regression estimates, we winsorize the $\Delta \ln(Light_{km}^X)$ observations at the 1st and 99th percentiles within each year-month.

Panel A of Figure C.3 reports the cumulative estimated coefficients $\sum_{\tau=-6}^{\tau=t} \hat{\delta}^\tau$ for the US tariff shock, using the baseline night lights variable without stray light correction. The tariffs on China's exports to the US have a statistically and economically insignificant impact on night lights prior to and upon their implementation (i.e., $\tau \leq 0$). This alleviates two concerns, namely that there could have been anticipatory effects occurring before the tariff changes, and that there could be product-specific time trends correlated with the US tariff shocks. The adverse effect of tariff hikes reveals itself and becomes significant three months after implementation; this remains persistent at least for the next three months. This pattern is particularly distinct when we use the VIIR-DNB night lights data series that includes the stray light correction (Panel B). This finding echoes that in Panel A of Figure C.1 in the main paper, where we also see that the effect of the US' discretionary tariffs on the log value of China's product-level

exports to the US intensifies three months after implementation.

To investigate the effects of China's retaliatory tariffs, we reconstruct the product-level measure of night lights growth, denoted by $\Delta \ln(Light_{km}^M)$, with $s_{ik} = \frac{M_{ik0}^{US}}{M_{i\kappa 0}}$, these being the initial shares on which the Bartik measure of exposure to the retaliatory tariffs in (3) is based. Consistent with the previous analysis, we restrict the set of products considered to intermediate inputs and capital goods, and winsorize the $\Delta \ln(Light_{km}^M)$ observations at the 1st and 99th percentiles within each year-month. The corresponding estimation equation is:

$$\Delta \ln(Light_{km}^M) = \sum_{\tau=-6}^{\tau=6} \kappa^\tau \Delta CHNInputTariff_{k,m+\tau}^{US} + D_k + D_{sm} + \nu_{km}^M. \qquad (C.5)$$

The estimated cumulative effects are never statistically significant during the window we examine, both for the baseline night lights measure (Panel C) and the stray light corrected measure (Panel D). This dovetails with the grid-level analysis in the main paper, which also did not uncover any significant effects of the retaliatory tariffs on inputs on economic outcomes within China.

As corroborating evidence to these findings on night lights, Figure C.4 illustrates two national-level economic indicators and how these evolved over the course of the tariff war. These are the year-on-year growth in respectively industrial value added (Panel A) and in the generation of electricity (Panel B), as reported by the National Bureau of Statistics of China. While there is a fair bit of month-to-month fluctuation in these growth rates, both variables nevertheless paint the picture that economic activity slowed down in the quarters following the onset of US Section 301 tariff rounds, especially after List 3 in September 2018.

C.3   Share of Ordinary Imports and Tariff Shocks

In Figure C.2, we provide product-level evidence of within-product switching of imports towards processing trade following China's retaliatory tariff actions against the US. Specifically, we estimate the following equation:

$$\Delta \frac{M_{km}^{US,Proc}}{M_{km}^{US}} = \sum_{\tau=-6}^{\tau=6} \lambda_1^\tau \Delta CHNTariff_{k,m+\tau} + \sum_{\tau=-6}^{\tau=6} \lambda_2^\tau \Delta CHNMFNTariff_{k,m+\tau}$$
$$+ D_k + D_{sm} + \varepsilon_{km},$$

where $M_{km}^{US,Proc}/M_{km}^{US}$ measures the share of imports from the US organized through processing trade for product k in month m; D_k's are HS 6-digit fixed effects, and D_{sm}'s are HS-section-by-month fixed effects. We restrict the sample to intermediary inputs and capital goods. Observations are weighted by the initial value of imports in 2017, and the standard errors are clustered at the 2-digit HS level.

Panel A of Figure C.2 reports the cumulative estimated coefficients $\sum_{\tau=-6}^{\tau=t} \lambda_1^\tau$. It reveals

that, in response to import tariff hikes, the share of imports from the US organized through processing trade increases significantly. In Panel B, we repeat the analysis, but replace the dependent variable by the Davis-Haltiwanger-Schuh approximation of the year-on-year log growth rate of processing imports from the US, i.e., $\frac{M_{km}^{US,Proc} - M_{k,m-12}^{US,Proc}}{M_{km}^{US,Proc} + M_{k,m-12}^{US,Proc}}$. It appears that firms started switching to processing imports two months before the implementation of retaliatory tariffs, implying an anticipatory effect of the import tariff shock.[42] Panels C and D conduct placebo tests, where the dependent variables are replaced by the corresponding measures of processing imports from the ROW. As is expected, the retaliatory tariffs against the US have little impact on the choice of trade mode for imports from the ROW.

---

[42]The administrative barriers of switching to processing trade appear to be low in China during the trade war period. Before 1 January 2019, processing trade was administered through the measures governing the applications for the Certificate of Production Capacity of Processing Enterprise and the record filing of processing trade operation. To engage in processing trade, enterprises should apply for the Certificate through the Ministry of Commerce's certification system online. Upon approval, enterprises could obtain the Certificate from the local commerce department. The process took 5 business days. With the Certificate, enterprises embarking on processing trade should go to the Customs and complete the formalities for obtaining a Processing Trade Handbook. Customs would issue the Handbook based on the scope of tax items (the first four digits of the HS codes) listed in the Certificate, and no further verification of the related licences is required. This process took 5 business days. (http://big5.www.gov.cn/gate/big5/www.gov.cn/gongbao/content/2014/content_2697077.htm) As a result of ongoing reforms, the administrative process has been simplified, lowering the costs of switching to processing trade. For example, since 1 January 2019, enterprises are no longer required to apply for the Certificate. (http://www.mofcom.gov.cn/article/b/e/201812/20181202821589.shtml) In China, a significant portion of processing importers are hybrid importers engaging in both ordinary and processing imports. These enterprises may have a lower cost of switching trade modes.

Figure C.1: Product-Level Analysis: Lead-Lag Specification

Panel I: US Tariffs and China's Exports

A. Exports to US

B. Exports to ROW
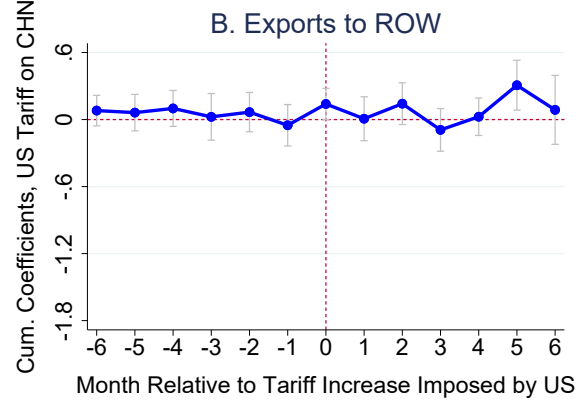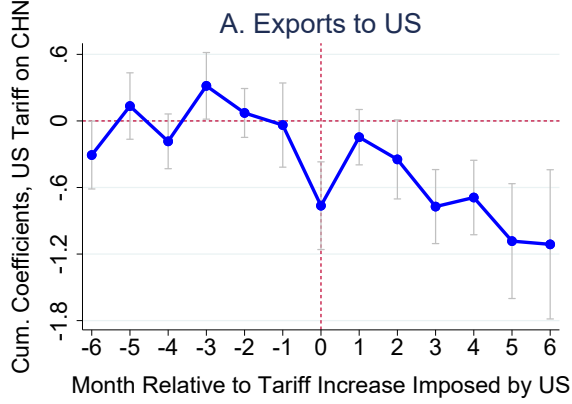
Panel II: China's Retaliatory Tariffs and China's Imports

A. Imports from US

B. Import from ROW

C. Imports from US

D. Imports from ROW
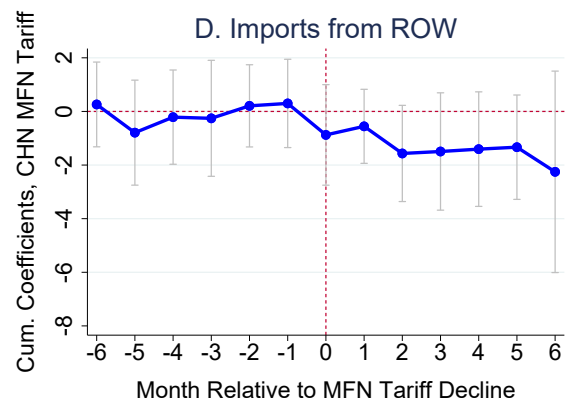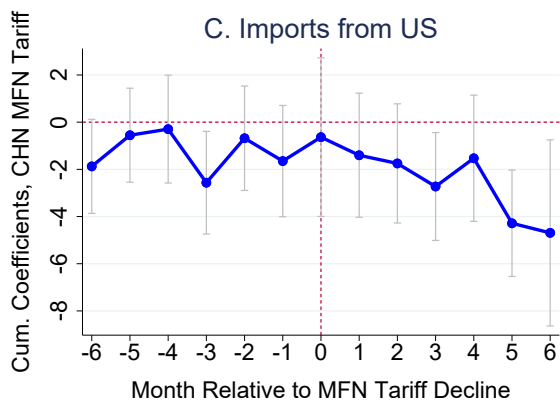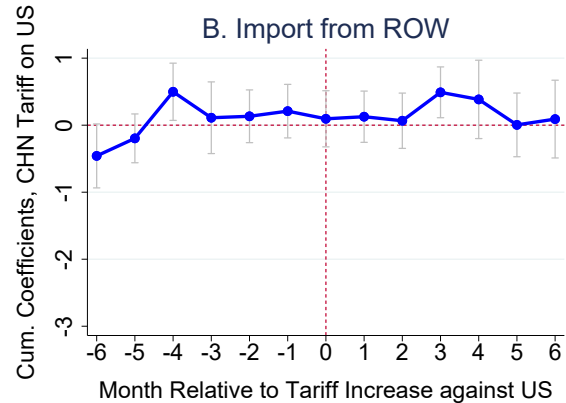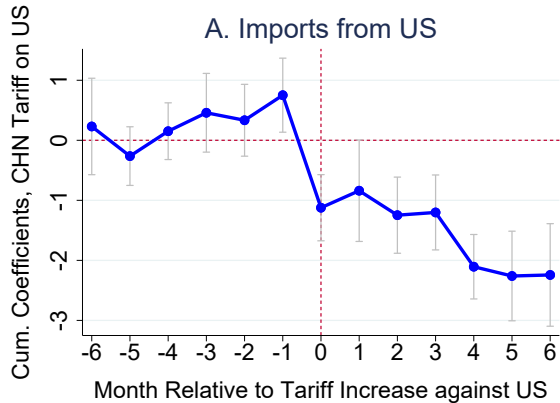
Notes: The figure plots the cumulative sum of φ^τ coefficients in equation (C.1) (Panel I), and the cumulative sum of θ_1^τ coefficients (and respectively, θ_2^τ coefficients) in equation (C.2) (Panel II). For import regressions, the sample is restricted to intermediate and capital goods. Standard errors are clustered at the HS 2-digit level. Error bands show 90% confidence intervals. The sample period is 01/2018 to 12/2019.

Figure C.2: Product-Level Analysis: Imports Under Processing Trade
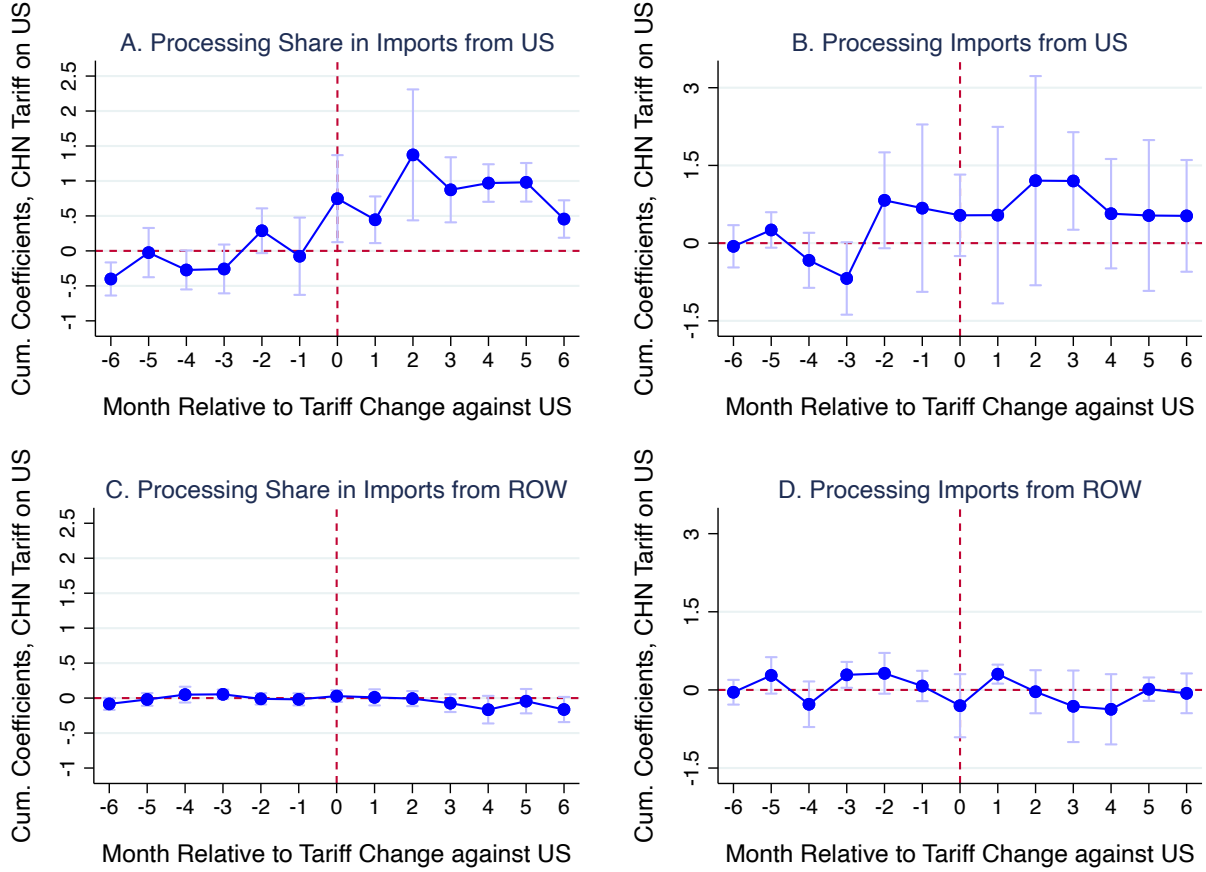
Notes: The figure plots the cumulative sum of λ_1^τ coefficients in equation (C.6). For all regressions, the sample is restricted to intermediate and capital goods. The dependent variable in Panels A and B are the change in share of imports from the US that is organized through processing trade and the change in log processing imports from the US, respectively. The dependent variable in Panels C and D are the change in share of imports from the ROW that is organized through processing trade and the change in log processing imports from the ROW, respectively. Standard errors are clustered at the HS 2-digit level. Error bands show 90% confidence intervals. The sample period is 01/2018 to 12/2019.

Figure C.3: Product-Level Analysis: Dynamic Specification
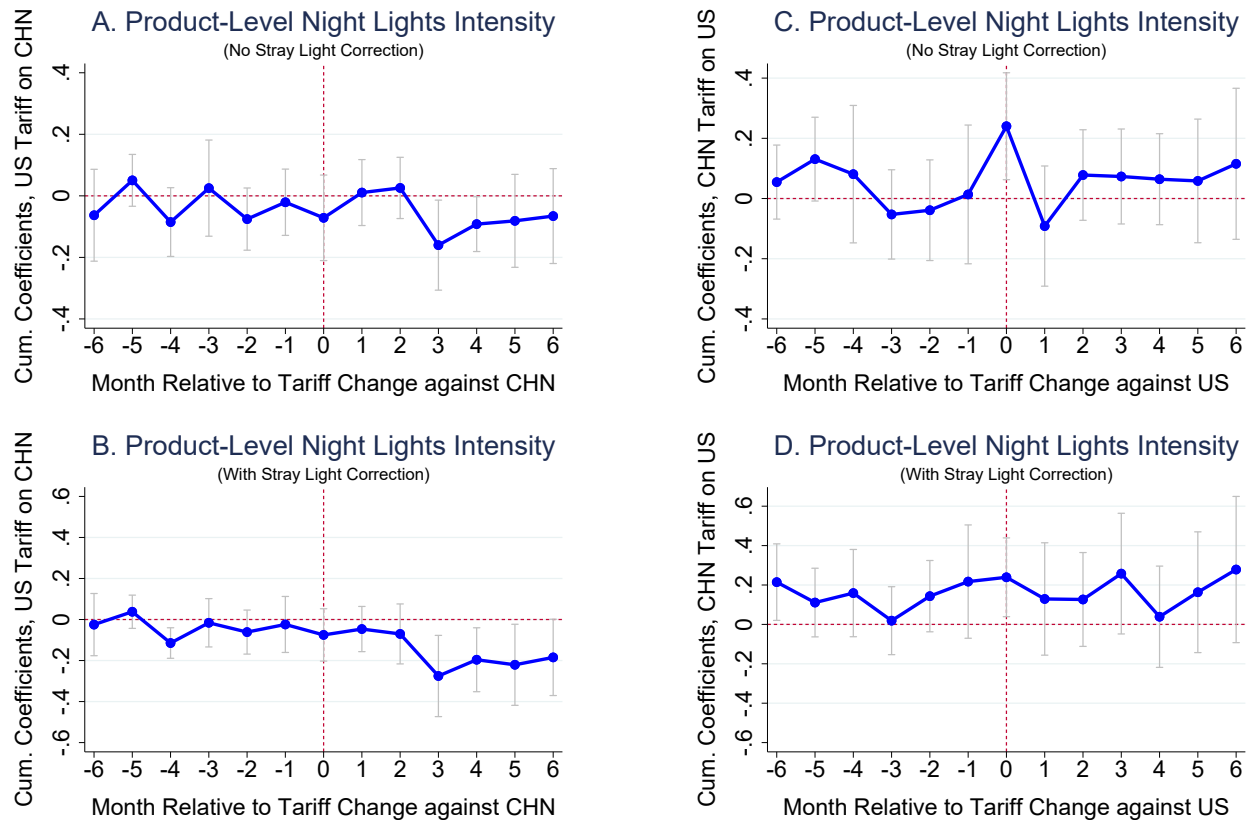
Notes: The figure plots the cumulative sum of δ^τ coefficients in equation (C.4) (Panels A, B), and the cumulative sum of κ^τ coefficients in equation (C.5) (Panels C, D). Panels A and C use a dependent variable constructed from the raw night lights data that deletes observations exposed to the stray light problem; observations from the months of May, June, and July that are particularly subject to this measurement problem are omitted from the sample. Panels B and D use a night lights growth dependent variable that corrects for the stray lights problem. For the regression in Panels C and D, the sample is restricted to intermediate and capital goods. Standard errors are clustered at the HS 2-digit level. Error bands show 90% confidence intervals. The sample period is 04/2018 to 12/2019.

Figure C.4: Corroborating Evidence

Panel I: Value Added of Industry
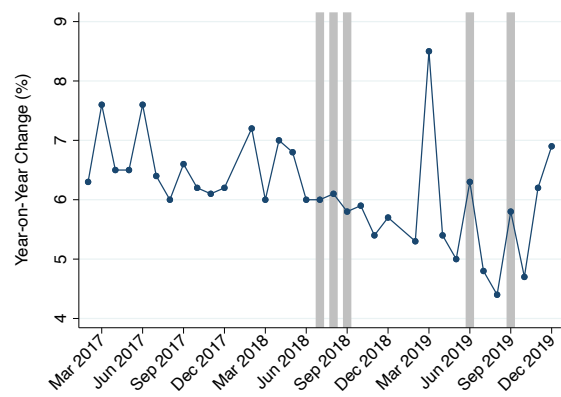
Panel II: Production of Electricity
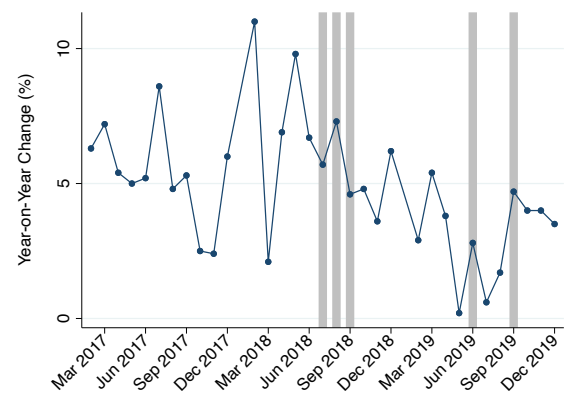
Sources: National Bureau of Statistics.
Notes: The shaded areas indicate the onsets of different phases of the US Section 301 tariff actions.

D Additional Empirical Results and Checks

In this appendix, we report on additional results and checks related to our empirical analysis of: (i) the relationship between tariff shocks and night lights intensity (Section D.1); (ii) the relationship between night lights and GDP per capita (Section D.2); and (iii) the effects of nonlocal tariff shocks (Section D.3).

D.1 Basic Specification Checks

Binned Scatterplot. In our exploration of the relationship between the tariff shocks and night-time luminosity, the baseline specification we have focused on has been that in Column 4 of Table 1. We start our series of checks by illustrating residual binned scatterplots based on this specification.

Figure D.1 illustrates the impact of the US tariff shock, $\Delta USTariff_{i,t-1}$ (Panel A) and the China retaliatory tariff shock on inputs, $\Delta CHNInputTariff_{i,t-1}$ (Panel B). For each of these tariff shock variables, we first compute their predicted values based on the first stage of the 2SLS regression from the Table 1, Column 4 specification. We then residualize these predicted values by regressing them against grid fixed effects D_i, prefecture-year-quarter fixed effects D_{pt}, and the grid initial characteristics interacted with year-quarter dummies that are used in Column 4, $W_{i0} \times D_t$; the regressions are run with grid-level population weights, with a minimum population of 1 imputed for grid cells with zero reported population. The US tariff residuals (respectively, China input tariff residuals) are placed into 50 bins with equal population, and these are illustrated on the horizontal axis in Panel A (respectively, Panel B). We similarly residualize the grid-level year-on-year change in night lights, $\Delta \ln(Light_{it})$; we compute a population weighted-average of this residual night lights growth, and this is the measure that is illustrated on the vertical axis.

The binned scatterplots confirm that there is a larger decline in night lights intensity for bins that experienced a greater US tariff increase (Panel A). On the other hand, the relationship between night lights growth and the China tariff hikes across the 50 bins has a positive slope, but this is not statistically significant (Panel B). These plots moreover provide assurance that the relationships are not being unduly driven by influential bins.

Extended Sample Period. Table D.1 extends the baseline specification in (1) in two ways: (i) the sample period for the night lights growth dependent variable now covers $t = Q1/2018, \ldots, Q4/2020$ (instead of $t = Q2/2018$ to $Q4/2019$ in our baseline); and (ii) we accommodate the possibility of heterogeneous effects over time, by estimating a separate US tariff shock and China input tariff shock coefficient for each half-year period (i.e., $Q1\&2/2018, \ldots, Q3\&4/2020$). (We once again lag each tariff shock explanatory variable by one quarter.)

The columns across Table D.1 differ in the set of additional controls that are included. Column 1 controls for grid and prefecture-year-quarter fixed effects (as in Column 3, Table 1), while Column 2 further adds initial grid characteristics interacted with time dummies (as in

Column 4, Table 1). Column 3 controls for the possible influence of the Covid-19 pandemic on night lights; we use here a dummy variable for whether a grid is in the decile of cells that are closest in distance to Wuhan (the epicenter of the pandemic within China), interacted with time dummies for the year-quarters from $Q4/2019$ to $Q4/2020$. Last but not least, Column 4 augments the specification in Column 2 by adding grid-specific linear time trends (as in Column 6, Table 1). We find across the regression columns a negative impact of the US tariff shock, particularly on night lights growth in the second half of 2018 and the first half of 2019, a timing that coincides with the advent of the Section 301 tariffs in July 2018. We also detect a persistent negative effect of the US tariffs into the first half of 2020, suggesting that the Covid-19 pandemic was not the only source of headwinds for local economic activity. Interestingly, we do find that proximity to Wuhan is associated with a fall in night lights growth in $Q2/2020$, although this does not alter much the estimated effects of the US tariff shock. On the other hand, we do not find evidence of an impact of the retaliatory tariffs on imported inputs that is consistent across columns.

Pre-Trend Checks. In Table D.2, we re-run the Column 4, Table 1 specification using various lags of the grid-level night lights growth measure as the left-hand side variable. Column 1 in this table reproduces the estimates from the baseline 2SLS specification, while the successive columns use $\Delta \ln(Light_{i,t-1})$, $\Delta \ln(Light_{i,t-2})$, and $\Delta \ln(Light_{i,t-3})$, as the dependent variable. We obtain statistically insignificant coefficients on the tariff shock explanatory variables in Columns 2-4, which confirms that these trade policy changes are uncorrelated with grid-level pre-trends in night lights growth.

As discussed in the main paper, another threat to identification stems from the possibility that there could be initial grid-level features driving subsequent movements in night lights intensity. This is why we control for a set of initial grid characteristics W_{i0} – the US share in exports, the US share in imports of inputs, log exports per capita, log imports of inputs per capita, and log mean 2016 night lights intensity – each interacted with time fixed effects in our baseline specification. Table D.3 augments this set of initial grid characteristics that we consider. In Column 1, we further include log grid population in the set W_{i0}. In Column 2, we add the initial grid-level share of exports for each of the 15 HS sections, and the analogous set of initial grid-level share of intermediate imports by HS section.[43] In Column 3, we add the initial exports to the US by HS section expressed as a share of total grid-level exports, and likewise add the initial imports of intermediates from the US by HS section expressed as a share of total grid-level imports of intermediates. In Column 4, we include the share of total grid-level exports that are accounted for by state-owned enterprises (SOEs), as inferred from the ten-digit firm identifiers in the China customs database; the sixth digit of the firm identifier is equal to '1' for SOEs. These help to capture the effects of policies that may have been implemented during

---

[43]As a reminder, the HS sections are: (i) Animal & Animal Products; (ii) Vegetable Products; (iii) Foodstuffs; (iv) Mineral Products; (v) Chemical & Allied Industries; (vi) Plastics/Rubbers; (vii) Raw Hides, Skins, Leather & Furs; (viii) Wood & Wood Products; (ix) Textiles; (x) Footwear/Headgear; (xi) Stone/Glass; (xii) Metals; (xiii) Machinery/Electrical; (xiv) Transportation; and (xv) Miscellaneous.

this period to bolster SOEs, for example through preferential access to bank credit, that could have affected the intensity of local economic activity. Column 5 then jointly includes all of these preceding initial grid characteristics together in a single regression. The negative impact of the US tariffs that we obtain remains stable in both size and statistical significance. In particular, this is reassuring that initial grid-level patterns of export specialization or input sourcing by HS sections (and the time trends that emanate from these) are not driving our baseline results. It moreover indicates that it is the grid-level profile of product-level trade shares *within* broader HS sections that is the key identifying source of variation for our Bartik tariff shock variables.

Checks on Baseline Specification. In Table D.4, we consider a series of basic checks related to our preferred regression specification. In Column 1, we estimate the regression model in levels rather than in changes, as follows:

$$\ln(Light_{it}) = \pi_1 USTariff_{i,t-1} + \pi_2 CHNInputTariff_{i,t-1} + \psi_{iq} + \phi_{pt} + \theta_i \times t + \varepsilon_{it}. \quad \text{(D.1)}$$

Here, $Light_{it}$ is the night-time luminosity of grid i during time t. The variables $USTariff_{i,t-1}$ and $CHNInputTariff_{i,t-1}$ are the analogues of (2) and (3) in which the initial trade shares are multiplied with the corresponding product-level tariffs in levels (i.e., without time-differencing); we once again use one-period lags of these explanatory variables to accommodate a lagged response. The ψ_{iq}'s in equation (D.1) denote grid-by-quarter-of-year fixed effects, which control for location-specific seasonality in night lights intensity. The ϕ_{pt}'s are prefecture-by-year-quarter fixed effects. Lastly, the $\theta_i \times t$ term captures a grid-specific linear time trend in log night lights. Note in particular that taking year-on-year differences of (D.1) yields precisely the regression model (1) in changes in the main paper. The results in Column 1 show that this alternative fixed effects model in levels yields similar estimates as the year-on-year-difference specification.

Column 2 addresses the concern that several of the initial grid-level characteristics (W_{i0}) whose time-varying effects we control for – specifically, the US share in exports, the US share in imports of inputs, log exports per capita, log imports of inputs per capita – are constructed using Amap geo-coordinates, which could be subject to measurement error inherent in that web-mapping service. We thus run a specification in which we use the Google Maps-based W_{i0} measures interacted with year-quarter fixed effects, and instrument for these using the interactions of the Amap-based W_{i0} measures with year-quarter fixed effects. The coefficient estimates in this column remain stable. In Column 3, we revert to our baseline specification in Table 1, Column 4, but instead use the tariff shocks constructed with Google Maps geo-information as the instrumental variable for the Amap-based tariff shocks. The US tariff shock coefficient remains similar in magnitude and statistically significant (albeit at the 10% level).

In Column 4, we adopt the VIIR-DNB measure that applies the stray light correction (instead of our baseline measure where observations impacted by stray light during the summer months are dropped). In Column 5, we drop all grid cells with a zero reported population, rather than imputing a minimum population of 1. Neither of these last checks affects our key conclusion of a negative US tariff shock effect on night lights growth; in particular, the estimates

we obtain in Column 5 are virtually identical to our baseline results, indicating that the grids with zero population in the raw data were not driving our findings.

One may be concerned that due to spillover effects of tariff shocks across grid cells, the estimate based on a continuous difference-in-differences framework may be biased. In particular, our baseline specification controls for prefecture-by-year-quarter fixed effects. Although these fixed effects control for a large set of unobserved factors, the aforementioned concern could be compounded as the identification stems from the variation of differential tariff shocks across geographically nearby grid cells within a prefecture. While we explore spatial spillovers using various formal approaches in Section 4.4, we also present an alternative specification that replaces the prefecture-by-year-quarter fixed effects with province-by-year-quarter fixed effects. If there are strong spatial spillovers that decay rapidly with distance, we should expect the estimates to be sensitive to the inclusion of time-varying fixed effects of geographic units at different aggregation levels. As is shown in Column 6, the estimated coefficient of $\Delta USTariff_{i,t-1}$ is statistically similar to the baseline estimate, albeit slightly larger in magnitude. If anything, our baseline quantitative analysis is likely to yield a lower bound of the total impact of the US tariffs on China's economy.

Using web mapping services provided by Google Maps and the Amap, we geo-locate firms based on firm names. Given the information available in the Chinese customs data, we cannot rule out the possibility that some transactions are reported by firm headquarters and hence may not reflect production in the local economy. To alleviate this concern of systematic measurement errors, in Column 7, we exclude observations in the top 5 prefectures by 2017 GDP (Beijing, Shanghai, Guangzhou, Shenzhen and Chongqing) where headquarters are more likely located. The estimates remain robust.[44]

In the baseline analysis, we cluster standard errors at the province level, which allows for arbitrary within-province correlation in the error terms. This may be inappropriate if there is substantial cross-province correlation due to the similarity of trade structure across grids that are not geographically proximate (Adão et al., 2019). We adopt two approaches to alleviate this concern. As a first check, we consider an alternative clustering protocol. Specifically, for each grid, we identify the 2-digit HS code that has the largest export share. We then two-way cluster the standard errors by province and by these HS 2-digit codes. As shown in Column 6, this makes little change to the standard errors. As a second check, we will shortly below substantiate the robustness of the statistical inference by performing random permutation tests, in the same spirit as the Monte Carlo exercises in Adão et al. (2019).

Controlling for Other Policy Shocks. Table D.5 accounts for other policy changes that occurred within the same time frame as the US-China tariff war, and which could have similarly impacted economic outcomes through a grid location's initial export or intermediate import trade shares. We do so by constructing analogous Bartik measures to control for these

---

[44]In the unreported results, we verify that the results are robust to the exclusion of top 10 prefectures by 2017 GDP, and to the exclusion of top 5 or 10 prefectures by 2017 export value.

other policy shocks.

Column 1 examines the effects of the adjustments made by China to its MFN tariff rates. As discussed in Appendix A, China reduced MFN tariffs on a range of products during the tariff war, which would have offset some of the retaliatory tariffs hikes vis-à-vis the US, while making it less expensive to source these products from the rest of the world. To capture the change in input costs induced by the MFN tariff cuts, we construct an MFN input tariff shock measure as follows:

$$\Delta CHNMFNInputTariff_{it} = \sum_{k \in \mathcal{K}} \frac{M_{ik0}}{M_{i\mathcal{K}0}} \Delta ImportTariff_{kt}^{MFN},$$

where $M_{ik0}/M_{i\mathcal{K}0}$ is the imports of HS 6-digit product k attributable to firms in grid i in the base year (2016), expressed as a share of total imports of inputs in that year. $\Delta ImportTariff_{kt}^{MFN}$ denotes the change in the MFN tariff rate for product k at time t relative to a year ago. As in the main paper, we limit the construction of these shares to products $k \in \mathcal{K}$ that are deemed to be intermediates or capital goods under the UN BEC, Revision 5. We augment the baseline regression from Table 1, Column 4 with this additional $\Delta CHNMFNInputTariff_{i,t-1}$ variable; in particular, we use the MFN tariff shock constructed using Google Maps geo-coordinates, and instrument for this using the Amap-based MFN tariff shock measure. A potential caveat of this specification is that the changes in MFN tariffs for some products could have been endogenous responses by the Chinese government, to strategically reduce MFN tariffs to mitigate the adverse effects of the tariff war on economic activities. In addition, a number of the MFN tariff cuts for high-technology goods had already been scheduled prior to the tariff war, and so there could be anticipation effects. Due to these considerations, we only use this MFN tariff shock as a control in a robustness check. We obtain a negative but statistically insignificant coefficient for $\Delta CHNMFNInputTariff_{i,t-1}$, while the estimated effect of the US tariff shock changes little.

Column 2 controls for the potential confounding effects of exchange rate movements. As Figure B.2 has shown, the RMB depreciated against the US dollar between 2018 and 2019. On the one hand, this would have benefited Chinese exporters for whom the US is a major destination market, by making their exports cheaper for US buyers. On the other hand, the weaker RMB would have raised the cost for Chinese firms of imported inputs from the US. To capture the grid-level exposure faced by Chinese exporters to exchange rate movements with respect to their destination markets, we construct:

$$\Delta ExportExRate_{it} = \sum_{c} \frac{X_{i0}^{c}}{X_{i0}} \Delta \ln ExRate_{ct},$$

where $ExRate_{ct}$ measures the amount of country c's currency that can be purchased by one unit of RMB at time t; and X_{i0}^{c}/X_{i0} is the share of grid-i exports that are sold in country c in 2016. (As with the previous shock variables, we examine year-on-year changes in the country exchange rates.) Similarly, we capture the exposure faced by Chinese firms that import

intermediate inputs to exchange rate movements with respect to their source countries with:

$$\Delta ImportInputExRate_{it} = \sum_c \frac{M_{i\mathcal{K}0}^c}{M_{i\mathcal{K}0}} \Delta \ln ExRate_{ct},$$

where $M_{i\mathcal{K}0}^c/M_{i\mathcal{K}0}$ is the share of grid i's imports of inputs originating from country c in the base year. Once again, we use the Amap-based versions of these measures as instrumental variables for the Google Maps-based versions in the 2SLS regressions. As was the case with the MFN tariff adjustments, movements in the strength of the RMB could be an endogenous response by policymakers to help dampen any negative effects of the tariff war on domestic economic activity. We therefore do not attribute a causal interpretation to the exchange rate shock coefficient, and view the results here more as a robustness check. When these Bartik exchange rate shock measures are included in Column 2, we find no discernible effects on night lights intensity of the depreciation in the RMB during the tariff war period, either through the export or import exposure channels. More importantly, the estimated effect of the US tariff shock remains stable.

In Column 3, we explicitly account for the contemporaneous reductions in China's value-added tax (VAT) rates (see Figure B.3), which could have mitigated the negative impact of the US-China tariff war on economic activity within China. We do so by incorporating grid-level Bartik measures of exposure to product-level VAT rate changes. On the exporting side, this is constructed as:

$$\Delta ExportValAddTax_{it} = \sum_k \frac{X_{ik0}}{X_{i0}} \Delta ValAddTax_{kt},$$

where X_{ik0}/X_{i0} is the product-k share in grid-i's total exports, as observed in 2016; and $\Delta ValAddTax_{kt}$ is the change in VAT tax rate implemented in time t relative to a year ago. On the importing side, this grid-level VAT exposure is captured by:

$$\Delta ImportInputValAddTax_{it} = \sum_{k \in \mathcal{K}} \frac{M_{ik0}}{M_{i\mathcal{K}0}} \Delta ValAddTax_{kt},$$

where $M_{ik0}/M_{i\mathcal{K}0}$ is the product-k share in grid-i's total imports of inputs, as observed in 2016. We include both of these measures of exposure to VAT changes in Column 3, using the two AMAP-based VAT exposure measures as instrumental variables for the two Google Maps-based measures. We find some evidence that the VAT rate cuts enjoyed by importing firms are associated with an increase in night lights growth, an interpretation that is based on the negative coefficient (significant at the 10% level) estimated for $\Delta ImportInputValAddTax_{i,t-1}$. Importantly though, our key finding – that exposure to the US tariffs on Chinese exports reduced night lights growth – is preserved.

Lastly, in Column 4, we consider a specification that incorporates all the three sets of preceding policy shocks just discussed. The estimated coefficient of $\Delta USTariff_{i,t-1}$ remains stable, while none of the MFN tariff, exchange rate or VAT shocks displays an effect that is

significant at conventional levels.

Alternative Tariff Shock Measures. Table D.6 explores alternative constructions of the tariff shock measures. Note that in each of the columns in this table, we use the Amap-based version of each tariff shock measure as an IV for the Google Maps-based version of that measure.

We first conduct a falsification test in Column 1, in which we construct a pair of placebo tariff shocks that are based on grid-level trade shares with respect to a set of eight other developed countries, rather than the US. These eight countries are Australia, Denmark, Finland, Germany, Japan, New Zealand, Spain, and Switzerland, these being the set of countries that Autor et al. (2013) used to construct their widely-adopted instrumental variable for Chinese import penetration in the US.[45] Specifically, we define:

$$\Delta USTariff_{it}^{ADH8} = \sum_k \frac{X_{ik0}^{ADH8}}{X_{i0}} \Delta ExportTariff_{kt}^{US},$$

where X_{ik0}^{ADH8}/X_{i0} denotes the exports from grid i of product k to these eight countries, expressed as a share of total grid-level exports in 2016. Note that the above continues to us the product-level US tariff shocks, but instead applies initial export shares that capture the importance of exports to the ADH8 countries. Analogously, the placebo input tariff shock is built according to:

$$\Delta CHNInputTariff_{it}^{ADH8} = \sum_{k \in \mathcal{K}} \frac{M_{ik0}^{ADH8}}{M_{i\mathcal{K}0}} \Delta ImportTariff_{kt}^{US}.$$

where $M_{ik0}^{ADH8}/M_{i\mathcal{K}0}$ denotes the imports of inputs by grid i from the ADH8 countries, expressed as a share of total grid-level imports of intermediates in 2016. Column 1 of Table D.6 uses these placebo tariff shocks *in lieu* of our baseline tariff shocks (that were constructed with shares specific to trade with the US). Both placebo variables yield statistically insignificant coefficients, with their economic magnitude being much smaller than our baseline estimates. The finding that the adverse effect is stronger where US tariff hikes should bite more is reassuring. This also alleviates the concern that the baseline results might be spuriously driven by unobserved factors correlated with initial comparative advantage in producing products that are in demand in high-income markets.

Our baseline measures in (2) and (3) implicitly assume that only grids with firms exporting to or importing from the US are affected by the tariff shocks. This formulation aligns with our regression analysis that focuses more on the short-run responses of local night lights growth to the tariff actions during the trade war. Another view is that, regardless of export destinations or import origins, all grids with production in sectors impacted by the US punitive tariffs or in downstream sectors affected by China's retaliatory tariffs should have a positive exposure in

---

[45]In 2017, exports to these eight countries accounted for 12.8% of China's total exports, while exports to the US accounted for 19.0%.

the general equilibrium or in a long-time horizon. To account for this view, we re-weight the product-level tariffs according to:

$$\Delta USTariff_{it}^{All} = \sum_k \frac{X_{ik0}}{X_{i0}} \Delta ExportTariff_{kt}^{US},$$

$$\text{and} \quad \Delta CHNInputTariff_{it}^{All} = \sum_{k \in \mathcal{K}} \frac{M_{ik0}}{M_{i\mathcal{K}0}} \Delta ImportTariff_{kt}^{US},$$

where X_{ik0}/X_{i0} (respectively, M_{ik0}/M_{i0}) is the exports from (respectively, imports by) grid i of product k to all destinations (respectively, from all origins) as a share of total grid-level exports (respectively, imports) in 2016. Column 2 reruns the regression but replaces the tariff shocks by these alternative measures. The estimated coefficient for the US tariff shock turns marginally insignificant with a p-value of 0.11.[46] We detect a positively significant effect of $\Delta CHNInputTariff_{it}^{All}$, which implies a possible substitution towards inputs from non-US countries.

While our baseline analysis in Column 4, Table 1 focuses on the retaliatory tariffs levied by China on imported inputs, we account next for any possible impact on local economic activity that might arise from tariffs levied on imported consumption goods. To do so, we construct:

$$\Delta CHNConsTariff_{it} = \sum_{k \in \mathcal{C}} \frac{M_{ik0}^{US}}{M_{i\mathcal{C}0}} \Delta ImportTariff_{kt}^{US},$$

where $\mathcal{C}$ is the set of HS 6-digit products classified as consumption goods under the UN BEC, Revision 5. $M_{ik0}^{US}/M_{i\mathcal{C}0}$ is now the imports of products k sourced from the US, expressed as a share of total grid-level imports of consumption goods in 2016. Adding this variable in Column 3 of Table D.6, we continue to obtain a similar negative coefficient for the effects of the US tariff shock, but detect no statistically significant impact arising from either the retaliatory tariffs on intermediates or on consumption goods.

Column 4 explores whether there may have been substitution towards domestic sources of inputs as a result of the retaliatory tariffs on imports from the US. A limitation here is the lack of direct data on the domestic input purchases of Chinese firms, although we do have information from the customs data on whether grid locations within China may have been exporting intermediates and capital goods prior to the tariff war that overlap with the set of HS 6-digit codes on which retaliatory tariffs against the US were imposed. We use this

---

[46]The implied magnitude of the US tariff shock is also smaller. More specifically, a population-weighted standard deviation of $\Delta USTariff_{it}^{All}$ over Q1/2017-Q3/2019 (0.096) depresses night lights growth by 1.15(=-0.119×0.096×100) log points, while our baseline estimate reported in in Column 4 implies a magnitude of 1.63(=-0.59×0.028×100). The attenuation probably results from a larger degree of measurement error embedded in the alternative measure $\Delta USTariff_{it}^{All}$.

information to construct:

$$\Delta CHNExpWtdInputTariff_{it} = \sum_{k \in \mathcal{K}} \frac{X_{ik0}}{X_{i\mathcal{K}0}} \Delta ImportTariff_{kt}^{US},$$

where $X_{ik0}/X_{i\mathcal{K}0}$ is the exports of product $k \in \mathcal{K}$ in the base year, expressed as a share of total grid-i exports of intermediate and capital goods; this trade share is multiplied by the retaliatory tariff levied on imports of product k from the US. $\Delta CHNExpWtdInputTariff_{it}$ thus reflects whether exporters in grid i could have been in a position to supply inputs to other Chinese firms that were affected by the retaliatory tariffs. If such substitution were occurring, one might expect to see an increase in demand for these inputs, and hence an intensification of local economic activity associated with higher values of $\Delta CHNExpWtdInputTariff_{it}$. The coefficient estimate we obtain when we include this additional Bartik variable in Column 4 is statistically indistinguishable from zero. That said, we cannot exclude the possibility that producers may have switched to sourcing inputs from other Chinese firms that sell the bulk of their output domestically (i.e., that engage in minimal exporting and thus would not be picked up by this additional Bartik measure). Column 5 controls for an analogous export-share-weighted import tariff shock for consumption goods, $\Delta CHNExpWtdConsTariff_{i,t-1}$. Again, the estimated effect of the US tariff shock remain similar. It is worth pointing out that the specifications in Columns 4 and 5 to some extent account for the import competition channel if the export shares mimic local output (or employment) shares in the tradable sector. Without fine-grained data on industrial output and employment, we are not able to further tease out the effect of retaliatory tariffs on local economy through shielding import competition.

Column 5 considers an alternative set of initial share weights for the China input tariff shock Bartik variable. The variant we consider is:

$$\Delta CHNInputTariff_{it}^{alt} = \sum_{k \in \mathcal{K}} \frac{M_{ik0}^{US}}{M_{i0}} \Delta ImportTariff_{kt}^{US},$$

with the key difference being that we use the initial share of imports of inputs k when these are expressed as a share of total grid-level imports M_{i0}, instead of restricting this denominator to be just total grid-level imports of intermediates and capital goods. As Column 4 shows, this choice of initial share weights used to construct the China input tariff shock has little bearing on our results.

We next turn to ensure that the null effect of the input tariff shock detected in Table 1 is not driven by our choice of measurement. Specifically, using China's 2017 input-output (IO) table,[47]

---

[47]This IO table is obtained from the National Bureau of Statistics (NBS) of China, and is likely to reflect China's production technology across industries at the start of the trade war. There are 149 5-digit IO codes. To aggregate up the data on tariffs and trade shares, we construct a concordance between HS 6-digit codes and 5-digit IO codes based on the following bridges: (i) a crosswalk between 4-digit Chinese Standard Industry Classification (CSIC) codes (2017 version) and 5-digit Chinese IO codes (2017 version) from the NBS, (ii) a crosswalk between 4-digit CSIC codes (2017) and 4-digit ISIC Rev.4 codes from the NBS, and (iii) a crosswalk

we propose an alternative measure that leverages the variations stemming from cross-industry differences in input tariff shocks and cross-grid differences in industry structure:

$$\Delta CHNInputTariff_{it}^{io} = \sum_{\omega} \frac{X_{i\omega 0}}{X_{i0}} \Delta InputTariff_{\omega t},$$

where $\Delta InputTariff_{\omega t}$ denotes the year-on-year change in input tariffs of a 5-digit IO code ω faced by Chinese importers. Specifically, $\Delta InputTariff_{\omega t} = \sum_{\omega'} \alpha_{\omega'\omega} \Delta CHNTariff_{\omega't}$ à la Amiti and Konings (2007). Here, $\alpha_{\omega'\omega}$ is the direct requirement coefficient of an input ω' for a unit output of ω, and $\Delta CHNTariff_{\omega't}$ is China's retaliatory tariffs aggregated to the IO code level. We aggregate the industry-level tariff shocks to the grid level based on initial export shares, X_{iw0}/X_{i0}, which proxy for the sectoral composition in grid i. By construction, the measure captures the spillover impacts of retaliatory tariffs through import-export linkages within grid cells. As is shown in Column 7, consistent with our baseline findings, the exposure to input tariff shocks measured by $\Delta CHNInputTariff_{it}^{io}$ has a statistically insignificant impact on night lights growth.

In Column 8, we additively decompose the US tariff shock in (2) into a component for differentiated products and a component for non-differentiated products, based on the Rauch (1999) classification. Likewise, we additively decompose the China input tariff shock in (3) into two terms attributable to the tariff changes on differentiated and non-differentiated intermediate input products respectively. We find that the US tariff hikes on China's exports of differentiated goods had a more pronounced negative effect on night lights growth than that associated with exports of homogeneous goods. This suggests that Chinese exporters may have been less able to divert output with a high degree of product specificity to the domestic market or other destination countries.

Random Permutation Test. We conduct two random permutation tests to assess the sensitivity of the statistical inference to concerns about possible cross-grid correlation in the unobserved shocks.

First, following Adão et al. (2019), we randomly reshuffle the product-level US tariff shocks across 6-digit products, and at the same time reshuffle the product-level China input tariff shocks; we then re-build the respective Bartik regressors by combining the actual grid-level trade shares in 2016 with the placebo product-level shifters. (More specifically, we reshuffle the time series of both the US and China input tariff shocks over Q1/2018-Q3/2019 across HS 6-digit products.) This procedure is repeated for 300 sets of random permutations. We then re-run the baseline specification (Column 4 in Table 1) using the fictitious data. Since the shifters are randomly reshuffled, their effects on average should be close to zero. Moreover, if the actual tariff shocks have a causal effect on local economic outcomes, our baseline estimates of the respective tariff shock coefficients should be outliers in the distribution of placebo coefficients. Both of these features are verified in Figure D.2, which presents the cumulative distributions of

---

between 4-digit ISIC Rev.4 codes and HS 6-digit codes from Liao et al. (2020).

the placebo coefficients for the US tariff and China input tariff shocks; the baseline estimates from Column 4 of Table 1 are indicated by the vertical lines. Importantly, in both panels, the standard deviations of the placebo estimates are smaller than our baseline robust standard errors that are clustered at the province level. At the same time, the empirical p-value with which we would obtain a US tariff shock coefficient that is this large in magnitude is < 0.000. This alleviates the concern that our baseline standard errors may be downward-biased due to an underlying cross-grid correlation arising from similarity in grid-level export and/or import structure, that is not adequately accounted for by the province clusters.

In the second permutation test, we instead randomly reshuffle initial export and import shares across grids within a prefecture.[48] Figure D.3 presents the cumulative distributions of placebo coefficients for the US tariff and China input tariff shocks derived from 300 placebo samples, together with the respective baseline estimates from Table 1, Column 4 (vertical red lines). The standard deviations of the placebo estimates are similar to the baseline standard errors. We moreover find that only 2.3% of the placebo estimates of the effect of the US tariff shock are larger in absolute value than the baseline estimate of -0.5903, which suggests that this coefficient estimate is unlikely to be driven by coincidence.[49]

Robustness to Time-Varying Heterogeneous Treatment Effects. Building on the discussion in de Chaisemartin and D'Haultfoeuille (2020), if the treatment effects (i.e., of the tariff shocks) are heterogeneous both in timing across grids and in magnitude, the coefficient estimates obtained from a two-way fixed effects regression such as our equation (1) will be a weighted average of the treatment effects across grid-by-period (i, t) cells. As some of these weights can be negative, our baseline tariff shock coefficient can be negative even when the average treatment effect on the treated (ATT) is zero or even when the treatment effects across all (i, t) cells are positive. In such cases, our conclusion drawn from the baseline findings is misleading.

As a robustness check, we adopt the alternative estimator (i.e., DID_M) proposed by de Chaisemartin and D'Haultfoeuille (2020). This is an unbiased estimator of the ATT under reasonable assumptions and can be employed in cases where the treatment takes a finite number of ordered values. we adapt the estimator to our context where the grid-level treatment (i.e., the tariff shocks) is a continuous variable. Specifically, we group the observations into 20 equally-spaced bins based on $\Delta USTariff_{i,t-1}$. Within each bin, we assign the observations with the mid-point value of the corresponding bin. This discretized variable is denoted as $\Delta USTariff^d_{i,t-1}$. Since the DID_M estimator is designed for OLS estimation, we focus in the following analysis on OLS regressions that relate the change in night lights intensity to the grid-level measures based on Google Maps geo-information.[50]

---

[48]In practice, this is equivalent to reshuffling the time series of grid-level tariff shocks over Q1/2018 to Q3/2019 across grids within a prefecture.

[49]We obtain similar results when reshuffling tariff shocks across grids within provinces (available upon request).

[50]The results are similar when we employ the grid-level tariff measures based on the Amap geo-information

Column 1 in Table D.7 reports the estimated coefficient on the discretized version of the US tariff shock, $\Delta USTariff_{i,t-1}^d$, in an OLS specification in which we control for grid and prefecture-year-quarter fixed effects. Column 2 then applies the DID_M estimator; the coefficient of interest remains negative and statistically significant, similar to the baseline estimate in Column 1.[51] The finding provides some reassurance that our baseline results are robust to concerns about heterogeneous treatment effects. Columns 3 and 4 repeat the analysis, but replace the independent variable by the discretized China input tariff shock, $\Delta CHNInputTariff_{i,t-1}^d$. Both the conventional OLS and the DID_M estimators yield statistically insignificant coefficients.

D.2 Benchmarking the Inverse Elasticity of Night Lights

In this appendix section, we elaborate on how the inverse elasticity of night lights we have estimated in Table 2 compares against what has been reported in the prior literature, as well as against what one obtains in more conventional cross-country panel datasets.

Comparison with Henderson et al. (2012). A starting point of reference is the work of Henderson et al. (2012). We have adopted the same statistical framework that Henderson et al. (2012) laid out to link observed night lights to actual and observed income respectively in a location (see Section 4.1 in the main paper). There are however several differences to bear in mind: Henderson et al. (2012) examine real GDP rather than real GDP per capita. Their methodology moreover focuses on cross-sectional variation across countries, while we work instead with a panel of observations at the more detailed grid level.[52] Notwithstanding these differences, given the attention that Henderson et al. (2012) have received in the empirical literature on night lights, it is useful to discuss how our inverse elasticity estimate compares against what they have reported.

More specifically, Henderson et al. (2012)'s methodology for backing out the inverse elasticity of night lights proceeds as follows. The statistical framework implies three moment conditions for: (i) the variance of observed night lights, $var(x_{js})$; (ii) the variance of observed GDP, $var(z_{js})$; and (iii) the covariance between observed night lights and observed GDP, $cov(x_{js}, z_{js})$. (The notation here follows that in Section 4.1.) These data moments are functions of four parameters of interest: (i) the variance of the error term in measured night lights, σ_x^2; (ii) the variance of true GDP, σ_y^2; (iii) the variance of the error term in measured GDP, σ_z^2; and (iv) the inverse elasticity of night lights, $1/\beta$. The setup is thus under-identified, with one more parameter than data moment. The approach that Henderson et al. (2012) take is then to compute a range of plausible values of β, corresponding respectively to different assumed

---

(available upon request).

[51]The standard error in Column 2 is larger. As is shown in de Chaisemartin and D'Haultfoeuille (2020), the DID_M estimator could be less efficient than the conventional two-way fixed effects estimator when the treatment effect is in fact constant.

[52]Another point of departure is that many existing studies, including Henderson et al. (2012), use the night lights data from the DMSP-OLS satellite which is top-coded. This data series ceased in 2013, and has been superseded by the VIIR-DNB data that we have used in our analysis; the latter is not subject to top-coding.

values for the signal-to-total-variance ratio, $\sigma_y^2/(\sigma_y^2 + \sigma_z^2)$, in the GDP variable. In practice, Henderson et al. (2012) work with a generalization of the statistical framework that allows for a different signal-to-total-variance ratio across two subsets of countries, where the categorization is based on a World Bank assessment of the data quality of countries' reported national accounts statistics.

In terms of empirical implementation, Henderson et al. (2012) use a sample of 113 low- and middle-income countries, and work with long-differences of the data between 1992/1993 and 2005/2006. Table 5 in their paper reports the implied β values they obtain. The estimates of β range from 1.034 to 1.724, across the values for the signal-to-total-variance ratio in GDP they consider. Reciprocating these estimates, this translates into inverse night lights elasticities with respect to GDP that range from 0.58 to 0.97, as we have reported in Section 4.2.

A noteworthy extension that builds on Henderson et al. (2012) is the recent work of Hu and Yao (2022). They generalize the statistical framework from above to allow: (i) the measurement error term $\varepsilon_{z,js}$ in the relationship between observed and actual income to be drawn from a distribution that depends on countries' statistical capacity; and (ii) the measurement error term $\varepsilon_{x,js}$ in the relationship between observed night lights and actual income to be drawn from a distribution that is indexed by locations. Hu and Yao (2022) then use nonparametric sieve maximum likelihood methods to estimate the measurement error distributions. Using data from 162 countries and annual growth in GDP from 1993-2013, they obtain a central estimate for the elasticity of night lights with respect to GDP of 1.3, or an inverse elasticity of 0.77 that sits in the middle of the range that Henderson et al. (2012) had earlier found.

In sum, the prior work that adopts country real GDP as the income measure of interest yields inverse elasticity estimates that are generally larger than what we have found in Table 2, Panel A, for real GDP per capita in China's prefectures.

Comparison with Pinkovskiy and Sala-i-Martin (2016). A more direct benchmark to provide would be to size up our estimates against what one would obtain from applying the novel instrumental variable strategy we propose on a conventional panel dataset of country income per capita. For this purpose, we use the dataset of Pinkovskiy and Sala-i-Martin (2016), comprising annual observations of log GDP per capita (adjusted for purchasing power parity), from 1993-2010. We focus here on the subset of these countries which had a population greater than 1 million in 1993.

We should first point out that the elasticities that Pinkovskiy and Sala-i-Martin (2016) estimate are not directly comparable to those we have reported in our Table 2, Panel A. This is because Pinkovskiy and Sala-i-Martin (2016) run regressions in which log night lights is the dependent variable against country income per capita and various sets of fixed effects, whereas our estimating equation in (7) has instead country income per capita as the left-hand side variable. To perform this benchmarking exercise, we therefore run the specification in our equation (7) on the Pinkovskiy and Sala-i-Martin (2016) panel dataset, using a one-period lag of log night lights as an instrumental variable for $\ln(Light_{js})$; *in lieu* of prefecture and province-

year fixed effects, we control for country and year fixed effects instead, and we report standard errors clustered by country.

Table D.8 reports the results, with Columns 1-7 being the analogues of the corresponding columns in Table 2 in the main paper. As a reminder, Columns 1-3 report OLS estimates, while Columns 4-7 report 2SLS estimates; the columns differ in terms of whether or not we drop the tail 1% or 5% within each year of income per capita values, and Column 7 further weights observations by country population. The OLS estimates from Columns 1-3 yield inverse night lights elasticities with respect to GDP per capita from 0.26 to 0.29. As was the case in Table 2, the 2SLS specifications deliver larger estimates that range from 0.37 to 0.41; this could be indicative of measurement error in the night lights data that the instrumental variable helps to address, to the extent that this error term is serially uncorrelated.

In Panel B of Table D.8, we re-run the Panel A specifications, but estimate separate $\ln(Light_{js})$ coefficients for those countries that are classified as high versus non-high income (by the World Bank) through the use of interaction terms with dummy variables for each of these subsets of countries. The coefficients we obtain for the non-high income countries are much in the same ballpark as the inverse elasticity estimates that we reported in Table 2 from the Chinese prefecture-level data. This provides some reassurance that the relationship between observed night lights and true income per capita is broadly stable across different levels of geographic aggregation.

Estimations of $1/\beta$ with Data at Different Aggregation Levels. We examine the sensitivity of the estimate of $1/\beta$ using different datasets with geographic units defined at various aggregation levels. To this end, we compile an unbalanced county-level panel data using the data reported in China Statistical Yearbooks (County-Level),[53] and a balanced province-level panel data based on China Statistical Yearbooks.

Columns 1 and 2 in Table D.11 report the results of county-level regressions in which the lagged night lights variable, $\ln(Light_{js-1})$, is used as an instrument for $\ln(Light_{js})$. The estimates resemble the baseline estimate based on the prefecture-level analysis. Columns 3 and 4 conduct the analysis at the province level. Again, we find statistically similar estimates, although they are less precise due to the smaller sample size. In sum, the finding that the estimated elasticity remains stable across analyses at different administration levels lends us some confidence in extrapolating the estimated inverse elasticity to the grid-level to infer the impacts of tariff shocks on income growth.

Visualizing the grid-level night lights relationships (Figure D.4). Last but not least, we return to our regression estimates from Table 2, to provide more visual evidence on the linear nature of the relationship between log GDP per capita (respectively, log manufacturing employment) and log night lights across Chinese prefectures. Figure D.4 presents residualized scatterplots based on the 2SLS specifications, where the variable on the vertical axis is log GDP per capita (respectively, log manufacturing employment) after residualizing out the variation

---

[53]There are 2044 counties in the unbalanced panel.

that can be explained by province-year and prefecture fixed effects. Likewise, the variable on the horizontal axis is predicted log night lights (from the first-stage regression) after residualizing out the role of these same fixed effects. Panels A and B present these relationships based on regressions using all available data points (i.e., Columns 4 and 11 in Table 2 respectively), while Panels C and D drop observations in the tail 5% of the distribution within each year (i.e., these are based on Columns 6 and 13 in Table 2). The figures reveal smooth upward-sloping relationships, with no clear signs of non-linearities or overly influential outliers.

D.3 Effects of Nonlocal Tariff Shocks

We report in this appendix section on the regressions exploring the potential impact of non-local tariff shocks on grid-level night lights. As discussed in Section 4.3, such regressions are informative of the full effect of the US-China tariff war – taking into account both partial and general equilibrium forces – on local economic performance, when viewed through the lens of the quantitative spatial model in Adão et al. (2020).

Tables D.9 and D.10 explore several approaches for capturing the potential impact of non-local tariff shocks. In Table D.9, we investigate whether there is evidence of spillovers from tariff shocks in neighboring grid cells on local night lights intensity. For each grid cell i, these neighboring shocks are constructed as the population-weighted average of the US and China input tariff shocks in equations (2) and (3) across grids whose centroids are within: (i) a 15km radius (equivalently, grids contiguous with i); (ii) a (15,30] km ring; (iii) a (30,50] km ring, and; (iv) a (50,100] km ring. We then augment our baseline regression specification in (1) – as in equation (8) – successively with these neighboring tariff shock terms to explore whether there is evidence of significant spillovers on local night lights.

Columns 1 to 5 in Table D.9 present the results from specifications that include grid and prefecture-year-quarter fixed effects; we use the tariff shock terms for each neighboring ring radius in turn in Columns 1-4, before including all of them jointly in Column 5. (Throughout the exploration in this section, we use the Amap-based versions of these nonlocal shock variables as instruments for the Google-based versions in the 2SLS estimation.) The coefficient estimates point to negative spillover effects from US tariff shocks and the China input tariff shocks in adjacent rings that are within 15km of the grid in question, from US tariff shocks within the 15-30km radius, as well as from China input tariff shocks within the 30-50km radius. These neighboring grid spillover effects are however not robust in Column 6 to the inclusion of the grid-level initial characteristics W_{i0} interacted with year-quarter fixed effects. Of note, the coefficient of the US tariff shock in the own-grid cell remains negative and significant throughout all columns, with a magnitude that is virtually unchanged from what we have found in our baseline results in Table 1, while the China input tariff shock in the own-grid cell is always statistically insignificant. It thus appears that neighboring spillover effects, if any, would tend to reinforce the negative effect of a grid cell's own direct exposure to the US tariff shock.

In Columns 1-3 of Table D.10, we aggregate these neighboring ring tariff shocks using a

"market-potential" weighted average. Specifically, we summarize the US tariff shocks experienced within the neighboring rings in Table D.9 as follows:

$$\text{Non-local } \Delta USTariff_{it} = \sum_{r=1}^{4} \frac{L_{r0} D_{ir}^{-\delta}}{\sum\limits_{h=1}^{4} L_{h0} D_{ih}^{-\delta}} \Delta USTariff_{Ring_r(i),t},$$

where $Ring_r(i)$ (with $r = 1, \ldots, 4$) denotes the set of grid cells that lie within each of the four distance rings considered in Table D.9 with respect to grid i; $\Delta USTariff_{Ring_r(i),t}$ is the population weighted average of tariff shocks across grids in $Ring_r(i)$; L_{r0} is the population located in grids in $Ring_r$ in the baseline period; and D_{ir} is the distance between grid i and $Ring_r$, which we take to be 7.5km, 22.5km, 40km, and 75km respectively. Intuitively, more weight is assigned to neighboring grid rings that have a higher population and that are less distant from grid i, where we set the distance exponent to $\delta = 5$ following the empirical implementation in Adão et al. (2020). Columns 1-3 of Table D.10 include this and an analogously-constructed nonlocal China input tariff shock term; all columns include grid fixed effects, but they differ in terms of whether year-quarter or prefecture-year-quarter fixed effects are used, and whether the time-varying effects of initial grid characteristics are controlled for. The results here are in line with Table D.9, suggesting that there may have been negative spillovers on own-grid night lights intensity from nonlocal US tariff shocks, but not from the China input tariff shocks in neighboring rings.

One concern that emerges with the preceding nonlocal measures is that grid cells that are more than 100km away are excluded from consideration. We therefore supplement our analysis in Columns 4-6 with a nonlocal tariff shock measure that is a market-potential weighted average measure across all prefectures j, where:

$$\text{Non-local } \Delta USTariff_{it} = \sum_{j} \frac{L_{j0} D_{ij}^{-\delta}}{\sum\limits_{n} L_{n0} D_{in}^{-\delta}} \Delta USTariff_{j(i),t},$$

where L_{j0} is the population of prefecture j in the baseline period; D_{ij} is the distance between grid i and the population-weighted centroid of prefecture j; and $\delta = 5$. The prefecture-level US tariff shock, $\Delta USTariff_{j(i),t}$, is defined according to:

$$\Delta USTariff_{j(i),t} = \begin{cases} \sum\limits_{p \in \mathcal{J}} \frac{L_{p0}}{\sum\limits_{q \in \mathcal{J}} L_{q0}} \Delta USTariff_{p,t} & \text{if } i \notin \mathcal{J} \\ \sum\limits_{p \in \mathcal{J}, p \neq i} \frac{L_{p0}}{\sum\limits_{q \in \mathcal{J}, q \neq i} L_{q0}} \Delta USTariff_{p,t} & \text{if } i \in \mathcal{J} \end{cases}$$

where $\mathcal{J}$ is the set of grid cells located in prefecture j; this excludes the own-grid cell i from the constructed prefecture-level tariff shock if i is located in the prefecture in question.[54] The

---

[54]We aggregate the tariff shocks first to the prefecture level in this manner, rather than directly computing market-potential weighted averages across the grid-level tariff shocks. This is because we run into computational

nonlocal China input tariff shock is constructed analogously. We find some hints that this alternative nonlocal US tariff shock measure correlates negatively with local night lights growth (Columns 4-5), although this is not precisely estimated and is not robust to the inclusion of the grid-level initial W_{i0}'s interacted with time fixed effects. The nonlocal China input tariff shock once again displays no distinctive relationship with grid-level night lights.

Summing up, we have investigated several measures for capturing the nonlocal incidence of tariff shocks on economic activity within a given location. The reduced-form elasticities, when significant, point to a potential negative influence of US tariff shocks in neighboring locations, even while the coefficient on the own-grid's direct exposure to the US tariff shocks remains stable in magnitude. This leads us to conclude that general equilibrium forces related to the US tariff shocks are likely reinforcing the negative impact on local economic activity of direct tariff exposure, and hence that our difference-in-differences estimates are likely on average to be under-stating the full adverse effects of the tariff war.

D.4 County-Level Analysis

In Table D.12, we re-estimate equation (1) using the data at the county level. Due to the lack of information on county of location in the customs data, we map firms to the corresponding counties based on their geo-coordinates. Again, to alleviate the attenuation bias, the measures on the basis of Amap geo-coordinates serve as instrumental variables for the corresponding measures constructed using geo-coordinates from Google Maps. Parallel to the grid-level analysis, we control for county fixed effects, prefecture-by-year-quarter fixed effects, and time-varying effects of initial county characteristics. Standard errors are clustered at the province level. We also winsorize the $\Delta \ln(Light_{it})$ observations that are above the 97.5th percentile or below the 2.5th percentile within each period t to reduce the influence of outliers.

As is detected in Column 1, the estimated coefficient for the US tariff shock has a slightly larger magnitude, but remains statistically similar to the baseline grid-level estimate (-0.63 v.s. -0.59). The estimated effect of the China input tariff shock is insignificant both statistically and economically. Columns 2 and 3 present the county-level evidence that the adverse impacts of the US tariff shocks are more concentrated in locations with a higher commuting intensity, which is in line with the findings in Section 4.4.1.

---

constraints, with the latter approach requiring us to maintain a matrix of 10^{12} bilateral distances.

Table D.1: Tariff Shocks and Night Lights Intensity, 2SLS
(Extended Sample Period through End-2020)

Dep. Var.: $\Delta \ln(Light_{it})$	(1)	(2)	(3)	(4)
$\mathbf{1}(Q1\&2/2018) \times \Delta USTariff_{i,t-1}$	2.7736**	1.4906	1.4910	1.4782
	(1.3084)	(1.4876)	(1.4860)	(1.4919)
$\mathbf{1}(Q3\&4/2018) \times \Delta USTariff_{i,t-1}$	-0.3759	-1.3801*	-1.3791*	-1.3821*
	(0.6352)	(0.8046)	(0.8043)	(0.8052)
$\mathbf{1}(Q1\&2/2019) \times \Delta USTariff_{i,t-1}$	-0.5985*	-0.8980**	-0.8978**	-0.8998**
	(0.2965)	(0.4374)	(0.4370)	(0.4375)
$\mathbf{1}(Q3\&4/2019) \times \Delta USTariff_{i,t-1}$	-0.0022	-0.2376	-0.2359	-0.2364
	(0.1259)	(0.2347)	(0.2344)	(0.2335)
$\mathbf{1}(Q1\&2/2020) \times \Delta USTariff_{i,t-1}$	-0.4954**	-0.5407**	-0.5489**	-0.5371**
	(0.1859)	(0.2588)	(0.2588)	(0.2542)
$\mathbf{1}(Q3\&4/2020) \times \Delta USTariff_{i,t-1}$	-1.2513**	0.2374	0.2359	0.2345
	(0.4749)	(0.4325)	(0.4330)	(0.4337)
$\mathbf{1}(Q3\&4/2018) \times \Delta CHNInputTariff_{i,t-1}$	1.3679	0.5910	0.5950	0.5844
	(1.2380)	(1.1958)	(1.1942)	(1.1920)
$\mathbf{1}(Q1\&2/2019) \times \Delta CHNInputTariff_{i,t-1}$	0.5689	0.2216	0.2265	0.2171
	(0.5565)	(0.9437)	(0.9427)	(0.9413)
$\mathbf{1}(Q3\&4/2019) \times \Delta CHNInputTariff_{i,t-1}$	0.5512	-0.0584	-0.0394	-0.0594
	(0.3741)	(0.4934)	(0.4916)	(0.4925)
$\mathbf{1}(Q1\&2/2020) \times \Delta CHNInputTariff_{i,t-1}$	0.0944	-0.2552	-0.2788	-0.2553
	(0.5494)	(0.7415)	(0.7414)	(0.7397)
$\mathbf{1}(Q3\&4/2020) \times \Delta CHNInputTariff_{i,t-1}$	-2.4048**	-0.7868	-0.7805	-0.7883
	(0.9683)	(1.1232)	(1.1209)	(1.1214)
$\mathbf{1}(Q4/2019) \times \mathbf{1}(DistDecWuhan)$			0.0230*	
			(0.0126)	
$\mathbf{1}(Q1/2020) \times \mathbf{1}(DistDecWuhan)$			0.0119	
			(0.0141)	
$\mathbf{1}(Q2/2020) \times \mathbf{1}(DistDecWuhan)$			-0.0587*	
			(0.0302)	
$\mathbf{1}(Q3/2020) \times \mathbf{1}(DistDecWuhan)$			0.0085	
			(0.0273)	
$\mathbf{1}(Q4/2020) \times \mathbf{1}(DistDecWuhan)$			-0.0014	
			(0.0119)	
Grid FE	Y	Y	Y	Y
Prefecture×Year-Quarter FE	Y	Y	Y	Y
Grid W_{i0}×Year-Quarter FE	N	Y	Y	Y
Grid $\ln(DistWuhan)$× Covid-quarter FE	N	N	N	Y
Observations	1,147,689	1,147,689	1,147,689	1,147,689
F-stat	1.843	1.584	1.584	1.584

Notes: The coefficients reported are from the regression specification that generates Figure 2. All columns report 2SLS estimates, using the Amap grid-level tariff shocks as instrumental variables for the corresponding Google Maps grid-level tariff shocks. The initial grid characteristics, W_{i0}, whose time-varying effects are included in Columns 2-4 are: the US share in exports, the US share in imports of intermediates, log exports per capita, log intermediate imports per capita, and log 2016 mean night lights intensity; grid-level exports and imports geolocated via Amap are used to construct the first four of these W_{i0} variables. All regressions are weighted by grid population in 2015, with a minimum population of 1 imputed for cells with zero population in the raw data. The $\mathbf{1}(DistDecWuhan)$ variable in Column 3 is an indicator for whether a grid cell is within the first decile of observations in terms of proximity (grid-cell distance) to Wuhan; this is interacted with a set of Covid-quarter fixed effects, for Q4/2019 to Q4/2020. Column 4 includes the log grid-cell distance to Wuhan interacted with the set of Covid-quarter fixed effects (estimates available on request). Standard errors are clustered at the province level. *** p<0.01, ** p<0.05, * p<0.1.

Table D.2: Basic Pre-Trend Checks, 2SLS

Dep. Var.:	$\Delta \ln(Light_{it})$	$\Delta \ln(Light_{i,t-1})$	$\Delta \ln(Light_{i,t-2})$	$\Delta \ln(Light_{i,t-3})$
	(1)	(2)	(3)	(4)
$\Delta USTariff_{i,t-1}$	-0.5903**	-0.2631	0.1072	0.0808
	(0.2673)	(0.2699)	(0.2584)	(0.3750)
$\Delta CHNInputTariff_{i,t-1}$	0.5509	0.3239	-0.0516	0.1986
	(0.5555)	(0.4651)	(0.3561)	(0.5362)
Grid FE	Y	Y	Y	Y
Prefecture×Year-Quarter FE	Y	Y	Y	Y
Grid W_{i0}×Year-Quarter FE	Y	Y	Y	Y
Observations	669,845	669,845	669,846	673,052
F-stat	21.22	21.22	21.22	21.22

Notes: The dependent variable in Columns 1-4 is $\ln(Light_{it})$ and its successive one-period lags. All columns use the Amap grid-level tariff shocks as instrumental variables for the corresponding Google Maps grid-level tariff shocks. The initial grid characteristics, W_{i0}, whose time-varying effects are included are: the US share in exports, the US share in imports of intermediates, log exports per capita, log intermediate imports per capita, and log 2016 mean night lights intensity; grid-level exports and imports geolocated via Amap are used to construct the first four of these W_{i0} variables. All regressions are weighted by grid population in 2015, with a minimum population of 1 imputed for cells with zero population in the raw data. Standard errors are clustered at the province level. *** p<0.01, ** p<0.05, * p<0.1.

Table D.3: Robustness: Additional Time-varying controls, 2SLS

Dep. Var.: $\Delta \ln(Light_{it})$	(1)	(2)	(3)	(4)	(5)
$\Delta USTariff_{i,t-1}$	-0.5803**	-0.5407**	-0.6587**	-0.5768**	-0.6398***
	(0.2626)	(0.2471)	(0.2494)	(0.2629)	(0.2237)
$\Delta CHNInputTariff_{i,t-1}$	0.5219	0.2120	0.2969	0.5374	0.1754
	(0.5636)	(0.6546)	(0.8646)	(0.5565)	(0.8640)
Grid FE	Y	Y	Y	Y	Y
Prefecture×Year-Quarter FE	Y	Y	Y	Y	Y
Grid W_{i0}×Year-Quarter FE	Y	Y	Y	Y	Y
Additional Grid W_{i0}×Year-Quarter FE	Log Population	Trade shares by HS Segment	Trade Shares, US by HS Segment	State-Owned Export Share	All together
Observations	669,845	669,845	669,845	669,845	669,845
F-stat	21.36	21.92	25.01	21.10	25.09

Notes: All columns use the Amap grid-level tariff shocks as instrumental variables for the corresponding Google Maps grid-level tariff shocks. The baseline set of initial grid characteristics, W_{i0}, whose time-varying effects are included in all columns are: the US share in exports, the US share in imports of intermediates, log exports per capita, log intermediate imports per capita, and log 2016 mean night lights intensity. The additional grid W_{i0} controls whose time-varying effects are included are: log population (Column 1), export shares and imported input shares by HS segment (Column 2), the US share in exports and the US share in imports of intermediates by HS segment (Column 3), and the share of exports accounted for by state-owned enterprises (Column 4); these are used jointly in Column 5. Grid-level exports and imports geolocated via Amap are used to construct the relevant W_{i0} variables. All regressions are weighted by grid population in 2015, with a minimum population of 1 imputed for cells with zero population in the raw data. Standard errors are clustered at the province level. *** p<0.01, ** p<0.05, * p<0.1.

Table D.4: Robustness: Basic Specification Checks, 2SLS

	FE Model in Levels (1)	IVs for W_{i0} Grid Controls (2)	Interchange Google Maps & Amap (3)	Alternative Night Lights Measure (4)	Exclude Grids with Zero Population (5)	Province× Year-Quarter FE (6)	Excl. Top 5 Prefectures by GDP (7)	Two-Way Clustered SEs (8)
$USTariff_{i,t-1}$	-0.5236**							
	(0.2515)							
$CHNInputTariff_{i,t-1}$	0.4143							
	(0.5885)							
$\Delta USTariff_{i,t-1}$		-0.5949**	-0.6400*	-1.2920**	-0.5903**	-0.7097*	-0.5683**	-0.5903**
		(0.2707)	(0.3701)	(0.6084)	(0.2673)	(0.3832)	(0.2688)	(0.2625)
$\Delta CHNInputTariff_{i,t-1}$		0.5625	1.1291	1.3337	0.5509	0.4071	0.6150	0.5509
		(0.5548)	(0.7721)	(1.3794)	(0.5555)	(0.5812)	(0.5773)	(0.7061)
Grid FE	N	Y	Y	Y	Y	Y	Y	Y
Prefecture×Year-Quarter FE	Y	Y	Y	Y	Y	N	Y	Y
Grid W_{i0}×Year-Quarter FE	Y	Y	Y	Y	Y	Y	Y	Y
Grid×Quarter-of-Year FE	Y	N	N	N	N	N	N	N
Grid×Year-Quarter Linear Trend	Y	N	N	N	N	N	N	N
Observations	1,057,218	669,845	669,845	676,852	487,291	669,845	662,040	669,845
F-stat	19.83	1.681	34.57	21.22	21.22	10.12	15.32	10.20

Notes: All columns report 2SLS regressions. The dependent variable in Column 1 is $\ln(Light_{it})$, this being a specification that uses variables in levels rather than expressed in year-on-year changes; the dependent variable in all other columns is $\Delta \ln(Light_{it})$. Unless otherwise stated, the Amap grid-level tariff shocks are used as instrumental variables for the corresponding Google Maps grid-level tariff shocks. The initial grid characteristics, W_{i0}, whose time-varying effects are included in all columns are: the US share in exports, the US share in imports of intermediates, log exports per capita, log intermediate imports per capita, and log 2016 mean night lights intensity; grid-level exports and imports geolocated via Amap are used to construct the first four of these W_{i0} variables. Column 2 uses instead the corresponding Google Maps-based W_{i0} variables. Column 2 uses instead the corresponding Google Maps-based W_{i0} measures interacted with year-quarter fixed effects, and instruments for these using the Amap-based W_{i0}'s and their interactions with year-quarter fixed effects. Column 3 interchanges the roles of the Google Maps and Amap grid-level variables, by using the Google Maps tariff shocks as an IV for the Amap tariff shocks, while controlling for Google Maps-based grid controls W_{i0} interacted with year-quarter fixed effects. Column 4 uses the alternative VIIR-DNB night lights intensity measure that incorporates a correction for stray light. Column 5 drops grid cells i with zero population in the raw data. All regressions are weighted by grid population in 2015; a minimum population of 1 is imputed for zero-population cells in all columns other than Column 5. Column 6 drops prefecture×year-quarter fixed effects, while controlling for province×year-quarter fixed effects. Columns 7 drops the grid cells in the top 5 prefectures ranked by GDP in 2017. Standard errors in Column 8 are two-way clustered by province and by the 2-digit HS code that accounts for the most value in grid-level exports (geolocated via Google Maps). Standard errors in all other columns are clustered at the province level. *** p<0.01, ** p<0.05, * p<0.1.

Table D.5: Robustness: Controlling for Other Policy Shocks, 2SLS

Dep. Var.: $\Delta \ln(Light_{it})$	MFN Tariff (1)	Exchange Rate (2)	VAT (3)	All Policies (4)
$\Delta USTariff_{i,t-1}$	-0.5961**	-0.5970**	-0.5539**	-0.5723**
	(0.2706)	(0.2695)	(0.2546)	(0.2526)
$\Delta CHNInputTariff_{i,t-1}$	0.5495	0.5744	0.5195	0.5538
	(0.5562)	(0.5511)	(0.5619)	(0.5520)
$\Delta CHNMFNInputTariff_{i,t-1}$	-0.2598			-0.0657
	(0.5021)			(0.5488)
$\Delta ExportExRate_{i,t-1}$		-0.1284		-0.2056
		(0.1454)		(0.1694)
$\Delta ImportInputExRate_{i,t-1}$		-0.1619		-0.1629
		(0.1723)		(0.1813)
$\Delta ExportValAddTax_{i,t-1}$			1.0929	1.3712
			(0.9528)	(1.0768)
$\Delta ImportInputValAddTax_{i,t-1}$			-1.4104*	-1.1754
			(0.8231)	(0.8278)
Grid FE	Y	Y	Y	Y
Prefecture×Year-Quarter FE	Y	Y	Y	Y
Grid W_{i0}×Year-Quarter FE	Y	Y	Y	Y
Observations	669,845	669,845	669,845	669,845
F-stat	14.31	11.13	10.87	7.117

Notes: All columns report 2SLS regressions, using the Amap grid-level tariff, exchange rate and VAT shocks as instrumental variables for the corresponding Google Maps grid-level tariff, exchange rate and VAT shocks. The initial grid characteristics, W_{i0}, whose time-varying effects are included in all columns are: the US share in exports, the US share in imports of intermediates, log exports per capita, log intermediate imports per capita, and log 2016 mean night lights intensity; grid-level exports and imports geolocated via Amap are used to construct the first four of these W_{i0} variables. All regressions are weighted by grid population in 2015, with a minimum population of 1 imputed for cells with zero population in the raw data. Standard errors are clustered at the province level. *** p<0.01, ** p<0.05, * p<0.1.

Table D.6: Robustness: Alternative Measures of Tariff Shocks, 2SLS

Dep. Var:: $\Delta \ln(Light_{it})$	Placebo ADH8 Weights for Tariff Shocks (1)	Alternative Weights: All Ctry. (2)	Controlling for Consumption Tariff Shocks (3)	Controlling for Exp.-Weighted Input Tariffs (4)	Controlling for Exp.-Weighted Tariff Shocks (5)	Alternative Weights for Input Tariffs (6)	IO Table Based Input Tariffs (7)	Differentiated vs Homog. Products (8)
$\Delta USTariff f_{i,t-1}^{ADH8}$	-0.1714							
	(0.1670)							
$\Delta CHNInputTariff f_{i,t-1}^{ADH8}$	0.2528							
	(0.2249)							
$\Delta USTariff f_{i,t-1}^{All}$		-0.1192†						
		(0.0729)						
$\Delta CHNInputTariff f_{i,t-1}^{All}$		0.3041***						
		(0.0816)						
$\Delta USTariff f_{i,t-1}$			-0.6013**	-0.5921**	-0.5751**	-0.5952**	-0.5762**	
			(0.2723)	(0.2647)	(0.2652)	(0.2677)	(0.2719)	
$\Delta CHNInputTariff f_{i,t-1}$			0.5558	0.5433	0.5424			
			(0.5519)	(0.5550)	(0.5551)			
$\Delta CHNConsTariff f_{i,t-1}$			-0.2695					
			(0.3098)					
$\Delta CHNExpWtdInputTariff f_{i,t-1}$				-0.0633	-0.0705			
				(0.1296)	(0.1314)			
$\Delta CHNExpWtdConsTariff f_{i,t-1}$					0.0496			
					(0.0702)			
$\Delta CHNInputTariff f_{i,t-1}^{alt}$						0.6758		
						(0.5126)		
$\Delta CHNInputTariff f_{i,t-1}^{io}$							-0.0791	
							(0.1652)	
$\Delta USTariff f_{i,t-1}$, Diff.								-0.7763***
								(0.2586)
$\Delta USTariff f_{i,t-1}$, Homog.								-0.3053
								(0.4071)
$\Delta CHNInputTariff f_{i,t-1}$, Diff.								0.8983
								(0.6223)
$\Delta CHNInputTariff f_{i,t-1}$, Homog.								0.3368
								(0.7846)
Grid FE	Y	Y	Y	Y	Y	Y	Y	Y
Prefecture×Year-Quarter FE	Y	Y	Y	Y	Y	Y	Y	Y
Grid W_{i0}×Year-Quarter FE	Y	Y	Y	Y	Y	Y	Y	Y
Observations	669,845	669,845	669,845	669,845	669,845	669,845	669,845	669,845
F-stat	95.85	172.8	13.53	14.32	10.72	25.56	102.2	10.70

Notes: All columns report 2SLS regressions, using the respective versions of the Amap grid-level tariff shocks as instrumental variables for the corresponding Google Maps grid-level tariff shocks. The initial grid characteristics, W_{i0}, whose time-varying effects are included in all columns are: the US share in exports, log exports per capita, log intermediate imports per capita, and log 2016 mean night lights intensity; grid-level exports and imports geolocated via Amap are used to construct the first four of these W_{i0} variables. All regressions are weighted by grid population in 2015, with a minimum population of 1 imputed for cells with zero population in the raw data. Standard errors are clustered at the province level. *** p<0.01, ** p<0.05, * p<0.1, † p<0.15.

Table D.7: Tariff Shocks and Night Light Intensity: Alternative Estimators

Dep. Var.: $\Delta \ln(Light_{it})$	(1) FE estimator	(2) $\mathrm{DID_M}$	(3) FE estimator	(4) $\mathrm{DID_M}$
$\Delta ExportTariff_{i,t-1}^d$	-0.3477*** (0.1186)	-0.4519*** (0.1814)		
$\Delta InputTariff_{i,t-1}^d$			-0.1800 (0.1078)	-0.1604 (0.2264)
Grid FE	Y	Y	Y	Y
Prefecture×Quarter×Year FE	Y	Y	Y	Y
Observations	669,845	669,845	669,845	669,845

Notes: This table presents estimates of the effect of tariff shocks on the growth of night lights intensity. Columns 1 and 3 report the conventional two-way fixed effects estimates based on the specifications in Columns 1 and 2 of Table 1, respectively; Columns 2 and 4 report the corresponding $\mathrm{DID_M}$ estimates computed by the `did_multipleGT` Stata package. Standard errors in Columns 1 and 3 are clustered at the province level. Standard errors in Columns 2 and 4 are computed by the `did_multipleGT` Stata package based on 100 samples block bootstrapped at the province level. *** p<0.01, ** p<0.05, * p<0.1

Table D.8: GDP per capita and Night Lights Intensity
Country Panel Data (1993-2010)

	Dep. Var.: $\ln(GDPpc_{ct})$						
Panel A.	(1) OLS	(2) OLS	(3) OLS	(4) 2SLS	(5) 2SLS	(6) 2SLS	(7) 2SLS
$\ln(Light_{ct})$	0.2898***	0.2927***	0.2585***	0.3943***	0.4061***	0.3666***	0.3875***
	(0.0520)	(0.0524)	(0.0498)	(0.0661)	(0.0648)	(0.0591)	(0.1079)
Observations	2,567	2,538	2,347	2,567	2,538	2,347	2,347
R-squared	0.9919	0.9922	0.9939	—	—	—	—
F-stat	—	—	—	126.7	119.6	83.39	236.8
Panel B.	(8) OLS	(9) OLS	(10) OLS	(11) 2SLS	(12) 2SLS	(13) 2SLS	(14) 2SLS
$(1 - High_c) \times \ln(Light_{ct})$	0.3235***	0.3264***	0.2984***	0.4014***	0.4128***	0.3729***	0.3769***
	(0.0479)	(0.0480)	(0.0438)	(0.0675)	(0.0661)	(0.0607)	(0.1075)
$High_c \times \ln(Light_{ct})$	0.0445	0.0486	0.0351	0.2360**	0.2554**	0.2629**	0.5460**
	(0.0437)	(0.0450)	(0.0411)	(0.1181)	(0.1154)	(0.1182)	(0.2216)
Observations	2,567	2,538	2,347	2,567	2,538	2,347	2,347
R-squared	0.9922	0.9925	0.9941	—	—	—	—
F-stat	—	—	—	1.501	1.488	1.476	11.41
Year FE	Y	Y	Y	Y	Y	Y	Y
Country FE	Y	Y	Y	Y	Y	Y	Y
Trimmed	N	Tail 1%	Tail 5%	N	Tail 1%	Tail 5%	Tail 5%
Weighted by population	N	N	N	N	N	N	Y

Notes: Based on the cross-country panel dataset from Pinkovskiy and Sala-i-Martin (2016). The dependent variable is log country GDP per capita adjusted for purchasing power parity, from the World Bank. In each panel, the first three columns report OLS regressions, while the remaining columns perform 2SLS regressions in which the lagged night lights variable, $\ln(Light_{j,s-1})$ is used as an IV. Columns 2 and 5 drop observations where the annual change in log GDP per capita between years $s-1$ and s is below the 1st percentile or above the 99th percentile values of its distribution in that year. Columns 3, 6 and 7 further drop observations where the annual change in the dependent variable is below the 5th percentile or above the 95th percentile of its distribution in each given year. Column 7 weights the observations by initial prefecture population in 2015. $High_c$ is a dummy variable for whether the country is classified as high income by the World Bank. Countries with an initial population less than 1 million are excluded from the sample. Standard errors are clustered at the province level. *** p<0.01, ** p<0.05, * p<0.1.

Table D.9: Local and Neighboring Tariff Shocks and Night Lights Intensity, 2SLS

Dep. Var.: $\Delta \ln(Light_{it})$	(1)	(2)	(3)	(4)	(5)	(6)
$\Delta USTariff_{i,t-1}$	-0.6878***	-0.7649***	-0.7761***	-0.7731***	-0.6609***	-0.5426**
	(0.1918)	(0.2027)	(0.2141)	(0.2099)	(0.1902)	(0.2614)
$\Delta USTariff_{i,t-1}$, <15km ring	-0.9945*				-0.8538	-0.1753
	(0.5329)				(0.5424)	(0.5162)
$\Delta USTariff_{i,t-1}$, 15-30km ring		-1.0611***			-0.8094*	-0.1592
		(0.3795)			(0.4335)	(0.4344)
$\Delta USTariff_{i,t-1}$, 30-50km ring			0.3686		0.4288	0.8396
			(0.8256)		(0.8183)	(0.7730)
$\Delta USTariff_{i,t-1}$, 50-100km ring				0.9406	0.6876	0.6269
				(1.1608)	(1.3275)	(1.2528)
$\Delta CHNInputTariff_{i,t-1}$	0.2505	0.1390	0.0260	0.1028	0.1728	0.4127
	(0.3286)	(0.3468)	(0.3190)	(0.3371)	(0.3342)	(0.6082)
$\Delta CHNInputTariff_{i,t-1}$, <15km ring	-1.2920**				-1.3886**	0.1414
	(0.6003)				(0.6421)	(0.5975)
$\Delta CHNInputTariff_{i,t-1}$, 15-30km ring		-1.6279			-1.4659	-0.3996
		(1.0309)			(1.0011)	(0.9093)
$\Delta CHNInputTariff_{i,t-1}$, 30-50km ring			-2.5693*		-2.7819**	-1.8007
			(1.2818)		(1.2457)	(1.1936)
$\Delta CHNInputTariff_{i,t-1}$, 50-100km ring				-0.2535	-1.9600	-1.3087
				(2.3900)	(2.5769)	(2.4970)
Grid FE	Y	Y	Y	Y	Y	Y
Prefecture×Year-Quarter FE	Y	Y	Y	Y	Y	Y
Grid W_{i0}×Year-Quarter FE	N	N	N	N	N	Y
Observations	669,845	669,845	669,845	669,845	669,845	669,845
F-stat	8.019	15.84	18.85	19.62	2.242	2.370

Notes: All columns report 2SLS estimates, using the respective Amap grid-level and neighboring-grid tariff shocks as instrumental variables for the corresponding Google Maps grid-level and neighboring-grid tariff shocks. The initial grid characteristics, W_{i0}, whose time-varying effects are included in Column 6 are: the US share in exports, the US share in imports of intermediates, log exports per capita, log intermediate imports per capita, and log 2016 mean night lights intensity; grid-level exports and imports geolocated via Amap are used to construct the first four of these W_{i0} variables. All regressions are weighted by grid population in 2015, with a minimum population of 1 imputed for cells with zero population in the raw data. Standard errors are clustered at the province level. *** $p<0.01$, ** $p<0.05$, * $p<0.1$.

Table D.10: Nonlocal Tariff Shocks and Night Lights Intensity, 2SLS

Dep. Var.: $\Delta \ln(Light_{it})$	(1)	(2)	(3)	(4)	(5)	(6)
$\Delta USTariff_{i,t-1}$	-0.7784**	-0.6802***	-0.5799**	-0.7736***	-0.8050***	-0.5639*
	(0.3562)	(0.1972)	(0.2700)	(0.2025)	(0.2342)	(0.2844)
Non-local $\Delta USTariff_{i,t-1}$, in 100km ring	-1.9421**	-1.6113**	-0.4112			
	(0.9492)	(0.6961)	(0.6529)			
Non-local $\Delta USTariff_{i,t-1}$, all prefectures				-3.4265	-0.7375	0.8142
				(2.5720)	(1.6426)	(1.5034)
$\Delta CHNInputTariff_{i,t-1}$	0.3579	0.2930	0.4915	0.1172	0.0978	0.5876
	(0.4117)	(0.3450)	(0.5755)	(0.3522)	(0.3108)	(0.5437)
Non-local $\Delta CHNInputTariff_{i,t-1}$, in 100km ring	-0.6879	-1.4408	0.6153			
	(1.6849)	(1.0455)	(0.8451)			
Non-local $\Delta CHNInputTariff_{i,t-1}$, all prefectures				2.8121	-0.4393	1.0919
				(4.0103)	(1.7915)	(1.8993)
Grid FE	Y	Y	Y	Y	Y	Y
Year-Quarter FE	Y	N	N	Y	N	N
Prefecture×Year-Quarter FE	N	Y	Y	N	Y	Y
Grid W_{i0}×Year-Quarter FE	N	N	Y	N	N	Y
Observations	652,345	652,345	652,345	669,845	669,845	669,845
F-stat	12.45	12.66	7.265	16.95	16.19	10.28

Notes: All columns report 2SLS estimates, using the respective Amap grid-level and nonlocal tariff shocks as instrumental variables for the corresponding Google Maps grid-level and nonlocal tariff shocks. The initial grid characteristics, W_{i0}, whose time-varying effects are included in Column 6 are: the US share in exports, the US share in imports of intermediates, log exports per capita, log intermediate imports per capita, and log 2016 mean night lights intensity; grid-level exports and imports geolocated via Amap are used to construct the first four of these W_{i0} variables. All regressions are weighted by grid population in 2015, with a minimum population of 1 imputed for cells with zero population in the raw data. Standard errors are clustered at the province level. *** p<0.01, ** p<0.05, * p<0.1.

Table D.11: GDP and Night Lights Intensity: County- or Province-Level Analysis

| Dep. Var.: $\Delta \ln(GDPpc_{js})$	County-Level		Province-Level	
	(1)	(2)	(3)	(4)
	2SLS	2SLS	2SLS	2SLS
$\ln(Light_{js})$	0.5384**	0.4003**	0.4004†	0.3574†
	(0.2192)	(0.1692)	(0.2521)	(0.2396)
Province×Year FE	Y	Y	N	N
County FE	Y	Y	N	N
Year FE	N	N	Y	Y
Province FE	N	N	Y	Y
Trimmed	N	Tail 5%	N	Tail 5%
Observations	8,167	7,533	124	118
F-stat	3.546	3.522	4.112	4.509

Notes: All columns report 2SLS regressions in which the lagged night lights variable, $\ln(Light_{js-1})$ is used as an IV. The analysis is at the county-level in columns 1 and 2, and at the province-level in columns 3 and 4. The county-level data on GDP per capita is obtained from China Statistical Yearbooks (County-Level), and the province-level data on GDP per capita is obtained from China Statistical Yearbooks. Columns 2 and 4 drop observations where the annual change in the log GDP per capita is below the 5th percentile or above the 95th percentile of its distribution in each given year. Standard errors are clustered at the province level. *** p<0.01, ** p<0.05, * p<0.1, † p<0.1.

Table D.12: Tariff Shocks and Night Lights Intensity: County-Level Analyses, 2SLS

| | | Measure of Commuting Openness | |
| | | $1 - \lambda_{cc|c}^R$ | $1 - \lambda_{cc|c}^L$ |
Dep. Var.: $\Delta \ln(Light_{jt})$	(1)	(2)	(3)
$\Delta USTariff_{j,t-1}$	-0.5069*		
	(0.2804)		
$\Delta CHNInputTariff_{j,t-1}$	-0.0193		
	(0.5267)		
Commuting Openness$_j$: above median $\times \Delta USTariff_{j,t-1}$		-0.6812**	-0.7018*
		(0.3299)	(0.3656)
Commuting Openness$_j$: below median $\times \Delta USTariff_{j,t-1}$		-0.3396	-0.3764
		(0.2815)	(0.3309)
Commuting Openness$_j$: above median $\times \Delta CHNInputTariff_{j,t-1}$		-0.0857	0.6748
		(0.4712)	(0.4813
Commuting Openness$_j$: below median $\times \Delta CHNInputTariff_{j,t-1}$		0.0157	-0.4473
		(0.7506)	(0.5726)
County FE	Y	Y	Y
Prefecture×Year-Quarter FE	Y	Y	Y
W_{j0}×Year-Quarter FE	Y	Y	Y
Observations	11,222	11,222	11,222
F-stat	11.94	6.288	5.844

Notes: All columns report 2SLS estimates, using the respective Amap county-level tariff shocks and associated interaction terms as instrumental variables for the corresponding Google Maps county-level tariff shocks and associated interaction terms. The initial county characteristics, W_{j0}, whose time-varying effects are included across all regressions are: the US share in exports, the US share in imports of intermediates, log exports per capita, log intermediate imports per capita, and log 2016 mean night lights intensity; county-level exports and imports geolocated via Amap are used to construct the first four of these W_{i0} variables. All regressions are weighted by county population in 2010. *** p<0.01, ** p<0.05, * p<0.1, † p<0.15.

Figure D.1: Growth in Night Lights across Tariff Bins
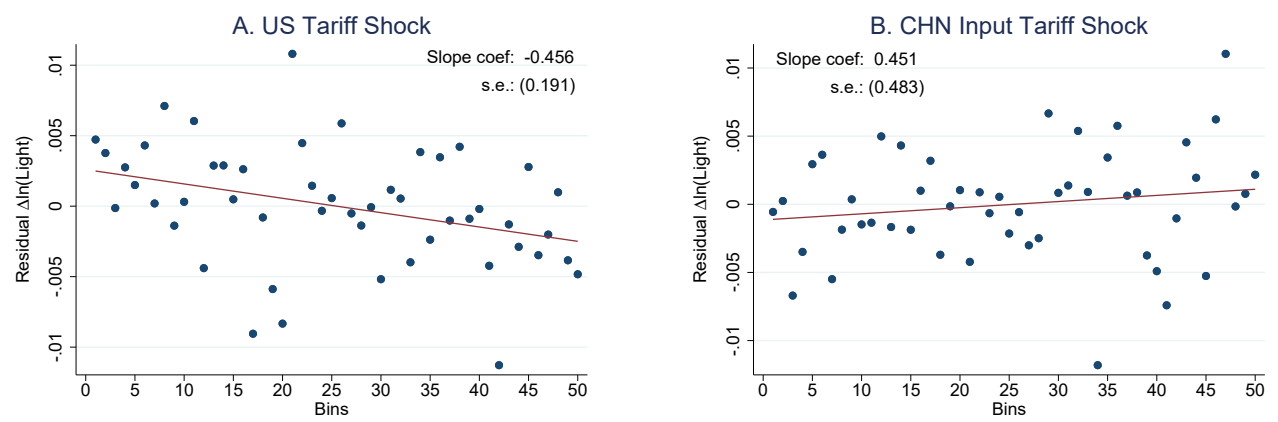
Notes: For the horizontal axis variable, we compute the predicted US tariff shock (Panel A) and the predicted CHN input tariff shock (Panel B) that emerge from running the first-stage of the IV regression corresponding to Column 4 in Table 1. We then regress these respective predicted variables against the grid and prefecture-year-quarter fixed effects, as well as the grid W_{i0} controls interacted with year-quarter fixed effects that are used in Column 4 of Table 1; the regressions are run with grid-level population weights, with a minimum population of 1 imputed for zero-population grid cells in the raw data. The grid observations are then grouped into 50 bins based on either the US tariff shock residual (Panel A) or the CHN input tariff shock residual (Panel B), with the bins constructed to be equal in population size. The night lights growth variable is constructed analogously, by residualizing $\Delta(Light)$ of the variation explained by grid and prefecture-year-quarter fixed effects, and by grid W_{i0} time-varying effects, and then computing a population weighted-average of residual night lights growth for the tariff shock bins on the respective horizontal axis. A simple linear regression line across the 50 bins is reported for each binned scatterplot.

Figure D.2: Baseline Estimated Coefficients versus Placebo Coefficients
(Constructing Placebo Tariff Shocks by Reshuffling Product-Level Shifters)
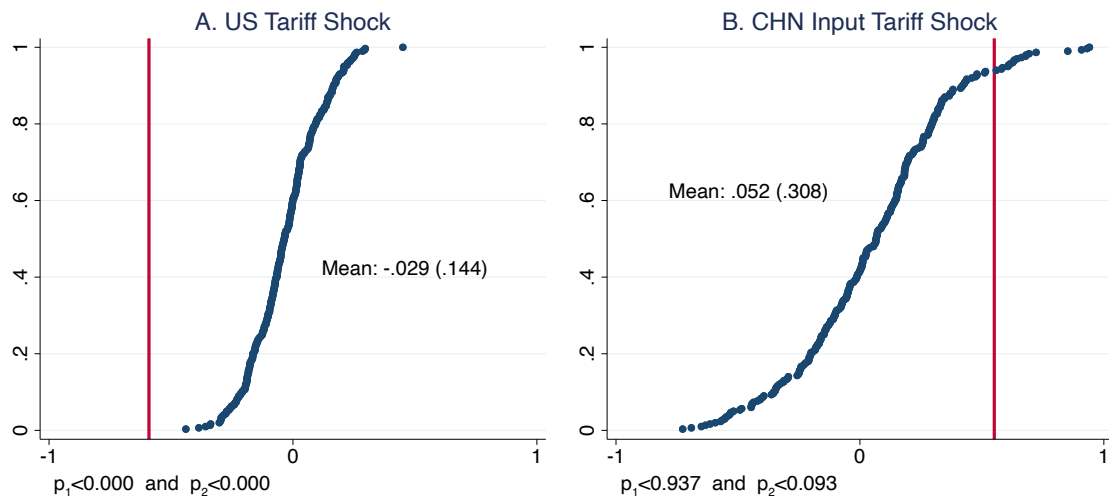
Notes: Panel A shows the cumulative distribution of the estimated coefficient of $\Delta USTariff_{i,t-1}$ when the regression specification from Column 4 of Table 1 is run on a series of 300 placebo grid samples. For each placebo grid, we build shift-share measures of the US and CHN input tariff shocks by combining actual grid trade shares for each of the HS 6-digit products with product-level shifters that are reshuffled. The mean of the $\Delta USTariff_{i,t-1}$ coefficient estimate across the 300 placebo grids is -0.029, and the standard deviation is 0.144; for comparison, the vertical line indicates the coefficient estimate obtained from the actual sample. Panel B illustrates the analogous cumulative distribution of the coefficient estimates of $\Delta CHNInputTariff_{i,t-1}$ across the 300 placebo grids. The mean of these coefficient estimates is 0.052, and the standard deviation is 0.308. Under each graph, two summary statistics are presented: p_1 is the fraction of placebo coefficient estimates that have a more negative value compared to the estimates obtained from the actual sample, and p_2 is the fraction with larger absolute values.

Figure D.3: Baseline Estimated Coefficients versus Placebo Coefficients
(Reshuffling Tariff Shocks across Grids within Prefectures)
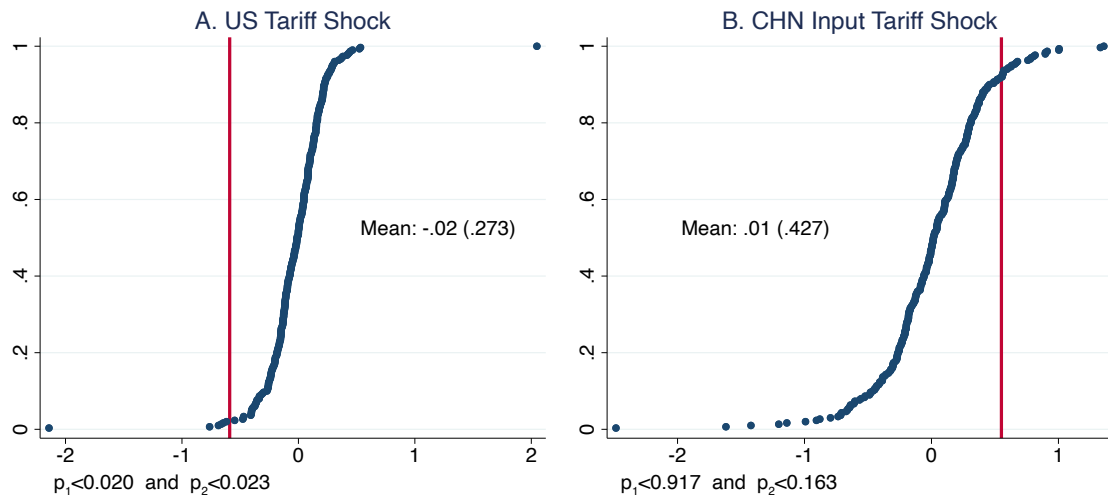
A. US Tariff Shock

Mean: -.02 (.273)

$p_1 < 0.020$ and $p_2 < 0.023$

B. CHN Input Tariff Shock

Mean: .01 (.427)

$p_1 < 0.917$ and $p_2 < 0.163$

Notes: Panel A shows the cumulative distribution of the estimated coefficient of $\Delta USTariff_{i,t-1}$ when the regression specification from Column 4 of Table 1 is run on a series of 300 placebo grid samples. For each placebo grid, we randomly reshuffle the US and CHN input tariff shocks over our sample period (that are associated with the same grid cell) across grids within a prefecture. The mean of the $\Delta USTariff_{i,t-1}$ coefficient estimate across the 300 placebo grids is -0.020, and the standard deviation is 0.273; for comparison, the vertical line indicates the coefficient estimate obtained from the actual sample. Panel B illustrates the analogous cumulative distribution of the coefficient estimates of $\Delta CHNInputTariff_{i,t-1}$ across the 300 placebo grids. The mean of these coefficient estimates is 0.010, and the standard deviation is 0.427. Under each graph, two summary statistics are presented: p_1 is the fraction of placebo coefficient estimates that have a more negative value compared to the estimates obtained from the actual sample, and p_2 is the fraction with larger absolute values.

Figure D.4: GDP per capita, Employment, and Night Lights Intensity at the Prefecture Level

A. Log GDP per capita (untrimmed)
Slope coef: 0.410
s.e.: (0.132)

B. Log Employment (untrimmed)
Slope coef: 0.470
s.e.: (0.145)

C. Log GDP per capita (trimmed)
Slope coef: 0.470
s.e.: (0.092)

D. Log Employment (trimmed)
Slope coef: 0.302
s.e.: (0.089)
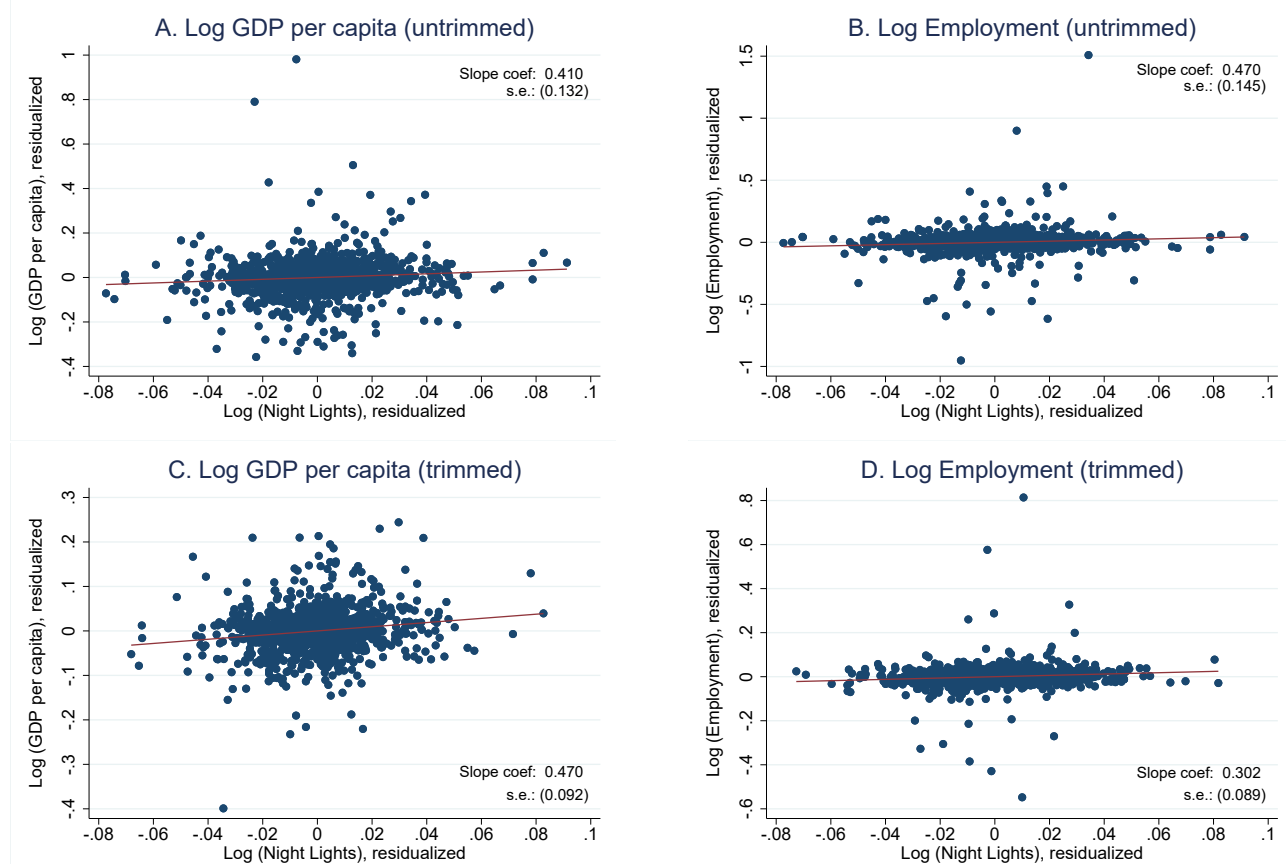
Notes: Panels A and C illustrate the relationship between log GDP per capita and log night lights intensity across prefecture-year observations from 2013-2016. These are based on the 2SLS specifications in Columns 4 and 6 of Table 2 respectively, after residualizing log GDP per capita and predicted log night lights (from the first-stage regression) by province-year and prefecture fixed effects. In Panel C, observations where the change in log GDP per capita relative to the prior year was smaller than the 5th and greater than the 95th percentiles of its distribution in that year are dropped. Panels B and D illustrate the analogous relationship between log employment and log night lights intensity, based on the 2SLS specification in Columns 11 and 13 of Table 2.